Generation of human hepatic progenitor cells with regenerative and metabolic capacities from primary hepatocytes

Takeshi Katsuda,[1] Juntaro Matsuzaki,[1] Tomoko Yamaguchi,[1,2] Yasuhiro Yamada,[3] Kazunori Hosaka,[1] Atsuko Takeuchi,[4] Yoshimasa Saito,[2] Takahiro Ochiya[1, 5]

1) Division of Molecular and Cellular Medicine, National Cancer Center Research Institute, 5-1-1 Tsukiji, Chuo-ku, Tokyo 104-0045, Japan
2) Division of Pharmacotherapeutics, Keio University Faculty of Pharmacy, 1-5-30 Shibakoen, Minato-ku, Tokyo, 105-8512, Japan
3) Department of Clinical Pharmaceutics, Nihon Pharmaceutical University, 10281 Komuro, Ina-machi, Kitaadachi-gun, Saitama 362-0806, Japan
4) Division of Analytical Laboratory, Kobe Pharmaceutical University, 4-19-1, Motoyamakitamachi, Higashinada-ku, Kobe, 658-8558, Japan
5) Corresponding author: tochiya@ncc.go.jp

Abstract

Hepatocytes are regarded as the only effective cell source for cell transplantation to treat liver diseases; however, their availability is limited due to a donor shortage. Thus, a novel cell source must be developed. We recently reported that mature rodent hepatocytes can be reprogrammed into progenitor-like cells with a repopulative capacity using small molecule inhibitors. Here, we demonstrate that hepatic progenitor cells can be obtained from human infant hepatocytes using the same strategy. These cells, named human chemically induced liver progenitors (hCLiPs), had a significant repopulative capacity in injured mouse livers following transplantation. hCLiPs redifferentiated into mature hepatocytes *in vitro* upon treatment with hepatic maturation-inducing factors. These redifferentiated cells exhibited cytochrome P450 (CYP) enzymatic activities in response to CYP-inducing molecules and these activities were comparable with those in primary human hepatocytes. These findings will facilitate liver cell transplantation therapy and drug discovery studies.

Keywords: hepatocyte, liver progenitor cell, transplantation, liver repopulation, cytochrome P450

Introduction

Expansion of functional human hepatocytes is a prerequisite for liver regenerative medicine. Human hepatocytes are currently regarded as the only competent cell source for transplantation therapy [1]; however, their availability is limited due to a shortage of donors. Moreover, the therapeutic application of hepatocytes is hampered by their inability to proliferate *in vitro*. To overcome this, researchers have sought to generate expandable cell sources as alternatives to primary hepatocytes. Such cell sources include embryonic stem cell- and induced pluripotent stem cell-derived hepatic cells [2–6], lineage-converted hepatic cells (induced hepatic cells; [7,8], and facultative liver stem/progenitor cells (LPCs) residing in adult liver tissue [9]. However, while primary hepatocytes efficiently repopulate injured mouse livers (repopulation indexes (RIs) > 50%), the repopulation efficiency of these laboratory-generated hepatocytes is limited, with reported RIs generally less than 5% (reviewed in [10]).

Researchers have also attempted to expand primary human hepatocytes (PHHs) *in vitro*. Several studies reported the expansion of these cells [11–15], suggesting that they are potentially applicable for transplantation therapy. However, the growth rate and proliferative lifespan of PHHs are limited. For example, Yoshizato's group reported that PHHs can be cultured for several passages, but their growth rate is slow (population doubling time of 20–300 days) [15]. This finding indicates that culture of PHHs must be improved for the clinical application of these cells.

We recently reported that a cocktail of small molecule signaling inhibitors reprograms rodent adult hepatocytes into culturable LPCs, named chemically induced liver progenitors (CLiPs) [16]. Notably, rat CLiPs extensively repopulate chronically injured mouse livers without causing any tumorigenic features. Here, using the same strategy, we demonstrate that human infant hepatocytes can be also converted into proliferative LPC-like cells, which are named human CLiPs.

Results

Small molecules support expansion of PHHS

In a pilot study, we tested whether the combination of Y-27632 (Y), A-83-01 (A), and CHIR99021 (C), the chemical cocktail used to reprogram rodent hepatocytes, also induced proliferation of commercially available cryopreserved adult PHHs (APHHs) (donor information is summarized in Table 1). In contrast with the basal culture medium (small hepatocyte medium (SHM)), culture in YAC-containing SHM (SHM+YAC) induced the proliferation of cells that morphologically resembled epithelial cells (Fig. S1A). These cells were small and had a higher nucleus-to-cytoplasm ratio than hepatocytes, which is a typical morphological feature of LPCs. When colonies became densely packed, rat and mouse CLiPs exhibited a compact polygonal cell shape delimited by sharply defined refractile borders with bright nuclei in phase contrast images (Fig. S1B, S1C). However, unlike rat and mouse CLiPs, the morphology of human cells did not clearly change after colonies became densely packed (Fig. S1A). Although we did not perform further characterization, these proliferating cells likely arose from non-hepatic cells, such as biliary epithelial cells (BECs) or so-called liver epithelial cells, the origins of which are not well-defined [17]. Thus, we speculated that human hepatocytes require additional proliferative stimuli. Therefore, we tested the ability of fetal bovine serum (FBS) to support the proliferation of these cells. One of three lots of APHHs formed proliferative and densely packed colonies, and exhibited a hepatocytic morphology upon culture in medium supplemented with YAC and 10% FBS (FYAC) (Fig. S1D). By contrast, all three lots of APHHs formed proliferative colonies with hepatic morphologies upon culture in medium supplemented with AC and 10% FBS (FAC) (Fig. S1E). However, the proliferative capacity of these hepatic colony-forming cells was limited, and the number of these cells markedly decreased after the first passage, while non-parenchymal cells (NPCs) with non-hepatic morphologies became the dominant population (data not shown).

Next, considering the previous finding that PHHs derived from young donors are optimal for *in vitro* expansion [14,15], we tested whether infant PHHs (IPHHs) expanded more efficiently in the presence of small molecules and FBS. Using IPHHs derived from a 10-month-old donor (lot FCL), we performed a mini-screen using all possible combinations of Y, A, and C in 10% FBS-supplemented SHM. The water-soluble tetrazolium salt-based (WST) assay demonstrated that these cells proliferated in the presence of A, YA, AC, and YAC (Fig. 1A). Consistent with the observations made in APHHs (Fig. S1E), these cells proliferated most efficiently in FAC and thus we used this medium in all subsequent

experiments. Robust proliferation of hepatocytes was not supported by culture in the presence of AC or FBS alone, but was synergistically supported by culture in the presence of both AC and FBS (Fig. 1B). Although proliferating cells cultured in FAC did not morphologically resemble hepatocytes when the cell density was low, they spontaneously acquired a hepatocyte-like morphology as colonies became densely packed (Fig. 1C). This observation strongly suggests that human proliferative cells cultured in FAC more closely resembled rodent CLiPs than those cultured in the presence of YAC. Unlike APHHs, IPHHs proliferated efficiently and became the predominant population over 2 weeks of culture. Two other lots of IPHHs (lot DUX from an 8-month-old donor and lot JFC from a 1-year-old donor) (Table 1) also proliferated in these culture conditions, although the proliferative capacity varied among the lots: FCL, DUX, and JFC proliferated 49.2 ± 9.34 (at day 14), 46.2 ± 2.12 (at day 14) and 3.66 ± 0.321 (at day 12) folds, respectively (mean ± SEM, determined by 2 repeated experiments for each lot). We also confirmed by microscopy that FAC enabled two more donors (11 mo and 2 yr old)-derived IPHHs and one juvenile donor (7 yr-old)-derived hepatocytes to proliferate and spontaneously change their morphologies to hepatocyte-like ones in the densely packed region of the proliferating colonies (Fig. S1F).

Characterization of proliferating cells cultured in FAC

These proliferating cells expressed multiple surface markers of LPCs, including EPCAM, CD44, PROM1 (also known as CD133), CD24, and ITGA6 (Fig. 1D, S2A). We performed microarray-based transcriptome analysis of previously identified BEC/LPC marker genes to further characterize these cells. Expression of many of these genes was induced during the 2 weeks of culture (Fig. 1E). Some of these genes, such as *PROM1* and *SPP1*, were expressed at comparable levels regardless of whether cells were cultured in the presence of AC, suggesting that their expression was spontaneously induced by the basal culture conditions (Fig. 1E). However, expression of multiple BEC/LPC marker genes, including *EPCAM*, *SOX9*, *KRT19*, *TACSTD2*, *AXIN2*, and *PROX1*, was increased in cells cultured in FAC (Fig. 1E, 1F). Of these, expression of *EPCAM*, *SOX9*, and *KRT19* was affected not only by the presence of AC but also by the culture duration, suggesting that AC induced expression of these genes during *in vitro* culture. By contrast, expression of *AXIN2* and *PROX1* was maintained, but not increased, upon culture in the presence of AC. Gene signature enrichment analysis (GSEA) comparing cells cultured in the presence of FBS and those cultured in FAC demonstrated that the majority of gene sets enriched in the latter cells

were related to hepatic function (Fig. 1G, Table S1), suggesting that AC also helped to maintain the hepatocytic characteristics of cultured hepatocytes. Although cell cycle-related gene sets were also identified by GSEA, their enrichment scores were relatively low (Fig. S2B, Table S1). This is likely because cell proliferation was also increased by culture in the presence of FBS. However, proliferating cells were contaminated by fibroblast-like NPCs upon culture in the presence of FBS. Proliferation-related gene sets were enriched in cells cultured in the presence of FBS and in FAC compared with cells at 1 day after plating (D1 hepatocytes) (Fig. S2C, S2D, Table S3 and S4). However, gene sets related to liver fibrogenesis, such as "p75 NTR receptor-mediated signaling", "PDGF signaling", and "TGFβ signaling", were also enriched in cells cultured in the presence of FBS (Fig. 1H, Table S2). Accordingly, expression of the hepatocytic connexin genes *GJB1* (also known as *CX32*) and *GJB2* (also known as *CX26*) was low in cells cultured in the presence of FBS, while the NPC connexin gene *GJA1* (also known as *CX43*) was sharply upregulated [18] (Fig. S2E). In addition, the gene set "epithelial to mesenchymal transition" was enriched in cells cultured in the presence of FBS compared with cells cultured in FAC (Fig. 1H), suggesting that the former cells acquired a mesenchymal phenotype. Overrepresentation of TGFβ signaling in hepatocytes reportedly leads to acquisition of a fibroblast-like dedifferentiated state both *in vitro* and *in vivo* [19,20]. In summary, two small molecules, AC, together with FBS, support the proliferation of hepatic epithelial cells with characteristics of both hepatocytes and LPCs/BECs.

Hepatic differentiation capacity of the proliferative cells

A hepatic differentiation capacity is an important feature of LPCs, particularly for their potential use as a candidate cell source for transplantation therapy. To investigate the hepatic differentiation capacity of these proliferative cells, we passaged and cultured them in the presence of oncostatin M (OSM), dexamethasone, and Matrigel, which induce maturation of LPCs into hepatocytes (Fig. S3A) [21]. As noted in Figure 1C, the proliferative cells spontaneously acquired hepatic morphologies when they reached 100% confluency, even in the absence of hepatic maturation inducers (Fig. 2A, S3B, middle panels for each lot). However, this morphological change was more evident in the presence of hepatic maturation inducers (Fig. 2A, S3B, right panels for each lot). In particular, cells acquired a polygonal and cytoplasm-rich morphology, which is similar to that of PHHs (Fig. 2B). Accordingly, microarray analysis confirmed that expression of representative hepatic marker genes,

including *ALB*, *TDO2*, and *SERPINA1* was increased after hepatic maturation induction (Fig. 2C). However, the expression levels of these genes were not markedly changed in cells from lot JFC. This is presumably because expression of hepatic maturation genes was already high in these cells even before hepatic induction. In contrast with the hepatic marker genes, expression of the BEC/LPC marker genes including *SOX9*, *KRT19*, and *KRT7* was decreased, suggesting that the proliferative cells lost their BEC/LPC phenotype and acquired a mature hepatic phenotype (Fig. S3C). Hierarchical cluster analysis of genes that were differentially expressed between cells cultured in the presence of hepatic maturation inducers (Hep-i(+)) and cells cultured for the same duration in the absence of hepatic maturation inducers (Hep-i(-)) indicated that the characteristics of Hep-i(+) cells were relatively similar to those of PHHs (Fig. 2D). Overrepresented pathways in Hep-i(+) cells in comparison with Hep-i(-) cells were associated with the immune response and metabolic processes (Fig. 2E), both of which are important functions of the liver. These findings were further validated by GSEA (Fig. 2F, Table S5). By contrast, overrepresented pathways in Hep-i(-) cells in comparison with Hep-i(+) cells were associated with developmental processes and morphogenesis, implying that Hep-i(-) cells were functionally immature compared with Hep-i(+) cells (Fig. S3D). In addition, cell cycle-related genes were overrepresented in Hep-i(-) cells (Fig. S3E, Table S6), which is consistent with the general notion that progenitor cells have a greater proliferative capacity than cells with a more mature phenotype. Taken together, proliferative cells derived from human hepatocytes via culture in FAC lost their immature phenotype and acquired a mature hepatocyte-like phenotype in response to hepatic maturation inducers. Thus, we hereafter designate these proliferative cells as human CLiPs (hCLiPs).

Expression and activities of drug-metabolizing enzymes in hCLiP-derived hepatocytes

Cytochrome P-450 (CYP) enzymes play a central role in the metabolic functions of the liver. Thus, we investigated the metabolic functions of hCLiP-derived hepatocytes. As noted in the previous section, overrepresented pathways in Hep-i(+) cells were associated with metabolism (Fig. 2E, 2F, Table S5). In addition, pathways involving CYPs were enriched in Hep-i(+) cells, as characterized by GSEA using both the KEGG and Reactome databases, although the p-values for these gene sets were higher than 0.05 (Fig. S4A). A heatmap revealed that expression of several *CYP* genes was higher in Hep-i(+) cells than in Hep-i(-) cells (Fig. 3A). These genes included *CYP2B6*, *CYP2D6*, *CYP2E1*, *CYP2C9*, and *CYP3A4*, which play crucial roles in metabolic functionality of the human liver [22]. The

enzymatic activities of multiple CYPs were investigated by liquid chromatography tandem mass spectrometry (LC-MS/MS) using a cocktail of substrates (Fig. 3B) [23]. This revealed that the enzymatic activities of CYP1A2, CYP2C19, CYP2C9, CYP2D6, and CYP3A were comparable, if not the same, in Hep-i(+) cells derived from lots FCL and JFC as in PHHs, but were lower in Hep-i(+) cells derived from lot DUX (Fig. 3B). Expression of CYP1A2, CYP2B6, and CYP3A4 is induced in hepatocytes via transcriptional activation in response to certain chemicals. Thus, we investigated whether the expression and activities of these CYPs were increased in hCLiP-derived hepatocytes treated with prototypical inducers of each CYP isoform, namely, omeprazole (aryl hydrocarbon receptor ligand) for CYP1A2, phenobarbital (indirect activator of constitutive active androstane receptor) for CYP2B6 and CYP3A4, and rifampicin (pregnane X receptor ligand) for CYP3A4. These *CYP* genes were markedly upregulated in cells derived from the three lots in response to the corresponding inducer (Fig. S4B, S4C). Although enzymatic activities of these CYPs were increased in both Hep-i(-) and Hep-i(+) cells upon treatment with the corresponding inducer, these increases were relatively larger in the latter cells than in the former cells (Fig. 3C, S3D), consistent with the changes in gene expression (Fig. S3C). We also directly quantified CYP protein expression by mass spectrometry. Protein expression of CYP1A2 and CYP3A4 in hCLiP-derived hepatocytes was increased in response to the corresponding inducer (Fig. 3D). In addition, activities of the phase II enzymes sulfotransferase (SULT) and UDP-glucuronosyltransferase (UGT) were comparable in hCLiP-derived hepatocytes and PHHs (Fig. 3E). These results demonstrate that hCLiPs differentiate into cells that are metabolically mature after induction of hepatic maturation and thus are potentially applicable for drug metabolism studies.

Long-term expansion of hCLiPs

Long-term culture of hepatocytes or LPCs with a sustained proliferative capacity is of great interest for liver regenerative medicine and drug discovery studies. Thus, we investigated the feasibility of long-term culture of hCLiPs. Cells derived from lots FCL and DUX could be serially passaged until at least passage 10 (P10) without growth arrest (Fig. 4A) or obvious morphological changes (Fig. S5A). The population doubling times of FCL and DUX hCLiPs were 1.27 ± 0.0066 and 1.43 ± 0.0086 d, respectively (Mean ± SEM, determined by 3 repeated experiments for each lot). However, non-hepatic cells with a fibroblast-like morphology were also observed (Fig. S4A, arrows), and the percentage of

these cells varied among repeated experiments for each lot, as assessed by flow cytometric analysis of the epithelial-cell surface marker proteins EPCAM and CD24 (Fig. S5B). Cultures of cells from lot JFC contained more fibroblast-like cells than cultures of cells from lots FCL and DUX (Fig. S5A). Upon culture of cells from lot JFC, the percentage of fibroblastic cells increased with the passage number and fibroblastic cells overwhelmed hCLiPs by P5, as assessed by microscopic observation (n = 3 repeated experiments) (Fig. S4A) and flow cytometric analysis of LPC markers (n = 1 experiment) (Fig. S4B). However, when $EPCAM^+$ cells were sorted from primary hCLiPs at the first passage, proliferative epithelial cells were observed for at least the next three passages (total of four passages) with their population doubling time 1.24 d (n = 1 experiment) during P1 and P4 (Fig. 4A, S5A), confirming the proliferative capacity of hCLiPs obtained from lot JFC. Although expression of surface markers varied among experimental batches at later passages (Fig. S5B), it was relatively stable up to P5 in cells derived from lots FCL and DUX (Fig. S5B). We also investigated the karyotype of cells derived from lots FCL and DUX at P7 (Fig. 4B). hCLiPs derived from lot JFC were contaminated by an increased percentage of fibroblast-like cells; therefore, we karyotyped FACS-sorted $EPCAM^+$ cells (at the first passage) which were then passaged four times after sorting (Fig. 4B). None of the analyzed cells exhibited any chromosomal abnormality (20 cells analyzed per lot) and all the analyzed cells were diploid (50 cells analyzed per lot) (Fig. 4B). This implies that hCLiPs were derived from diploid hepatocytes, which is consistent with our previous observations in rat CLiPs [16]. We further investigated transcriptomic changes in hCLiPs derived from lots FCL and DUX between P0 and P10 using cells from the experimental batches that maintained higher levels of EPCAM and CD24 expression (Fig. S5B) (experimental batch #2 and #3 for lots DUX and FCL, respectively). A heatmap of genes that were differentially expressed between P0 and P10 showed that the phenotype of hCLiPs gradually changed (Fig. S5C). As indicated on the right in Figure S5C, genes whose expression decreased included those related to hepatic functions, indicating that hCLiPs lose their hepatic phenotypes during repeated passage. Nonetheless, the heatmap suggested that hCLiPs retained at least some of their original characteristics until approximately P5 (Fig. S4C). Thus, we investigated the hepatic phenotype of hCLiPs at P3 and P5. Quantitative reverse transcription PCR (qRT-PCR) analysis of hCLiPs derived from each lot indicated that absolute expression levels of hepatic genes consistently decreased as the passage number increased (Fig. 4C). Nevertheless, hCLiPs derived from each lot, particularly lots FCL and DUX, could undergo hepatic differentiation (Fig. 4C).

Immunocytochemistry revealed that Hep-i(+) cells derived from lot FCL expressed hepatic marker proteins at P3 (Fig. S5D). We also investigated CYP enzymatic activities in these cells. Although the CYP enzymatic activities clearly decreased upon repeated passage, the basal activities of these enzymes, with the exception of CYP2C19, were maintained at P3 and P5 (Fig. 4D). Induction of CYP3A enzymatic activity in response to rifampicin and phenobarbital was relatively stable even at P3 and P5, especially in Hep-i(+) cells (Fig. 4E). In summary, functional decline of hCLiP-derived hepatocytes during continuous culture is unavoidable; however, CYP3A, the most important CYP in human drug metabolism, is still induced in these cells.

Repopulation of chronically injured mouse livers by hCLiPs

The capacity to repopulate injured livers is the most important and stringent criterion of a candidate cell source for liver regenerative medicine. Depending on the disease, 1–15% of hepatocytes must be replaced to achieve and sustain a therapeutic effect [10,24]. Consequently, we tentatively regard a RI of 15% as a benchmark of a significant repopulative capacity. Laboratory-generated hepatocytes typically have RIs of less than 5% [10], although a few studies reported maximum RIs of 20% or 30% in individual animals [2,8]. A previous study also reported that the repopulative capacity of authentic human hepatocytes decreases upon *in vitro* culture; the RI of cultured hepatocytes that successfully engrafted was 6.6% on average and reached 27% in an individual animal [13].

We assessed the repopulative capacity of hCLiPs in immunodeficient mice with chronically injured livers. Our previous study revealed that rat CLiPs repopulate the liver of cDNA-uPA/SCID mice [16]; therefore, we first transplanted hCLiPs derived from lots FCL, DUX, and JFC at P0–P2 into this model. After intrasplenic transplantation of primary hCLiPs that had been expanded *in vitro* for approximately 2 weeks (11–13 days) (hereafter designated P0-hCLiPs), the human ALB (hALB) level was exponentially increased in the blood of some, but not all, mice (Fig. 5A, red lines). The maximum hALB level in blood was > 10 mg/ml, which is comparable with that observed following transplantation of PHHs in this animal model [25]. Immunohistochemistry (IHC) of human-specific CYP2Cs (including CYP2C9 and other CYP2Cs according to the manufacturer's datasheet) demonstrated extensive repopulation in mouse livers extracted at 10–11 weeks after transplantation (Fig. 5B). Although the RI varied among mice (32.2 ± 13.5% for lot FCL, n = 11; 39.3 ± 13.5% for lot JFC, n = 11; 17.8 ± 16.4% for lot DUX, n =4, mean ± SEM), it reached > 90% in some

animals (Fig. 5C). This maximum RI is comparable with that achieved after transplantation of PHHs [10]. The repopulative capacity declined as the culture period increased (Fig. 5A, 5C). Nonetheless, one mouse transplanted with FCL-P1-hCLiPs (hCLiPs derived from lot FCL that were passaged once before transplantation) (67.4%) and two mice transplanted with JFC-P2-hCLiPs (hCLiPs derived from lot JFC that were passaged twice before transplantation) (83.1% and 91.1%) exhibited high RIs. We confirmed the repopulative capacity of FCL-P0-hCLiPs using another model, namely, TK-NOG mice [26]. In this model, the serum hALB level was dramatically elevated to at most 8.1 mg/ml (Fig. 5D). The maximum RI was lower in TK-NOG mice (57.5%) than in cDNA-uPA/SCID mice (96.0%) (Fig. 5E, 5F). However, engraftment was more efficient in TK-NOG mice than in cDNA-uPA/SCID mice; significant repopulation (> 15% RI) with FCL-P0-hCLiPs was observed in 83% (5/6 mice) of TK-NOG mice (Fig. 5F), but only in 50% (3/6 mice) of cDNA-uPA/SCID mice (Fig. 5C). Examination of the area repopulated by hCLiPs by staining with an antibody against human mitochondria showed that repopulating human cells expressed MDR1 and TTR, which are associated with hepatic function (Fig. 5G, 5H). MDR1 was detected on the apical side of adjacent mouse and human hepatocytes, suggesting that hCLiP-derived cells successfully reconstructed the normal liver architecture (Fig. 5G, arrows). Accordingly, hepatic zonation was correctly established in the repopulated regions, as assessed by investigating expression of glutamate-ammonia ligase (GLUL, also known as glutathione synthetase) (Fig. 5H), and CYP1A2 and CYP3A4 (Fig. 5I).

Functional characterization of hCLiP-derived hepatocytes in chimeric livers

Finally, we isolated human cells from chimeric mouse livers and investigated their functionality because it has been argued that some types of laboratory-generated hepatocytes are not fully functional *in vivo* [10]. We first performed microarray-based transcriptomic analysis. After isolating hepatocytes from chimeric livers of cDNA-uPA/SCID mice by a two-step collagenase perfusion method, we eliminated mouse cells using a magnetic bead separation system. Microscopic observation revealed that 32.7%, 16.8%, and 33.1% of hepatocytes isolated from chimeric livers of mice transplanted with hCLiPs derived from lots FCL, JFC, and DUX bound to magnetic beads conjugated with a specific anti-mouse antibody prior to magnetic separation, respectively, while these percentages were reduced to 2.9%, 0.0%, and 1.6% after magnetic separation, respectively. Thus, we assumed that the results of experiments performed with these cells should be mostly ascribed to human cells.

Magnetically separated human cells exhibited typical morphologies of mature hepatocytes (Fig. 6A). However, unexpectedly, hierarchical clustering and principle component analysis (PCA) of the entire transcriptome showed that chimeric liver-derived human cells were distinct from PHHs (Fig. 6B, 6C). A control sample of human hepatocytes isolated from chimeric livers following transplantation of IPHHs (lot JFC) yielded similar results as human hepatocytes isolated from chimeric livers following transplantation of hCLiPs (Fig. 6B, 6C), indicating that the transcriptomic difference between human hepatocytes in chimeric livers and PHHs is due to environmental differences between human and mouse livers. Surprisingly, GSEA demonstrated that multiple hepatic function-related gene sets were overrepresented in human hepatocytes isolated from chimeric livers in comparison with PHHs (Table S7). The majority of these gene sets were associated with metabolic pathways. Other hepatic functions were also enriched, such as pathways associated with coagulation and complement production (Fig. 6D, Table S7). BEC/LPC marker genes were underrepresented in hCLiP-derived hepatocytes isolated from chimeric livers and PHHs in comparison with hCLiPs (Fig. S6A), demonstrating that hCLiPs underwent hepatic maturation after repopulating mouse livers. We also investigated whether hCLiP-derived hepatocytes isolated from chimeric livers exhibited CYP activities. As expected based on the transcriptomic analysis, hCLiP-derived cells isolated from chimeric livers exhibited basal enzymatic activities of major CYPs comparable with those in PHHs (Fig. 6E). Enzymatic activities of CYP1A2, CYP2B6, and CYP3A were markedly induced in hCLiP-derived hepatocytes isolated from chimeric livers upon treatment with rifampicin, phenobarbital, and omeprazole (Fig. 6F). Consistently, qRT-PCR analysis demonstrated that expression of *CYP1A2*, *CYP2B6*, and *CYP3A4* was dramatically upregulated upon treatment with CYP inducers (Fig. S6B). Finally, activities of the phase II enzymes UGT and SULT in hCLiP-derived hepatocytes isolated from chimeric livers were comparable with those in PHHs (Fig. 6G). These results indicate that although their transcriptomic profiles are not identical to those of PHHs, including IPHHs and APHHs, hCLiPs functionally mature in mouse liver.

Discussion

In this study, we demonstrated that hCLiPs can repopulate chronically injured livers of immunodeficient mice. An efficient repopulative capacity is one of the most important requirements of a candidate cell source for transplantation therapy; however, it is very challenging to develop such a cultured cell source. Laboratory-generated hepatic cells, such

as pluripotent cell-derived hepatic cells and those transdifferentiated from cells of different lineage origins, have a poor repopulative capacity [10]. The RI of laboratory-generated hepatocytes is typically less than 5% [10]. After our report of rodent CLiPs [16], four groups recently reported methods for *in vitro* generation of proliferative human liver (progenitor) cells from human hepatocytes [27–30]. In three of these studies [27–29], the generated cells exhibited relatively low repopulative efficiency, approximately 13% of RI at maximum. In contrast, Hui's group reported strikingly high repopulation efficiency with as high as 64% RI [30]. Our study is, thus, not the first one to report substantial repopulation using an *in vitro*-generated human hepatic cell source. Nonetheless, to solidify a novel concept, more evidence must be provided independently from multiple laboratories. As such, we still believe that our work also plays an important role in pioneering this new field.

Our study also showed that hCLiPs may be a novel cell source for drug discovery studies. The major criterion for the application of cultured hepatic cells in drug discovery studies, particularly to evaluate the functions of drug-metabolizing enzymes, is the inducibility of CYP enzymatic activities. CYP enzymes play central roles in the metabolism of clinically used drugs and xenobiotics. In general, CYP induction accelerates the clearance of xenobiotics, leading to beneficial or harmful outcomes depending on the context. Thus, recapitulation of CYP induction in cultured hepatocytes or their equivalents is important to precisely predict the effects of a tested drug on hepatocytes. However, PHHs lose their hepatic functions, including CYP inducibility, upon *in vitro* culture. Laboratory-generated hepatocytes reportedly exhibit basal CYP activities after maturation [4,31–34]. Although a few groups described CYP inducibility in terms of enzymatic activity [35–37], such reports are very limited, to the best of our knowledge. We propose that hCLiPs are a novel platform for drug discovery studies.

In conclusion, we propose that hCLiPs are a novel platform for cell transplantation therapy as well as for drug discovery studies.

Materials and Methods

Primary human hepatocytes

Infant primary human hepatocytes (IPHHs) (lots FCL, DUX, and JFC) were purchased from Veritas Corporation (Tokyo, Japan). Adult primary human hepatocytes (APHHs) (lots HC1-14, HC3-14, HC5-25, and HC7-4) were purchased from Sekisui XenoTech (KS). Donor information is summarized in Table 1.

Culture medium

The basal medium for culture of PHHs was SHM (DMEM/F12 (Life Technologies, MA) containing 2.4 g/l $NaHCO_3$ and L-glutamine) [38,39] supplemented with 5 mM HEPES (Sigma, MO), 30 mg/l L-proline (Sigma), 0.05% bovine serum albumin (Sigma), 10 ng/ml epidermal growth factor (Sigma), insulin-transferrin-serine-X (Life Technologies), 10^{-7} M dexamethasone (Sigma), 10 mM nicotinamide (Sigma), 1 mM ascorbic acid-2 phosphate (Wako, Osaka, Japan), and antibiotic/antimycotic solution (Life Technologies). Depending on the experiment, this basal medium was supplemented with 10% FBS (Life Technologies), as well as small molecules, namely, 10 mM Y-27632 (Wako), 0.5 mM A-83-01 (Wako), and 3 mM CHIR99021 (Axon Medchem, Reston, VA). After a mini-screen of these three small molecules, PHHs were routinely cultured in SHM supplemented with 10% FBS, 0.5 mM A-83-01, and 3 mM CHIR99021.

Induction of hCLiPs from IPHHs

IPHHs were thawed in a water bath set to 37°C and suspended in 10 ml Leibovitz's L-15 Medium (Life Technologies) supplemented with Glutamax (Life Technologies) and antibiotic/antimycotic solution. After centrifugation at 50 ×g for 5 min, the cells were resuspended in William's E medium supplemented with 10% FBS, GlutaMAX, antibiotic/antimycotic solution, and 10^{-7} M insulin (Sigma). The number of viable cells was determined using trypan blue (Life Technologies). IPHHs from lot JFC were seeded in collagen I-coated plates (IWAKI, Shizuoka, Japan) at a density of approximately 5×10^3 viable cells/cm^2. IPHHs from lots FCL and DUX barely attached to the plates, and many of the small number that did attach subsequently detached prior to D3, as monitored by time-lapse imaging using a BZ-X700 microscope (Keyence, Osaka Japan) (data not shown). Therefore, IPPHs from lots FCL and DUX were seeded at a density of approximately 2×10^4 viable cells/cm^2, which was approximately 4-fold higher than the seeding density of IPHHs

from lot JFC. To determine the fold change in cell number during *in vitro* culture, the number of adherent cells on D3 was counted based on micrographs acquired at 10× magnification (5–10 fields per experiment).

Subculture of hCLiPs

Cells were harvested using TrypLE Express (Life Technologies, MA) when they reached 70–100% confluency and then re-plated into a 10 cm collagen-coated plate at a density of 1–2 × 10^5 cells/dish.

Cell proliferation assay

Numbers of viable cells were estimated based on the WST-8 assay using Cell Counting Kit 8 (Dojindo, Kumamoto, Japan), according to the manufacturer's instructions.

Flow cytometry and cell sorting

Flow cytometry and sorting of $EPCAM^+$ cells were performed using a S3e™ Cell Sorter (BioRad, Hercules, CA). Cells were labeled with APC-conjugated mouse anti-human CD44 (1:20; G44-26; BD, Franklin Lakes, NJ), APC-conjugated mouse anti-human EPCAM (1:20; EBA-1; BD), PE/Cy7-conjugated anti-human/mouse CD49f (ITGA6) (1:20; GoH3; Biolegend), PE/Cy7-conjugated anti-human CD24 (1:20; ML5; Biolegend), and APC-conjugated human anti-CD133 (1:11; AC133; Miltenyi Biotech) antibodies. An APC-conjugated mouse IgG1, κ isotype control antibody (Biolegend, MOPC-21) and a PE-Cy7-conjugated mouse IgG2b, κ isotype control (BD, 27-35) were used as controls.

Microarray analysis

One-color microarray-based gene expression analysis was performed using a SurePrint G3 Human Gene Expression v3 8x60K Microarray Kit (Agilent, Santa Clara, CA) following the manufacturer's instructions. The 75th percentile shift normalization was performed using GeneSpring software (Agilent).

Induction of hepatic differentiation of hCLiPs

hCLiPs were harvested using TrypLE Express (Life Technologies) and reseeded into a collagen I-coated 24-well plate at a density of 5 × 10^4 cells/well (2.5 × 10^4 cells/cm^2). When cells reached approximately 50–80% confluency, culture medium was replaced by SHM

supplemented with 2% FBS, 0.5 mM A-83-01, and 3 mM CHIR99021 in the absence (Hep-i(-)) or presence (Hep-i(+)) of 5 ng/ml human OSM (R&D) and 10^{-6} M dexamethasone. Cells were cultured for a further 6 days and fresh medium was provided every 2 days. On D6, cells were overlaid with a mixture of Matrigel (Corning, Corning, NY) and the aforementioned hepatic induction medium at a ratio of 1:7 and cultured for another 2 days. Thereafter, Matrigel was removed via aspiration, samples were washed with Hank's Balanced Salt Solution supplemented with Ca^{2+} and Mg^{2+} (Life Technologies), and cells were used for RNA extraction or CYP induction experiments.

CYP induction

SHM containing 2% FBS, but not A-83-01 or CHIR99021, was used as basal medium. CYP3A and CYP2B6 were induced via treatment with 10 μM rifampicin and 1 mM phenobarbital. An equal volume of methanol (1/100 dilution) and H_2O (1/1000 dilution) was used as the vehicle control for rifampicin and phenobarbital, respectively. CYP1A2 was induced via treatment with 50 μM omeprazole, and methanol (1/100 dilution) was used as the vehicle control. Each CYP induction medium was replaced by freshly prepared medium every day. After 3 days, CYP activity was measured by LC-MS/MS.

CYP activity assay using a cocktail of substrates

Cells were cultured in phenol red-free William's E medium supplemented with a cocktail of substrates (1/100 dilution) at 37°C for 1 hr. This cocktail contained 40 μM phenacetin as a CYP1A2 substrate, 50 μM bupropion as a CYP2B6 substrate, 0.1 μM amodiaquin as a CYP2C8 substrate, 5 μM diclofenac as a CYP2C9 substrate, 100 μM *S*-mephenytoin as a CYP2C19 substrate, 5 μM bufuralol as a CYP2D6 substrate, 5 μM midazolam as a CYP3A substrate, and 100 μM 7-hydroxycoumarin as a UGT and SULT substrate. Thereafter, the culture supernatant was harvested and metabolites were quantified by LC-MS/MS as described previously [40] with minor modifications.

Measurement of CYP protein expression

CYP protein levels were measured as described previously [41] with minor modifications. After trypsin digestion of cells, the target peptide of each CYP isoform was absolutely quantified by LC-MS/MS. The expression levels of each CYP were quantified using previously described peptide standards [41].

Measurement of cellular DNA

The cellular DNA content was measured to estimate the number of cells for CYP induction experiments. Following removal of Matrigel via aspiration, cells were washed once with phosphate-buffered saline (PBS) and any remaining Matrigel was removed by treating cells with Cell Recovery Solution (Corning) at 4°C for approximately 30 min. Thereafter, cells were washed once with PBS, and the cellular DNA content was determined using a DNA Quantity Kit (Cosmobio, Tokyo, Japan). To estimate the cell number from the DNA content, the correlation between these two parameters was determined using a dilution series of hCLiPs derived from each lot.

qRT-PCR

Total RNA was isolated using an miRNeasy Mini Kit (QIAGEN, Venlo, The Netherlands). Reverse transcription was performed using a High-Capacity cDNA Reverse Transcription Kit (Life Technologies) according to the manufacturer's guidelines. cDNA was used for PCR with Platinum SYBR Green qPCR SuperMix UDG (Lifetechnologies). Expression levels of target genes were normalized against that of *ACTB* as an endogenous control. The primers used for qRT-PCR are listed in the following table.

Primers for qRT-PCR

Gene	Forward	Reverse
ACTB	ACTCTTCCAGCCTTCCTTCC	AGCACTGTGTTGGCGTACAG
ALB	GCAAGGCTGACGATAAGGAG	CCTAAGGCAGCTTGACTTGC
TAT	ATCTCTGTTATGGGGCGTTG	ACTAACCGCTCCGTGAACTC
TTR	ATCTCCCCATTCCATGAGC	CATTCCTTGGGATTGGTGAC
TDO2	GGTGGTTCCTCAGGCTATCA	TGTCGGGGAATCAGGTATGT
G6PC	CCTTGCTGCTCATTTTCCTC	TGTGGATGTGGCTGAAAGTT
CYP1A2	CCCCAAGAAATGCTGTGTCT	AGGGCTTGTTAATGGCAGTG
CYP2B6	GGGGCACTGAAAAAGACTGA	AGTTCTGGAGGATGGTGGTG
CYP3A4	ATTGGCATGAGGTTTGCTCT	CGGGTTTTTCTGGTTGAAGA

Immunocytochemistry (ICC)

The antibodies used for ICC are listed in the table below. Cells were fixed in chilled methanol

(-30°C) on ice for 5 min. In some experiments, cells were fixed in 4% paraformaldehyde (PFA) (Wako, Osaka, Japan) at room temperature for 15 min and permeabilized by treatment with PBS containing 0.05% Triton X-100 for 15 min. Thereafter, cells were washed three times with PBS, incubated in Blocking One solution (Nacalai Tesque, Kyoto, Japan) at 4°C for 30 min, and labeled with primary antibodies at room temperature for 1 hr or at 4°C overnight. The primary antibodies were detected using Alexa Fluor 488- or Alexa Fluor 594-conjugated secondary antibodies (Life Technologies). Nuclei were counterstained with Hoechst 33342 (Dojindo).

Antibodies for ICC

Antibody	Host animal	Catalog #	Dilution	Manufacturer	Fixation
CYP3A4	Rabbit	Ab3572	1:200	Abcam	Methanol
MRP2	Mouse	Ab3373	1:200	Abcam	Methanol
HNF4A	Rabbit	sc-8987	1:200	Santa Cruz	4% PFA
MDR1	Rabbit	sc-53241	1:200	Santa Cruz	Methanol
CYP2C	Mouse	sc-53245	1:200	Santa Cruz	Methanol
CYP1A2	Mouse	sc-53241	1:200	Santa Cruz	Methanol
TTR	Rabbit	Ab75815	1:500	Abcam	Methanol

IHC

The antibodies used for IHC are listed in the table below. Formalin-fixed paraffin-embedded (FFPE) tissue samples were prepared. Following dewaxing and rehydration, heat-induced epitope retrieval was performed by boiling specimens in ImmunoSaver (Nissin EM, Tokyo, Japan) diluted 1/200 at 98°C for 45 min. Endogenous peroxidase was inactivated by treating specimens with methanol containing 0.3% H_2O_2 at room temperature for 30 min. Thereafter, specimens were permeabilized with 0.1% Triton X-100, treated with Blocking One solution at 4°C for 30 min, and incubated with primary antibodies at room temperature for 1 hr or at 4°C overnight. Sections were stained using ImmPRESS IgG-peroxidase kits (Vector Labs, Burlingame, CA) and a metal-enhanced DAB substrate kit (Life Technologies), according to the manufacturers' instructions. Finally, specimens were counterstained with hematoxylin, dehydrated, and mounted.

FFPE tissue samples were used for fluorescence IHC unless otherwise stated. Following dewaxing and rehydration, heat-induced epitope retrieval was performed by boiling

specimens in ImmunoSaver (Nissin EM) diluted 1/200 at 98°C for 45 min and then the following staining steps were performed. Fresh frozen tissue blocks prepared using Tissue-Tek® O.C.T. Compound (Sakura Finetek, Tokyo, Japan) were used for CYP1A2 and CYP3A4 staining. Fresh frozen liver sections prepared using a cryostat (Leica) were fixed in chilled (-30°C) acetone (Wako) for 5 min, washed three times with PBS, permeabilized with 0.1% Triton X-100, and treated with Blocking One solution at 4°C for 30 min. Thereafter, specimens were incubated with primary antibodies at room temperature for 1 hr or at 4°C overnight and then stained with a mixture of an Alexa Fluor 488-conjugated antibody (Invitrogen) (1:500) and an Alexa Fluor 594-conjugated antibody (Invitrogen) (1:500) at room temperature for 1 hr. Stained sections were mounted using Vectashield mounting medium containing DAPI (Vector Laboratories).

Antibodies for IHC

Antibody	Host animal	Catalog #	Dilution	Manufacturer	Tissue type
CYP2C	Mouse	sc-53245	1:200	Santa Cruz	FFPE/frozen
MDR1	Rabbit	sc-53241	1:200	Santa Cruz	FFPE
Human Mitochondria	Mouse	ab92824	1:1000	Abcam	FFPE
Human TTR	Rabbit	ab75815	1:500	Abcam	FFPE
GLUL	Rabbit	ab73593	1:1000	Abcam	FFPE
Human CYP1A2	Rabbit	BML-CR3130-0100	1:200	Enzo	Frozen
Human CYP3A4	Rabbit	BML-CR3340-0100	1:200	Enzo	Frozen

Liver repopulation assay using cDNA-uPA/SCID mice

hCLiPs derived from three lots of cells were used. For lots FCL and JFC, primary cultured cells at D11–14 (P0-hCLiPs), cells passaged once (P1-hCLiPs), and cells passaged twice (P2-hCLiPs) were used. For lot DUX, P0-hCLiPs were used. After harvesting cells using TrypLE Express, 0.2–1 × 10^6 cells/mouse were intrasplenically transplanted into 2–4-week-old cDNA-uPA/SCID mice (PhoenixBio Co., Ltd, Higashihiroshima, Japan) under isoflurane anesthesia. From 2 weeks after transplantation, 10 μl blood was retro-orbitally collected each

week and the hALB concentration was measured using a Human Albumin ELISA Quantitation Kit (Bethyl, TX) or a Latex agglutination turbidimetric immunoassay with a BioMajesty analyzer (JCA-BM6050; JEOL, Tokyo, Japan). Livers were extracted at 10–11 weeks after transplantation and histologically analyzed.

Liver repopulation assay using TK-NOG mice

FCL-P0-hCLiPs were used. Seven-week-old TK-NOG mice were obtained from the Central Institute of Experimental Animals (Kawasaki, Japan). One day after arrival at the National Cancer Center, mice were intraperitoneally injected with 10 mg/ml ganciclovir (Mitsubishi Tanabe Pharma Corporation, Osaka, Japan) at a dose of 10 μl/g body weight to induce thymidine kinase-mediated injury in host mouse hepatocytes. One day after injection, approximately 30 μl blood was obtained from the tail. Serum was separated and diluted 1/5 with PBS, and the serum ALT level was measured using a DRI-CHEM 3500 analyzer (Fujifilm, Tokyo, Japan). Mice with serum ALT levels of 500–1600 U/l were chosen as host animals for transplantation. At 1–3 days after ALT measurement, 0.4–1 × 10^6 cells were intrasplenically transplanted into these mice under isoflurane anesthesia. From 2 weeks after transplantation, approximately 20 μl blood was collected each week from the tail and the hALB concentration was measured using a Human Albumin ELISA Quantitation Kit (Bethyl, Montgomery, TX). Livers were extracted at 8–10 weeks after transplantation and histologically analyzed.

Estimation of RIs

Unless otherwise stated, RIs were estimated based on CYP2C positivity using image analysis software and a Keyence BZX-710 microscope. RIs in chimeric mice that were sacrificed to isolate primary hepatocytes were estimated based on magnetic bead separation, as described in the following section.

Isolation of human hepatocytes from chimeric livers of cDNA-uPA/SCID mice

Hepatocytes were isolated from chimeric livers of cDNA-uPA/SCID mice at 10 weeks after transplantation of FCL-P1-hCLiPs, DUX-P0-hCLiPs, and JFC-P0-hCLiPs using a two-step collagenase perfusion method. To remove contaminating mouse hepatocytes, isolated cells were incubated with the 66Z antibody, which recognizes the surface of mouse hepatocytes, but not of human hepatocytes [42]. Cells were washed with DMEM containing 10% FBS and

then incubated with Dynabeads M450-conjugated sheep anti-rat IgG (Dynal Biotech, Milwaukee, WI) for 30 min on ice. The tube was placed in a Dynal MPC-1 holder (Dynal Biotech) for 1–2 min to remove $66Z^+$ mouse hepatocytes. Human hepatocytes were collected as $66Z^-$ cells. $66Z^+$ and $66Z^-$ hepatocytes were counted using a hemocytometer before and after magnetic separation to estimate the repopulation efficiency and purity of human hepatocytes after separation, respectively.

Culture of chimeric liver-derived human hepatocytes

Magnetically purified human hepatocytes were resuspended in SHM containing 2% FBS and seeded into a 24-well collagen I-coated plate. One day later, RNA was prepared from cells in some wells for microarray-based transcriptomic analysis. As a control, RNA was also prepared from hepatocytes isolated from the chimeric liver of a mouse transplanted with IPHHs (lot JFC) immediately after thawing the original cell suspension (kindly prepared by PhoenixBio Co., Ltd). Other hCLiP-derived hepatocytes were used for the CYP activity assay, as described above.

Statistics

Data represent the mean ± SEM of independently repeated experiments or the mean ± SD of technical replicates in separate culture wells. Two groups were statistically compared using the Student's t-test, unless otherwise stated. Time-dependent alteration of gene expression was analyzed by the linear mixed models using IBM SPSS Statistics 23 (SPSS Inc., Chicago, IL, USA). Group allocation (FBS or FAC), time (culture period [day]), and the interaction of group and time were included in the model as fixed effects. A p-value less than 0.05 was considered statistically significant.

Acknowledgments

We thank Ms. Ayako Inoue for technical help; Dr. Chise Tateno and her colleagues (PhoenixBio Co., Ltd) for assistance with the transplantation experiments, kindly providing chimeric liver samples repopulated with IPHHs (lot JFC), and valuable advice; Drs. Taiji Yamazoe and Allyson J. Merrell for critically reading the manuscript; and Drs. Luc Gailhouste and Yusuke Yamamoto for valuable advice. This research was supported in part by Grants-in-Aid from the Research Program on Hepatitis from Japan Agency for Medical

Research and Development (AMED: 16fk0310512h0005 and 17fk0310101h0001, to T.O.), a grant from InterStem Co., Ltd (to T.O.), a Grant-in-Aid for Young Scientists B (16K16643, to T.K.).

Conflict of interests

T.O. received a research grant from InterStem Co., Ltd.

REFERENCES

1. Fisher R a, Strom SC. Human hepatocyte transplantation: worldwide results. *Transplantation*. 2006;82(4):441-449. doi:10.1097/01.tp.0000231689.44266.ac
2. Carpentier A, Tesfaye A, Chu V, et al. Engrafted human stem cell-derived hepatocytes establish an infectious HCV murine model. *J Clin Invest*. 2014;124(11):4953-4964. doi:10.1172/JCI75456
3. Woo DH, Kim SK, Lim HJ, et al. Direct and indirect contribution of human embryonic stem cellderived hepatocyte-like cells to liver repair in mice. *Gastroenterology*. 2012;142(3):602-611. doi:10.1053/j.gastro.2011.11.030
4. Liu H, Kim Y, Sharkis S, Marchionni L, Jang Y-Y. In Vivo Liver Regeneration Potential of Human Induced Pluripotent Stem Cells from Diverse Origins. *Sci Transl Med*. 2011;3(82):82ra39-82ra39. doi:10.1126/scitranslmed.3002376
5. Takebe T, Sekine K, Enomura M, et al. Vascularized and functional human liver from an iPSC-derived organ bud transplant. *Nature*. 2013;499(7459):481-484. doi:10.1038/nature12271
6. Zhu S, Rezvani M, Harbell J, et al. Mouse liver repopulation with hepatocytes generated from human fibroblasts. *Nature*. 2014;508(7494):93-97. doi:10.1038/nature13020
7. Huang P, Zhang L, Gao Y, et al. Direct reprogramming of human fibroblasts to functional and expandable hepatocytes. *Cell Stem Cell*. 2014;14(3):370-384. doi:10.1016/j.stem.2014.01.003
8. Du Y, Wang J, Jia J, et al. Human hepatocytes with drug metabolic function induced from fibroblasts by lineage reprogramming. *Cell Stem Cell*. 2014;14(3):394-403. doi:10.1016/j.stem.2014.01.008
9. Huch M, Gehart H, Boxtel R Van, et al. Article Long-Term Culture of Genome-Stable Bipotent Stem Cells from Adult Human Liver. *Cell*. December 2015:1-14.

doi:10.1016/j.cell.2014.11.050

10. Rezvani M, Grimm AA, Willenbring H. Assessing the therapeutic potential of lab-made hepatocytes. *Hepatology*. 2016;64(1):287-294. doi:10.1002/hep.28569
11. Hino H, Tateno C, Sato H, et al. A Long-Term Culture of Human Hepatocytes Which Show a High Growth Potential and Express Their Differentiated Phenotypes. *Biochem Biophys Res Commun*. 1999;256(1):184-191. doi:10.1006/bbrc.1999.0288
12. Shan J, Schwartz RE, Ross NT, et al. Identification of small molecules for human hepatocyte expansion and iPS differentiation. *Nat Chem Biol*. 2013;9(8):514-520. doi:10.1038/nchembio.1270
13. Utoh R, Tateno C, Yamasaki C, et al. Susceptibility of chimeric mice with livers repopulated by serially subcultured human hepatocytes to hepatitis B virus. *Hepatology*. 2008;47(2):435-446. doi:10.1002/hep.22057
14. Walldorf J, Aurich H, Cai H, et al. Expanding hepatocytes in vitro before cell transplantation: Donor age-dependent proliferative capacity of cultured human hepatocytes. *Scand J Gastroenterol*. 2004;39(6):584-593. doi:10.1080/00365520410005586
15. Yamasaki C, Tateno C, Aratani A, et al. Growth and differentiation of colony-forming human hepatocytes in vitro. *J Hepatol*. 2006;44(4):749-757. doi:10.1016/j.jhep.2005.10.028
16. Katsuda T, Kawamata M, Hagiwara K, et al. Conversion of Terminally Committed Hepatocytes to Culturable Bipotent Progenitor Cells with Regenerative Capacity. *Cell Stem Cell*. 2017;20(1):41-55. doi:10.1016/j.stem.2016.10.007
17. Mitaka T, Sato F, Mizuguchi T, Yokono T, Mochizuki Y. Reconstruction of hepatic organoid by rat small hepatocytes and hepatic nonparenchymal cells. *Hepatology*. 1999;29(1):111-125. doi:10.1002/hep.510290103
18. Maes M, Decrock E, Cogliati B, et al. Connexin and pannexin (hemi)channels in the liver. *Front Physiol*. 2014;4 JAN(January):1-8. doi:10.3389/fphys.2013.00405
19. Godoy P, Hengstler JG, Ilkavets I, et al. Extracellular matrix modulates sensitivity of hepatocytes to fibroblastoid dedifferentiation and transforming growth factor β-induced apoptosis. *Hepatology*. 2009;49(6):2031-2043. doi:10.1002/hep.22880
20. Zeisberg M, Yang C, Martino M, et al. Fibroblasts derive from hepatocytes in liver fibrosis via epithelial to mesenchymal transition. *J Biol Chem*. 2007;282(32):23337-23347. doi:10.1074/jbc.M700194200

21. Kamiya A, Kojima N, Kinoshita T, Sakai Y, Miyaijma A. Maturation of fetal hepatocytes in vitro by extracellular matrices and oncostatin M: induction of tryptophan oxygenase. *Hepatology*. 2002;35(6):1351-1359. doi:10.1053/jhep.2002.33331
22. Martignoni M, Groothuis GMM, de Kanter R. Species differences between mouse, rat, dog, monkey and human CYP-mediated drug metabolism, inhibition and induction. *Expert Opin Drug Metab Toxicol*. 2006;2(6):875-894. doi:10.1517/17425255.2.6.875
23. Ohtsuki S, Schaefer O, Kawakami H, et al. Simultaneous Absolute Protein Quantification of Transporters, Cytochrome P450s and UDP-glucuronosyltransferases as a Novel Approach for the Characterization of Individual Human Liver: Comparison with mRNA Levels and Activities. *Drug Metab Dispos*. 2011;40(1):83-92. doi:10.1124/dmd.111.042259
24. Jorns C, Ellis EC, Nowak G, et al. Hepatocyte transplantation for inherited metabolic diseases of the liver. *J Intern Med*. 2012;272(3):201-223. doi:10.1111/j.1365-2796.2012.02574.x
25. Tateno C, Kawase Y, Tobita Y, et al. Generation of Novel Chimeric Mice with Humanized Livers by Using Hemizygous cDNA-uPA/SCID Mice. *PLoS One*. 2015;10(11):e0142145. doi:10.1371/journal.pone.0142145
26. Hasegawa M, Kawai K, Mitsui T, et al. The reconstituted “humanized liver” in TK-NOG mice is mature and functional. *Biochem Biophys Res Commun*. 2011;405(3):405-410. doi:10.1016/j.bbrc.2011.01.042
27. Fu G-B, Huang W-J, Zeng M, et al. Expansion and differentiation of human hepatocyte-derived liver progenitor-like cells and their use for the study of hepatotropic pathogens. *Cell Res*. 2018;(September). doi:10.1038/s41422-018-0103-x
28. Kim Y, Kang K, Lee SB, et al. Small molecule-mediated reprogramming of human hepatocytes into bipotent progenitor cells. *J Hepatol*. 2018. doi:10.1016/j.jhep.2018.09.007
29. Hu H, Gehart H, Artegiani B, et al. Long-Term Expansion of Functional Mouse and Human Hepatocytes as 3D Organoids. *Cell*. 2018;175(6):1591-1606.e19. doi:10.1016/j.cell.2018.11.013
30. Zhang K, Zhang L, Liu W, et al. In Vitro Expansion of Primary Human Hepatocytes

with Efficient Liver Repopulation Capacity. *Cell Stem Cell*. 2018:1-14. doi:10.1016/j.stem.2018.10.018

31. Baxter M, Withey S, Harrison S, et al. Phenotypic and functional analyses show stem cell-derived hepatocyte-like cells better mimic fetal rather than adult hepatocytes. *J Hepatol*. 2015;62(3):581-589. doi:10.1016/j.jhep.2014.10.016
32. Takayama K, Hagihara Y, Toba Y, Sekiguchi K, Sakurai F, Mizuguchi H. Enrichment of high-functioning human iPS cell-derived hepatocyte-like cells for pharmaceutical research. *Biomaterials*. 2018;161:24-32. doi:10.1016/j.biomaterials.2018.01.019
33. Takayama K, Morisaki Y, Kuno S, et al. Prediction of interindividual differences in hepatic functions and drug sensitivity by using human iPS-derived hepatocytes. *Proc Natl Acad Sci*. 2014;111(47):16772-16777. doi:10.1073/pnas.1413481111
34. Kanninen LK, Harjumäki R, Peltoniemi P, et al. Laminin-511 and laminin-521-based matrices for efficient hepatic specification of human pluripotent stem cells. *Biomaterials*. 2016;103:86-100. doi:10.1016/j.biomaterials.2016.06.054
35. Pettinato G, Ramanathan R, Fisher RA, Mangino MJ, Zhang N, Wen X. Scalable Differentiation of Human iPSCs in a Multicellular Spheroid-based 3D Culture into Hepatocyte-like Cells through Direct Wnt/β-catenin Pathway Inhibition. *Sci Rep*. 2016;6(September):1-17. doi:10.1038/srep32888
36. Inamura M, Kawabata K, Takayama K, et al. Efficient Generation of Hepatoblasts From Human ES Cells and iPS Cells by Transient Overexpression of Homeobox Gene HEX. *Mol Ther*. 2010;450:1-6. doi:10.1038/mt.2010.241
37. Takayama K, Inamura M, Kawabata K, et al. Efficient Generation of Functional Hepatocytes From Human Embryonic Stem Cells and Induced Pluripotent Stem Cells by HNF4α Transduction. *Mol Ther*. 2012;20(1):127-137. doi:10.1038/mt.2011.234
38. Chen Q, Kon J, Ooe H, Sasaki K, Mitaka T. Selective proliferation of rat hepatocyte progenitor cells in serum-free culture. *Nat Protoc*. 2007;2(5):1197-1205. doi:10.1038/nprot.2007.118
39. Katsuda T, Hosaka K, Ochiya T. Generation of Chemically Induced Liver Progenitors (CLiPs) from Rat Adult Hepatocytes. *Bio-Protocol*. 2018;7(2):1-26. doi:10.21769/BioProtoc.2689
40. Kozakai K, Yamada Y, Oshikata M, et al. Reliable High-throughput Method for

Inhibition Assay of 8 Cytochrome P450 Isoforms Using Cocktail of Probe Substrates and Stable Isotope-labeled Internal Standards. *Drug Metab Pharmacokinet*. 2012;27(5):520-529. doi:10.2133/dmpk.DMPK-12-RG-014

41. Kawakami H, Ohtsuki S, Kamiie J, Suzuki T, Abe T, Terasaki T. Simultaneous absolute quantification of 11 cytochrome P450 isoforms in human liver microsomes by liquid chromatography tandem mass spectrometry with In silico target peptide selection. *J Pharm Sci*. 2011;100(1):341-352. doi:10.1002/jps.22255
42. Yamasaki C, Kataoka M, Kato Y, et al. In vitro evaluation of cytochrome P450 and glucuronidation activities in hepatocytes isolated from liver-humanized mice. *Drug Metab Pharmacokinet*. 2010;25(6):539-550. doi:10.2133/dmpk.DMPK-10-RG-047

Figure Legends

Figure 1. AC together with FBS support the expansion of IPHHs.

(A) WST assay assessing the effects of various combinations of Y, A, and C together with 10% FBS on proliferation of 8-month-old IPHHs (lot FCL). Absorbance at 450 nm was determined at D14 and normalized against that at D0. Data are the mean ± SEM of two repeated experiments.

(B) WST assay assessing the effects of AC and FBS on proliferation of IPHHs (lot FCL). Absorbance at 450 nm was determined at D14 and normalized against that at D0. Data are the mean ± SD of three technical replicates.

(C) Phase contrast images showing the morphological changes of IPHHs (lot FCL) upon culture in FAC. Inset images show spontaneous hepatic differentiation in densely packed regions at D14.

(D) Flow cytometric analysis of surface expression of LPC markers. Results of cells from lot FCL are shown as representative data (see also Fig. S1F).

(E) Heatmap showing expression of BEC/LPC marker genes, as assessed by microarray analysis. Each element represents normalized (log2) expression, as indicated by the color scale. Data are from three lots and two repeated experiments. Hierarchical clustering was performed based on Euclidean distance.

(F) Expression levels of genes that were differentially expressed between cells cultured in the presence of FBS and those cultured in FAC are shown as mean ± SEM of three lots per time point (each value is determined as the mean of 2 repeated experiments for each

lot). P-values were calculated by the linear mixed model to account for the covariance structure due to repeated measures at different time points. The meanings of the various colors are described in the figure.

(G) GSEA demonstrating enrichment of hepatic function-related gene sets in cells cultured in FAC in comparison with cells cultured in the presence of FBS at D14. P-values indicate nominal p-values.

(H) GSEA demonstrating enrichment of fibrosis-related and epithelial-to-mesenchymal transition-related gene sets in cells cultured in the presence of FBS in comparison with cells cultured in FAC at D14. P-values indicate nominal p-values.

Figure 2. FAC-cultured proliferative cells differentiate into mature hepatocytes *in vitro*.

(A) Phase contrast images showing the morphological changes of FAC-cultured human proliferative cells (lot FCL) treated with (Hep-i(+)) or without (Hep-i(-)) hepatic maturation-inducing factors (see Fig. S2A). Also see Fig. S2B for lots DUX and JFC.

(B) Phase contrast images of PHHs for reference.

(C) Quantified expression of hepatic function-related genes in hCLiPs derived from the three lots with or without hepatic induction and in PHHs. Data are shown as mean ± SEM of two repeated experiments for each lot of hCLiPs and the results of one experiment for each lot of PHHs.

(D) Hierarchical clustering based on Canberra distance of 990 genes that were differentially expressed (≥ 2-fold change on average for the three lots and $p < 0.05$ by the paired t-test) between Hep-i(-) and Hep-i(+). Data were obtained from two repeated experiments for each lot of hCLiPs and from one experiment for each lot of PHHs.

(E) Biological processes overrepresented in Hep-i(+) cells in comparison with Hep-i(-) cells, as identified using BiNGO, a Cytoscape plug-in. p-value is calculated by the default setting of the plug-in.

(F) GSEA demonstrating enrichment of hepatic function-related gene sets in Hep-i(+) cells in comparison with Hep-i(-) cells (see also Table S5). P-values indicate nominal p-values.

Figure 3. hCLiP-derived hepatocytes exhibit CYP enzymatic activity.

(A) Heatmap showing expression of *CYP* genes that were differentially expressed between Hep-i(-) and Hep-i(+) cells (≥ 1.5-fold change), as assessed by microarray analysis. Fold change was calculated using the mean values of 3 donor-derived CLiPs (experiments

were repeated twice for each donor-derived CLiPs). Hierarchical clustering was performed based on Euclidean distance.

(B) Basal enzymatic activities of major CYPs in Hep-i(-) cells, Hep-i(+) cells, and PHHs, as assessed by LC-MS/MS using a cocktail of substrates. Data were obtained from two repeated experiments for each lot of hCLiPs and from one experiment for each lot of PHHs.

(C) Inducibility of CYP1A2, CYP2B6, and CYP3A activities. Enzymatic activities in inducer-treated cells were compared with those in cells treated with the corresponding vehicle by LC-MS/MS analysis using a cocktail of substrates. Data are the mean ± SEM of two repeated experiments for each lot of hCLiPs and the results of one experiment for each lot of PHHs.

(D) LC-MS/MS analysis of the intracellular protein levels of CYP1A2 and CYP3A4 in Hep-i(-) and Hep-i(+) cells treated with inducers or the corresponding vehicle. Data are from one experiment for each lot of hCLiPs.

(E) Enzymatic activities of the phase II enzymes UGT and SULT, as assessed by LC-MS/MS analysis using a cocktail of substrates. Data are the mean ± SEM of two repeated experiments for each lot of hCLiPs and the results of one experiment for each lot of PHHs.

Figure 4. hCLiPs stably expand *in vitro* and retain their hepatic differentiation ability.

(A) Growth curves of hCLiPs from P0–10 (lots FCL and DUX) or P0–4 or P0–5 (lot JFC). Each curve represents data obtained in independent experiments. Data in each plot indicate the cumulative cell numbers at each time point normalized against that at D0 (set to one cell).

(B) Representative chromosomal images of hCLiPs derived from the three lots, as assessed by Q-band karyotyping.

(C) qRT-PCR analysis of hepatocyte-specific genes at P1, P3, and P5. Data are normalized against *ACTB* expression, and shown as mean ± SEM of two repeated experiments except JFC cells at P5 (n = 1).

(D) Basal enzymatic activities of major CYPs in Hep-i(-) and Hep-i(+) cells at P3 and P5, as well as in PHHs, as assessed by LC-MS/MS using a cocktail of substrates. Data are shown as one experiment or the mean ± SEM of two repeated experiments for each lot of hCLiPs and the results of one experiment for each lot of PHHs. N.d. indicates “not detected”.

(E) Inducibility of CYP1A2, CYP2B6, and CYP3A activities at P3 and P5. Enzymatic

activities in inducer-treated cells were compared with those in cells treated with the corresponding vehicle by LC-MS/MS analysis using a cocktail of substrates. Data are shown as one experiment or the mean ± SEM of two repeated experiments for each lot of hCLiPs and the results of one experiment for each lot of PHHs. N.d. indicates "not detected".

Figure 5. hCLiPs repopulate chronically injured mouse livers and contribute to reconstruction of the normal liver architecture.

(A) hALB levels in blood of cDNA-uPA/SCID mice. Each line indicates the level in an individual mouse. Colors denote the passage number of transplanted hCLiPs.

(B) Representative images of cDNA-uPA/SCID mouse livers highly (left and middle panels) and slightly (right panel) repopulated by hCLiPs. The percentages indicate RIs.

(C) Distribution of RIs in livers of cDNA-uPA/SCID mice at 10–11 weeks after transplantation of hCLiPs, as assessed by IHC of CYP2C (shown in B). Colors denote the passage number of transplanted hCLiPs. RIs were calculated for samples marked by asterisks using hepatocytes isolated from chimeric livers by two-step collagenase perfusion followed by incubation with magnetic beads conjugated with a specific anti-mouse antibody (see **Materials and Methods** for details). Bars indicate the mean ± SEM.

(D) hALB levels in sera of TK-NOG mice. Each line indicates the level in an individual mouse.

(E) Representative IHC of human CYP2C in TK-NOG mouse livers highly (left panel) and intermediately (right panel) repopulated by hCLiPs. The percentages indicate RIs determined based on this IHC.

(F) A dot plot showing the distribution of RIs in livers of cDNA-uPA/SCID mice at 10–11 weeks after transplantation of hCLiPs. Bars indicate the mean ± SEM.

(G) IHC of the hepatic function marker proteins MDR1 (left panels) and TTR (right panels). Sections were counterstained with an anti-human mitochondria antibody (green) and DAPI. Images of sections transplanted with hCLiPs derived from lot FCL are shown as representative data.

(H) IHC of the zone 3-specific protein GLUL. Sections were counterstained with an anti-human mitochondria antibody (green) and DAPI. Images of sections transplanted with hCLiPs derived from lot FCL are shown as representative data.

(I) IHC of the zone 3-specific CYPs CYP1A2 and CYP3A4. Sections were counterstained

with an antibody against human CYP2C, which does not show strong zone specificity. Nuclei were also counterstained with DAPI in merged images. Images of sections transplanted with hCLiPs derived from lot FCL are shown as representative data. PV and CV indicate portal vein and central vein, respectively.

Figure 6. Human cells isolated from chimeric livers of mice transplanted with hCLiPs have mature functions.

(A) Phase contrast images of human cells isolated from chimeric livers of mice transplanted with hCLiPs.

(B) Hierarchical clustering based on Euclidean distance of the entire transcriptome (27,459 probes) comparing hCLiPs prior to transplantation (hCLiP), hCLiP-derived hepatocytes from chimeric livers (transplanted cells were at P1, P0, and P0 for lots FCL, DUX, and JFC, respectively), and PHHs. Data for human hepatocytes isolated from chimeric livers of mice transplanted with PHHs (lot JFC) are shown for reference.

(C) PCA mapping of the samples described in (B).

(D) Gene sets enriched in hCLiP-derived cells from chimeric livers in comparison with PHHs (top panels) and their corresponding heatmaps (bottom panels). Hierarchical clustering was performed based on Euclidean distance.

(E) Basal enzymatic activities of major CYPs in hCLiP-derived cells from chimeric livers and PHHs, as assessed by LC-MS/MS using a cocktail of substrates. Each value is determined by one experiment with two replicate cultures.

(F) Inducibility of CYP1A2, CYP2B6, and CYP3A activities. Enzymatic activities in inducer-treated cells were compared with those in cells treated with the corresponding vehicle by LC-MS/MS analysis using a cocktail of substrates. Each value is determined by one experiment with two replicate cultures.

(G) Activities of the phase II enzymes UGT and SULT, as assessed by LC-MS/MS analysis using a cocktail of substrates. Each value is determined by one experiment with two replicate cultures.

Table 1. Donor information of primary human hepatocytes (PHHs) used in this study

Cell type	IPHH	IPHH	IPHH	IPHH	IPHH	APHH	APHH	APHH	APHH
Lot	FCL	DUX	JFC	MRW	187273	HC7-4	HC5-25	HC1-14	HC3-14
Age	10 mo	8 mo	1 yr	11 mo	2 yr	7 yr	56 yr	55 yr	45 yr
Sex	Female	Male	Male	Male	Male	Male	Male	Male	Male
Race	Hispanic	Caucasian	Caucasian	Caucasian	Caucasian	Caucasian	Caucasian	Caucasian	Caucasian
Cause of death	Anoxia/drowning	Anoxia/cardiovascular	Anoxia/second to blunt injury	Asphyxiation	NA	Anoxia	Cerebrovascular Accident	Anoxia	Cerebrovascular Accident
CMV	-	-	-	+	NA	+	+	-	-
HIV	-	-	-	-	-	-	-	-	-
HBV	-	+	+	-	-	-	-	-	-
HCV	-	-	-	-	-	-	-	-	-
EBV	-	NA	NA	NA	NA	NA	NA	NA	NA
RPR	-	NA	-	-	NA	NA	NA	NA	NA
HTLV	NA	NA	NA	-	NA	NA	NA	-	-

IPH: Infant primary human hepatocyte; APH: adult primary human hepatocyte; CMV: cytomegarovirus; HIV: human immunodeficiency virus; HBV: hepatitis B virus; HCV: hepatitis C virus; EBV: Epstein-Barr virus; RPR: rapid plasma reagin; HTLV: human T-cell leukemia virus

Figure 1

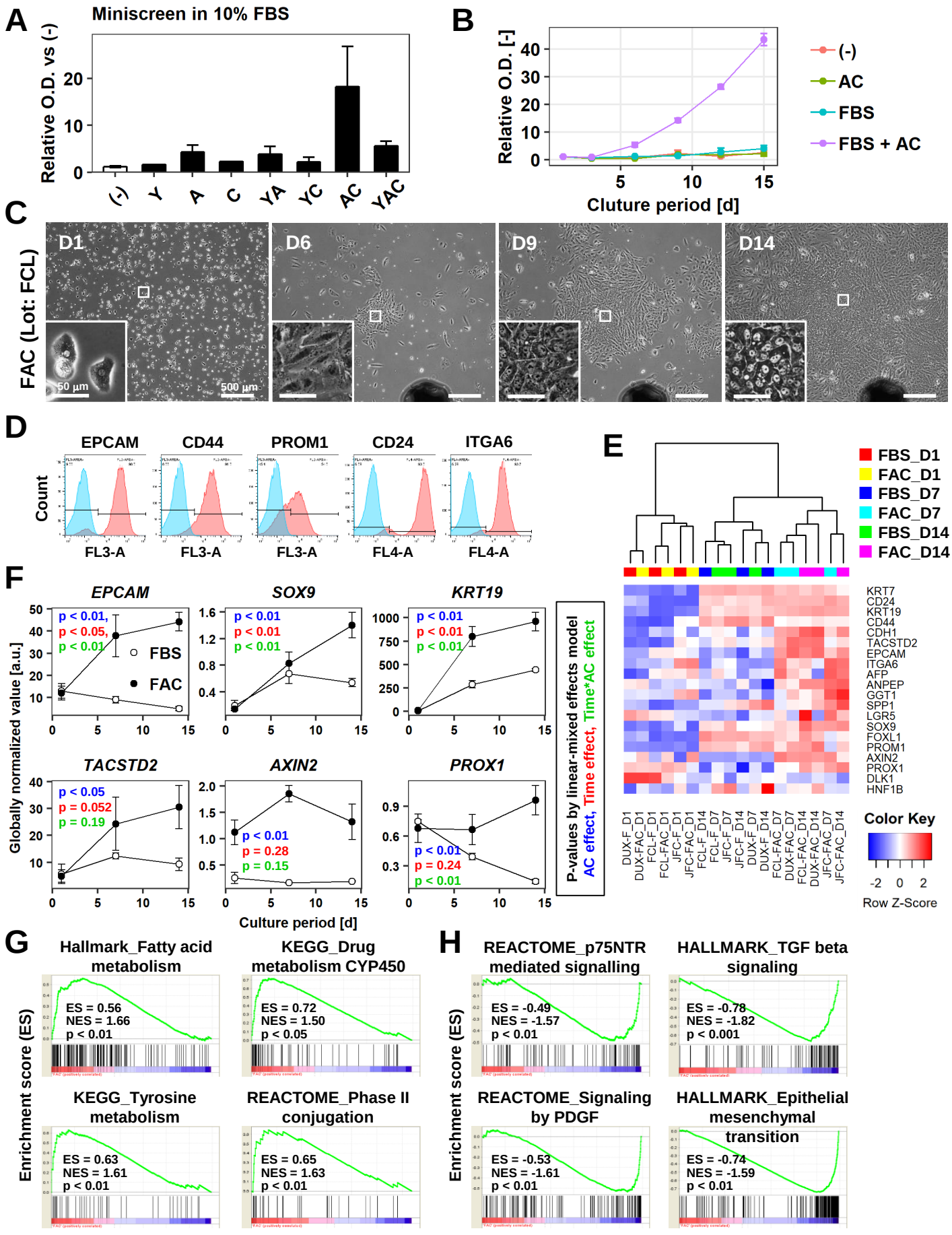
A
Miniscreen in 10% FBS
Relative O.D. vs (-)
(-)
Y
A
C
YA
YC
AC
YAC
B
Relative O.D. [-]
Cluture period [d]
(-)
AC
FBS
FBS + AC
C
FAC (Lot: FCL)
D1
D6
D9
D14
50 μm
500 μm
D
EPCAM
CD44
PROM1
CD24
ITGA6
Count
FL3-A
FL4-A
E
FBS_D1
FAC_D1
FBS_D7
FAC_D7
FBS_D14
FAC_D14
KRT7
CD24
KRT19
CD44
CDH1
TACSTD2
EPCAM
ITGA6
AFP
ANPEP
GGT1
SPP1
LGR5
SOX9
FOXL1
PROM1
AXIN2
PROX1
DLK1
HNF1B
Color Key
Row Z-Score
F
EPCAM
SOX9
KRT19
TACSTD2
AXIN2
PROX1
FBS
FAC
Globally normalized value [a.u.]
Culture period [d]
P-values by linear-mixed effects model
AC effect, Time effect, Time*AC effect
G
Hallmark_Fatty acid metabolism
ES = 0.56
NES = 1.66
p < 0.01
KEGG_Drug metabolism CYP450
ES = 0.72
NES = 1.50
p < 0.05
KEGG_Tyrosine metabolism
ES = 0.63
NES = 1.61
p < 0.01
REACTOME_Phase II conjugation
ES = 0.65
NES = 1.63
p < 0.01
Enrichment score (ES)
H
REACTOME_p75NTR mediated signalling
ES = -0.49
NES = -1.57
p < 0.01
HALLMARK_TGF beta signaling
ES = -0.78
NES = -1.82
p < 0.001
REACTOME_Signaling by PDGF
ES = -0.53
NES = -1.61
p < 0.01
HALLMARK_Epithelial mesenchymal transition
ES = -0.74
NES = -1.59
p < 0.01
Enrichment score (ES)

Figure 2

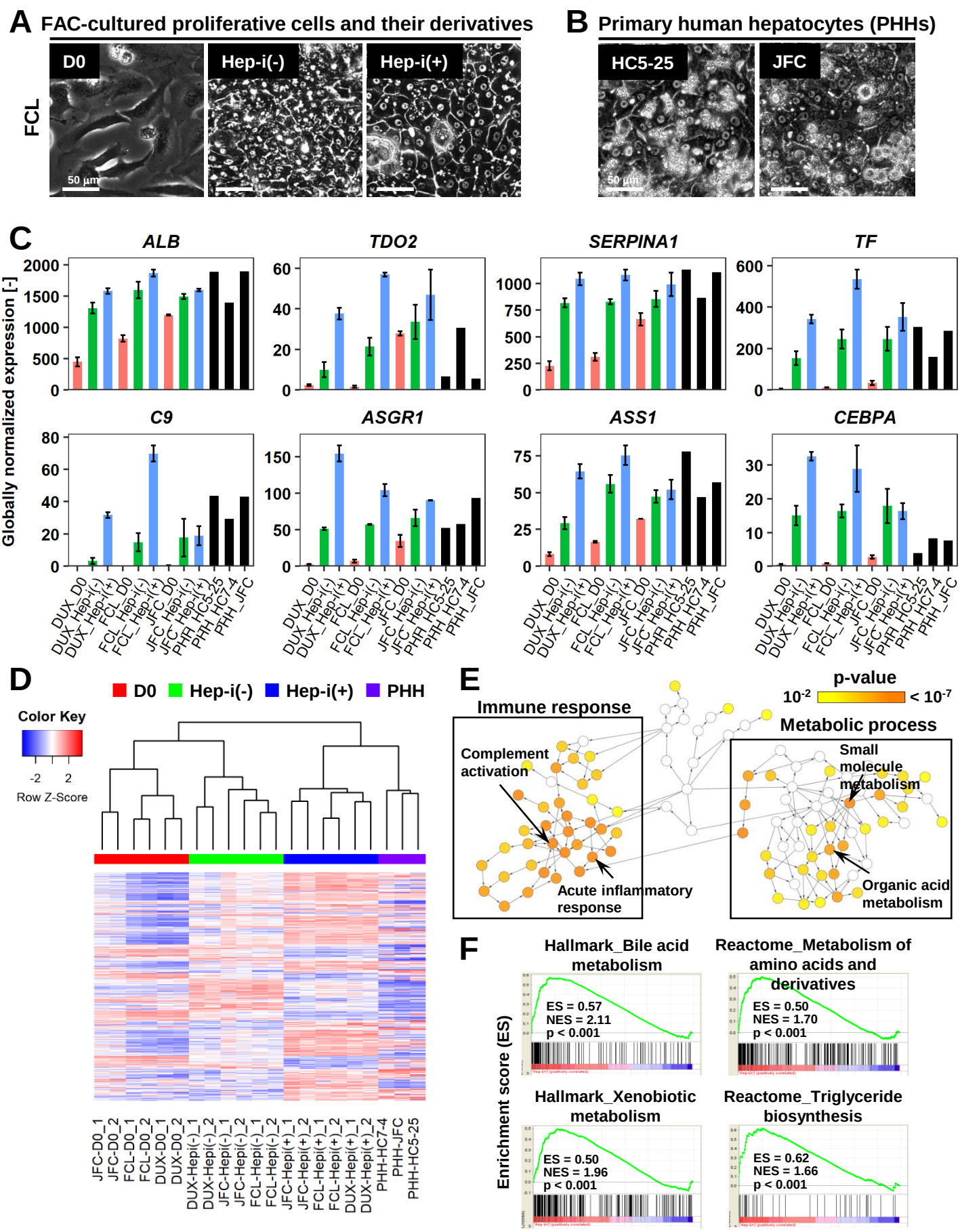
A
FAC-cultured proliferative cells and their derivatives
FCL
D0
Hep-i(-)
Hep-i(+)
50 μm
B
Primary human hepatocytes (PHHs)
HC5-25
JFC
50 μm
C
ALB
TDO2
SERPINA1
TF
C9
ASGR1
ASS1
CEBPA
Globally normalized expression [-]
DUX_D0
DUX_Hep-i(-)
DUX_Hep-i(+)
FCL_D0
FCL_Hep-i(-)
FCL_Hep-i(+)
JFC_D0
JFC_Hep-i(-)
JFC_Hep-i(+)
PHH_HC5-25
PHH_HC7-4
PHH_JFC
D
D0
Hep-i(-)
Hep-i(+)
PHH
Color Key
-2
2
Row Z-Score
JFC-D0_1
JFC-D0_2
FCL-D0_1
FCL-D0_2
DUX-D0_1
DUX-D0_2
DUX-Hepi(-)_1
DUX-Hepi(-)_2
JFC-Hepi(-)_1
JFC-Hepi(-)_2
FCL-Hepi(-)_1
FCL-Hepi(-)_2
JFC-Hepi(+)_1
JFC-Hepi(+)_2
FCL-Hepi(+)_1
FCL-Hepi(+)_2
DUX-Hepi(+)_1
DUX-Hepi(+)_2
PHH-HC7-4
PHH-JFC
PHH-HC5-25
E
p-value
10-2
< 10-7
Immune response
Complement activation
Acute inflammatory response
Metabolic process
Small molecule metabolism
Organic acid metabolism
F
Enrichment score (ES)
Hallmark_Bile acid metabolism
ES = 0.57
NES = 2.11
p < 0.001
Reactome_Metabolism of amino acids and derivatives
ES = 0.50
NES = 1.70
p < 0.001
Hallmark_Xenobiotic metabolism
ES = 0.50
NES = 1.96
p < 0.001
Reactome_Triglyceride biosynthesis
ES = 0.62
NES = 1.66
p < 0.001

Figure 3

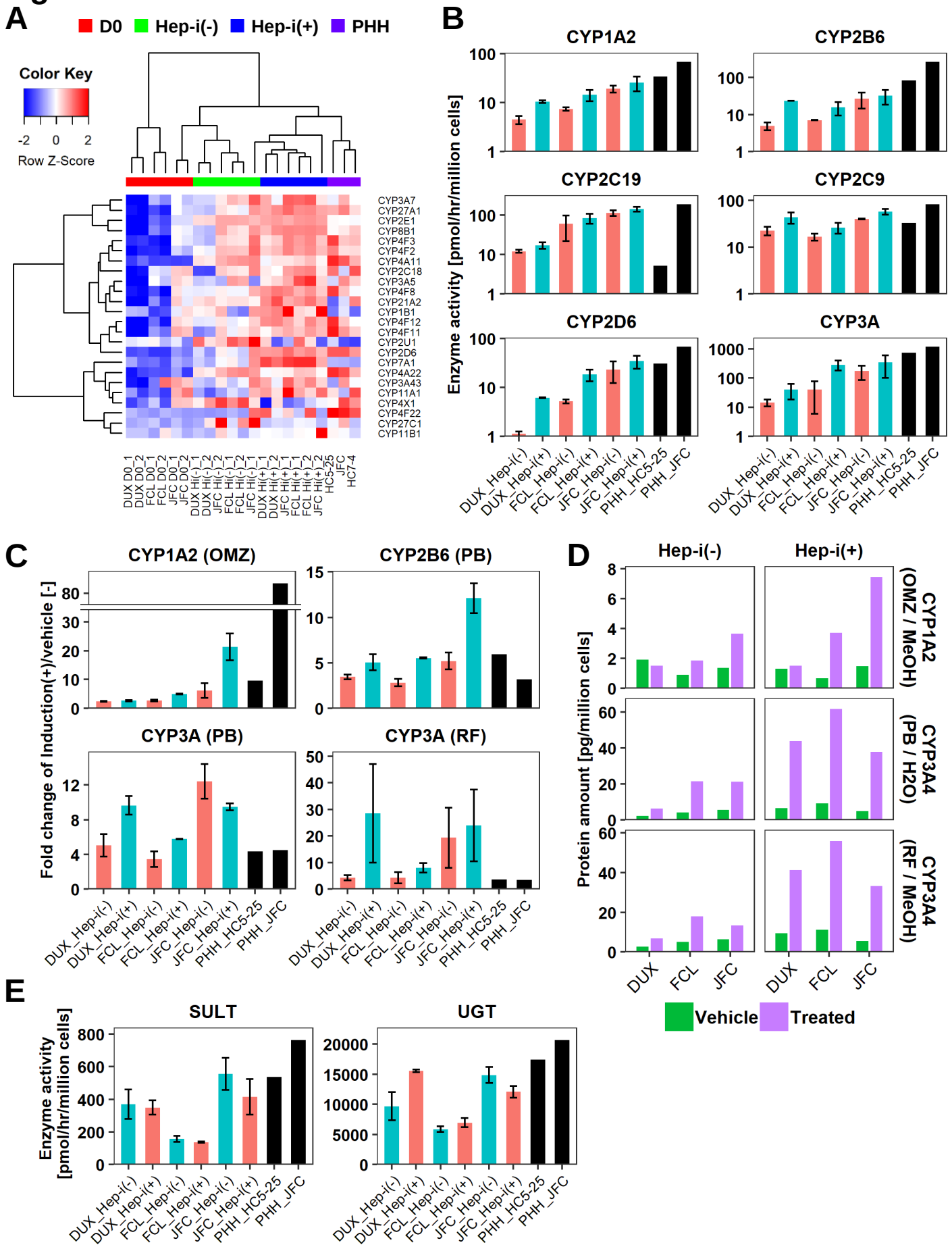
A
D0
Hep-i(-)
Hep-i(+)
PHH
Color Key
-2
0
2
Row Z-Score
CYP3A7
CYP27A1
CYP2E1
CYP8B1
CYP4F3
CYP4F2
CYP4A11
CYP2C18
CYP3A5
CYP4F8
CYP21A2
CYP1B1
CYP4F12
CYP4F11
CYP2U1
CYP2D6
CYP7A1
CYP4A22
CYP3A43
CYP11A1
CYP4X1
CYP4F22
CYP27C1
CYP11B1
DUX D0_1
DUX D0_2
FCL D0_1
FCL D0_2
JFC D0_1
JFC D0_2
DUX Hi(-)_1
DUX Hi(-)_2
JFC Hi(-)_2
FCL Hi(-)_1
FCL Hi(-)_2
JFC Hi(-)_1
DUX Hi(+)_1
DUX Hi(+)_2
JFC Hi(+)_1
FCL Hi(+)_1
FCL Hi(+)_2
JFC Hi(+)_2
HC5-25
JFC
HC7-4
B
CYP1A2
CYP2B6
CYP2C19
CYP2C9
CYP2D6
CYP3A
Enzyme activity [pmol/hr/million cells]
DUX_Hep-i(-)
DUX_Hep-i(+)
FCL_Hep-i(-)
FCL_Hep-i(+)
JFC_Hep-i(-)
JFC_Hep-i(+)
PHH_HC5-25
PHH_JFC
C
CYP1A2 (OMZ)
CYP2B6 (PB)
CYP3A (PB)
CYP3A (RF)
Fold change of Induction(+)/vehicle [-]
D
Hep-i(-)
Hep-i(+)
CYP1A2 (OMZ / MeOH)
CYP3A4 (PB / H2O)
CYP3A4 (RF / MeOH)
Protein amount [pg/million cells]
DUX
FCL
JFC
Vehicle
Treated
E
SULT
UGT
Enzyme activity [pmol/hr/million cells]

Figure 4

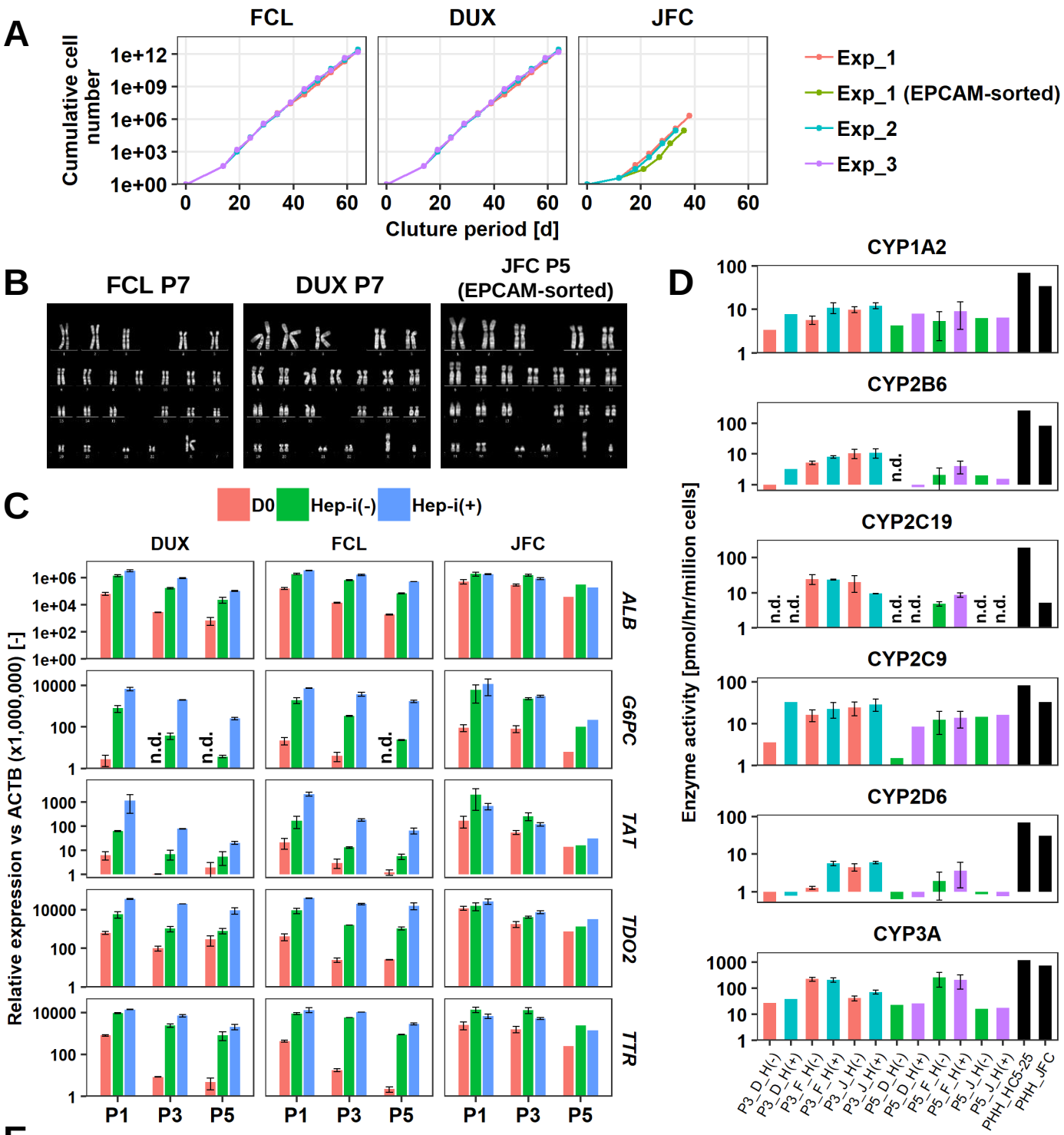
A
FCL
DUX
JFC
Cumulative cell number
1e+12
1e+09
1e+06
1e+03
1e+00
0
20
40
60
Cluture period [d]
Exp_1
Exp_1 (EPCAM-sorted)
Exp_2
Exp_3
B
FCL P7
DUX P7
JFC P5 (EPCAM-sorted)
C
D0
Hep-i(-)
Hep-i(+)
DUX
FCL
JFC
Relative expression vs ACTB (x1,000,000) [-]
ALB
G6PC
TAT
TDO2
TTR
n.d.
P1
P3
P5
D
CYP1A2
CYP2B6
CYP2C19
CYP2C9
CYP2D6
CYP3A
Enzyme activity [pmol/hr/million cells]
P3_D_H(-)
P3_D_H(+)
P3_F_H(-)
P3_F_H(+)
P3_J_H(-)
P3_J_H(+)
P5_D_H(-)
P5_D_H(+)
P5_F_H(-)
P5_F_H(+)
P5_J_H(-)
P5_J_H(+)
PHH_HC5-25
PHH_JFC
E
CYP1A2 (OMZ / MeOH)
CYP2B6 (PB / H2O)
CYP3A (PB / H2O)
CYP3A (RF / MeOH)
Fold induction [-]

Figure 5

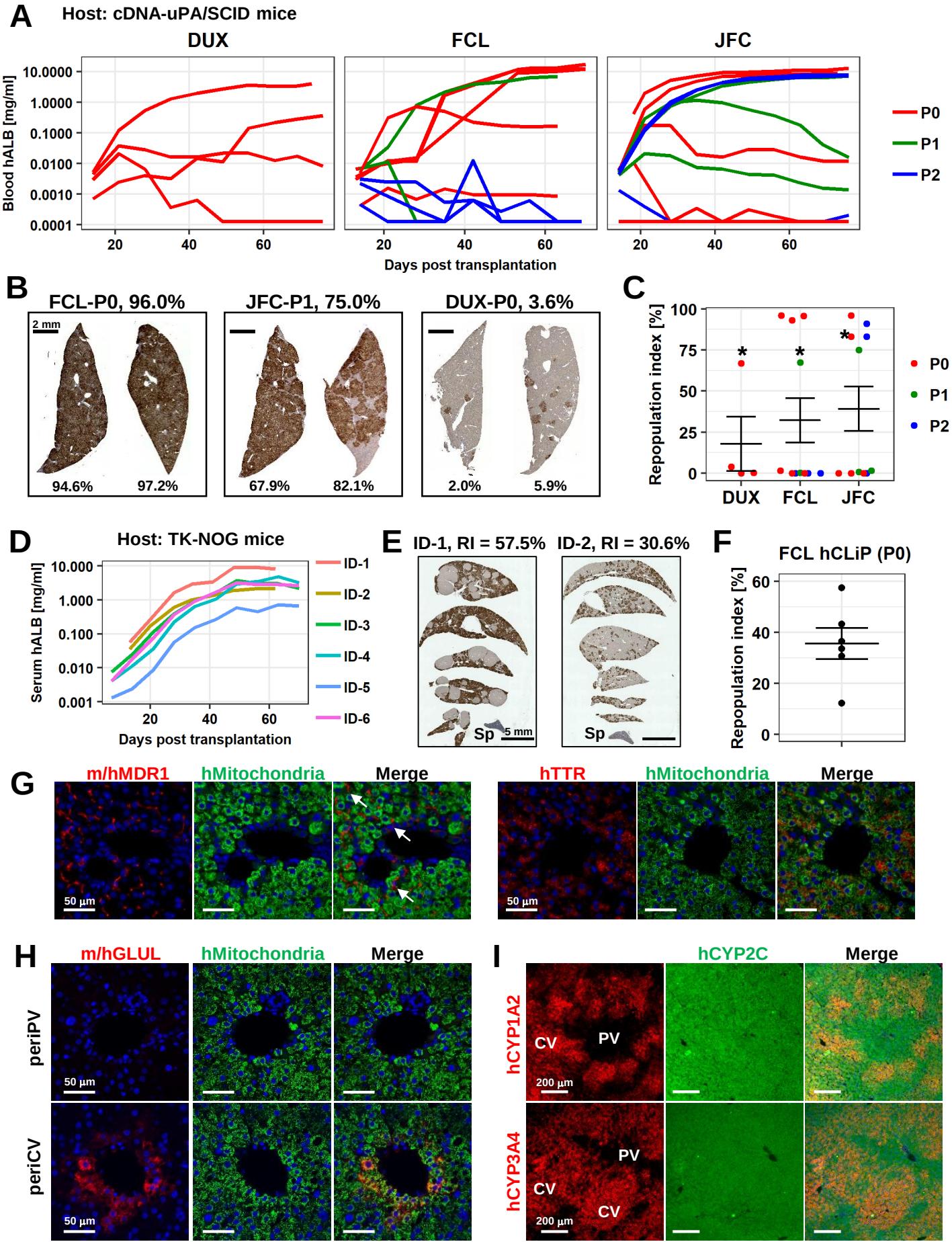
A
Host: cDNA-uPA/SCID mice
DUX
FCL
JFC
Blood hALB [mg/ml]
10.0000
1.0000
0.1000
0.0100
0.0010
0.0001
20
40
60
Days post transplantation
P0
P1
P2
B
FCL-P0, 96.0%
JFC-P1, 75.0%
DUX-P0, 3.6%
2 mm
94.6%
97.2%
67.9%
82.1%
2.0%
5.9%
C
Repopulation index [%]
100
75
50
25
0
DUX
FCL
JFC
P0
P1
P2
D
Host: TK-NOG mice
Serum hALB [mg/ml]
10.000
1.000
0.100
0.010
0.001
20
40
60
Days post transplantation
ID-1
ID-2
ID-3
ID-4
ID-5
ID-6
E
ID-1, RI = 57.5%
ID-2, RI = 30.6%
Sp
5 mm
Sp
F
FCL hCLiP (P0)
Repopulation index [%]
60
40
20
0
G
m/hMDR1
hMitochondria
Merge
50 µm
hTTR
hMitochondria
Merge
50 µm
H
m/hGLUL
hMitochondria
Merge
periPV
50 µm
periCV
50 µm
I
hCYP2C
Merge
hCYP1A2
CV
PV
200 µm
hCYP3A4
PV
CV
CV
200 µm

Figure 6

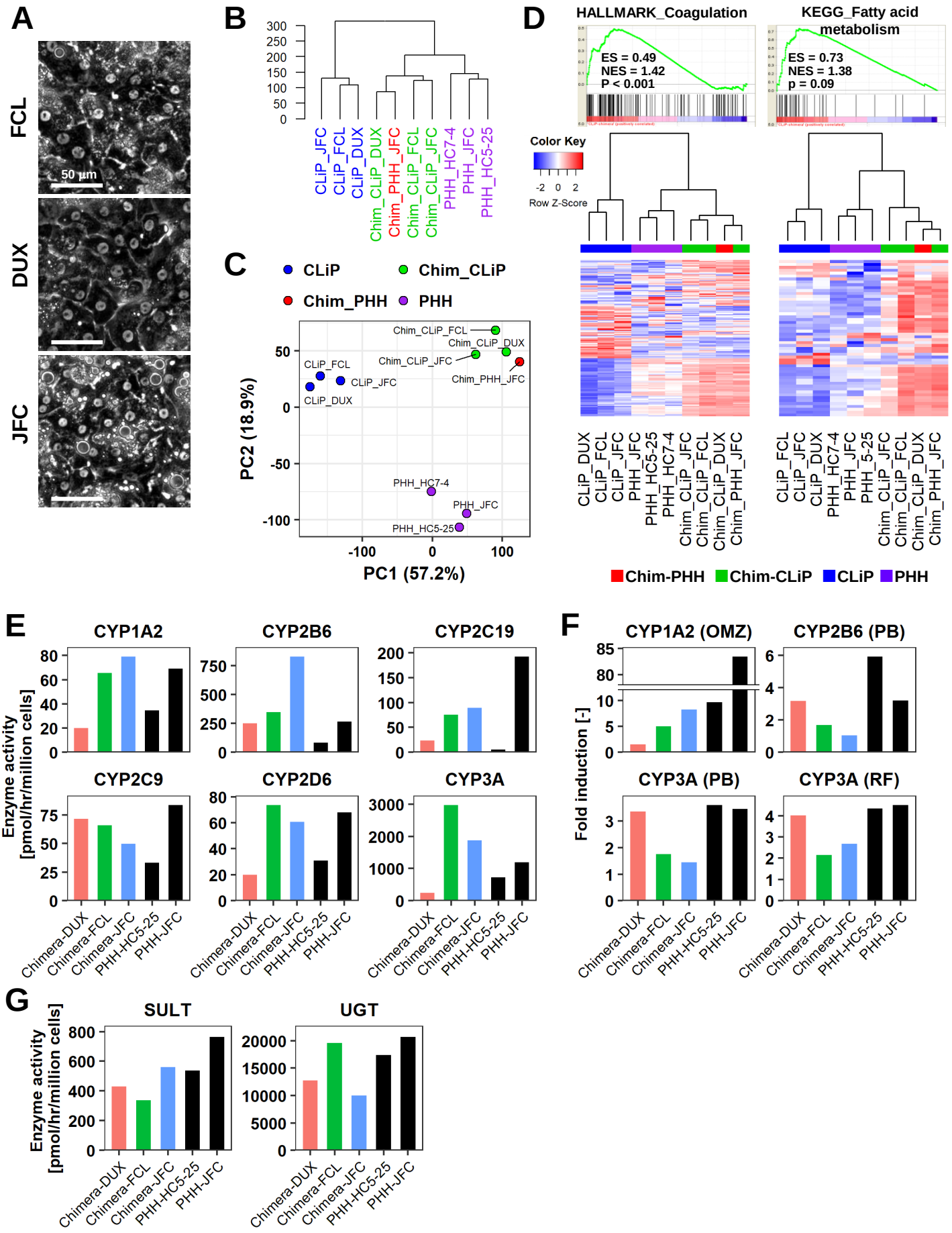
A
FCL
DUX
JFC
50 µm
B
CLiP_JFC
CLiP_FCL
CLiP_DUX
Chim_CLiP_DUX
Chim_PHH_JFC
Chim_CLiP_FCL
Chim_CLiP_JFC
PHH_HC7-4
PHH_JFC
PHH_HC5-25
C
CLiP
Chim_CLiP
Chim_PHH
PHH
PC2 (18.9%)
PC1 (57.2%)
D
HALLMARK_Coagulation
ES = 0.49
NES = 1.42
P < 0.001
KEGG_Fatty acid metabolism
ES = 0.73
NES = 1.38
p = 0.09
Color Key
Row Z-Score
Chim-PHH
Chim-CLiP
CLiP
PHH
E
CYP1A2
CYP2B6
CYP2C19
CYP2C9
CYP2D6
CYP3A
Enzyme activity [pmol/hr/million cells]
Chimera-DUX
Chimera-FCL
Chimera-JFC
PHH-HC5-25
PHH-JFC
F
CYP1A2 (OMZ)
CYP2B6 (PB)
CYP3A (PB)
CYP3A (RF)
Fold induction [-]
G
SULT
UGT
Enzyme activity [pmol/hr/million cells]

Figure 1-figure supplement 1

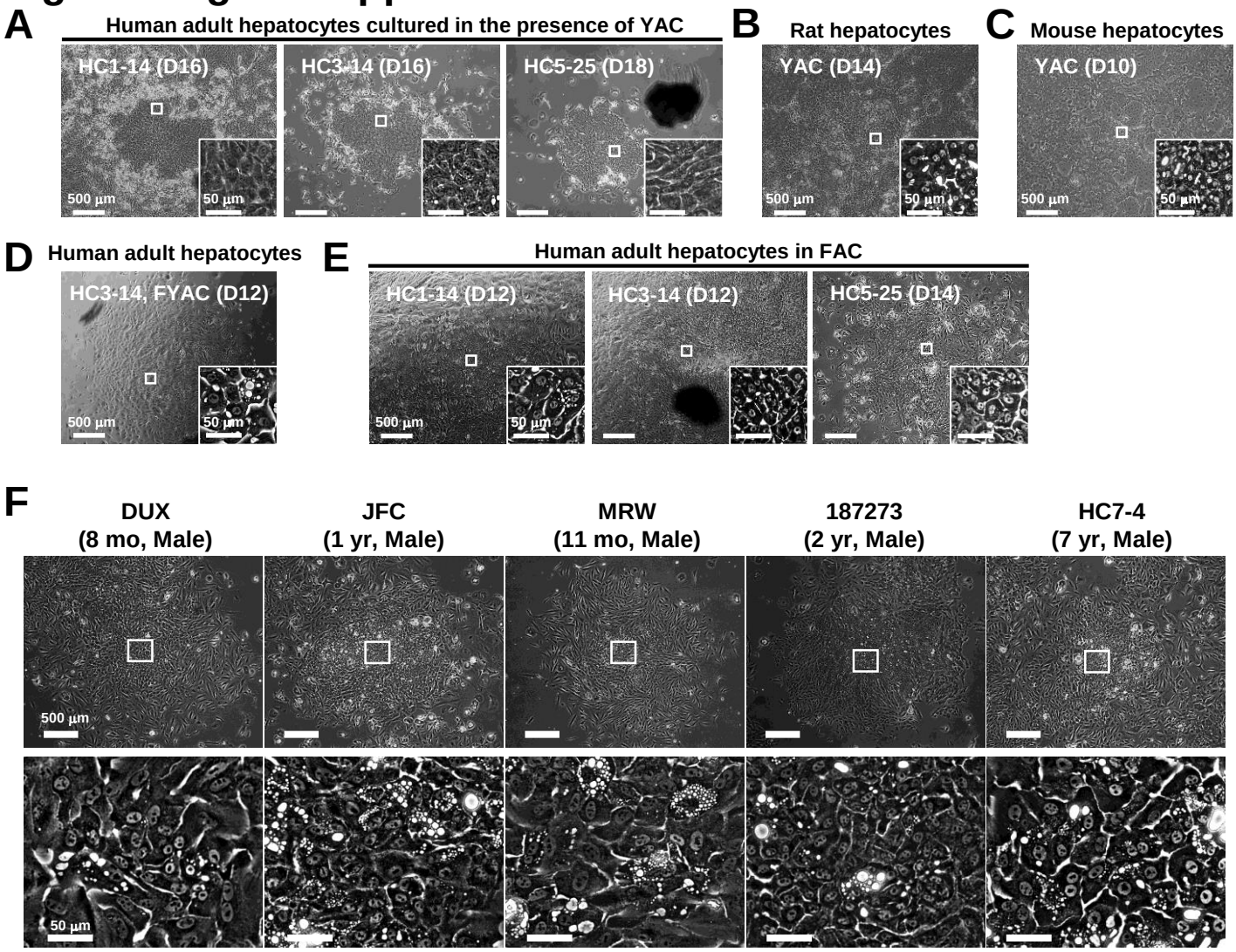

Figure 1-figure supplement 2

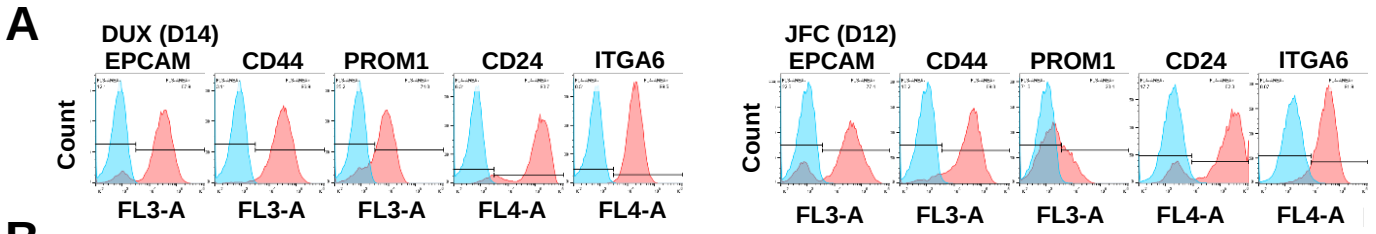

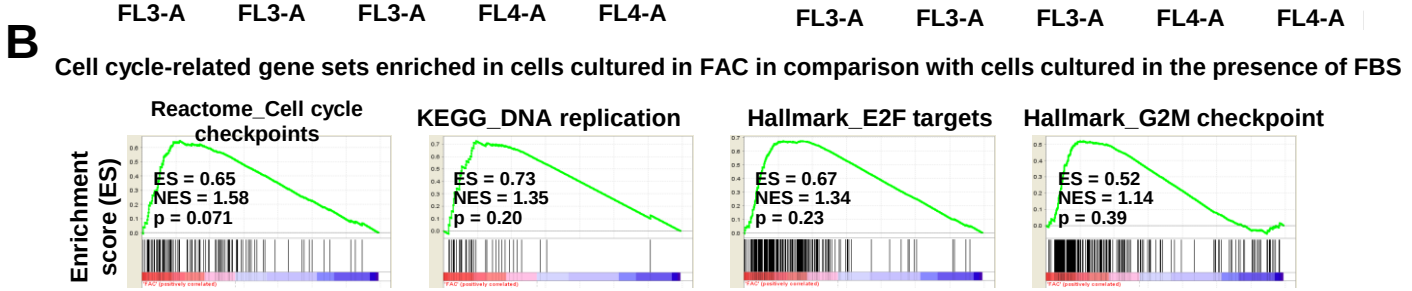

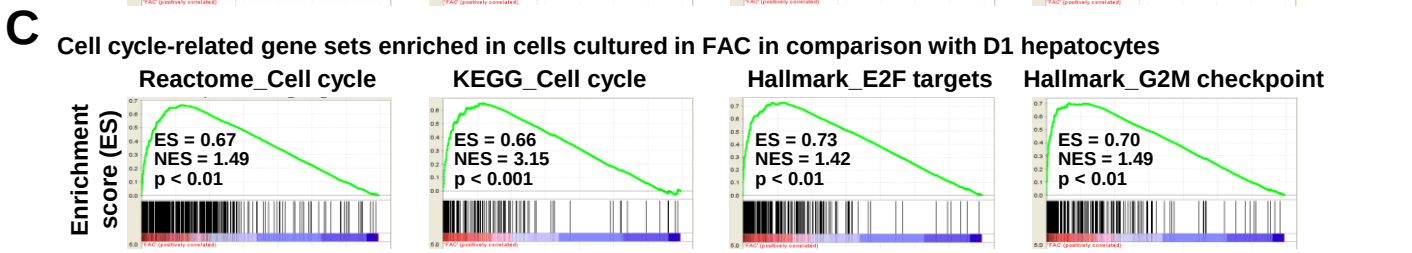

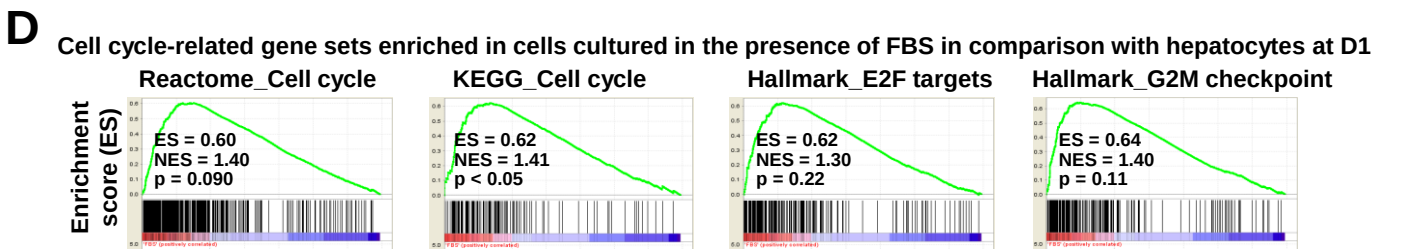

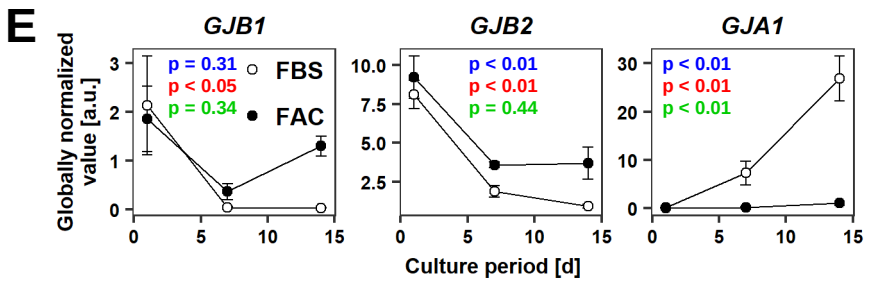

P-values by linear-mixed effects model AC effect, Time effect, Time*AC effect

Figure 2-figure supplement 1

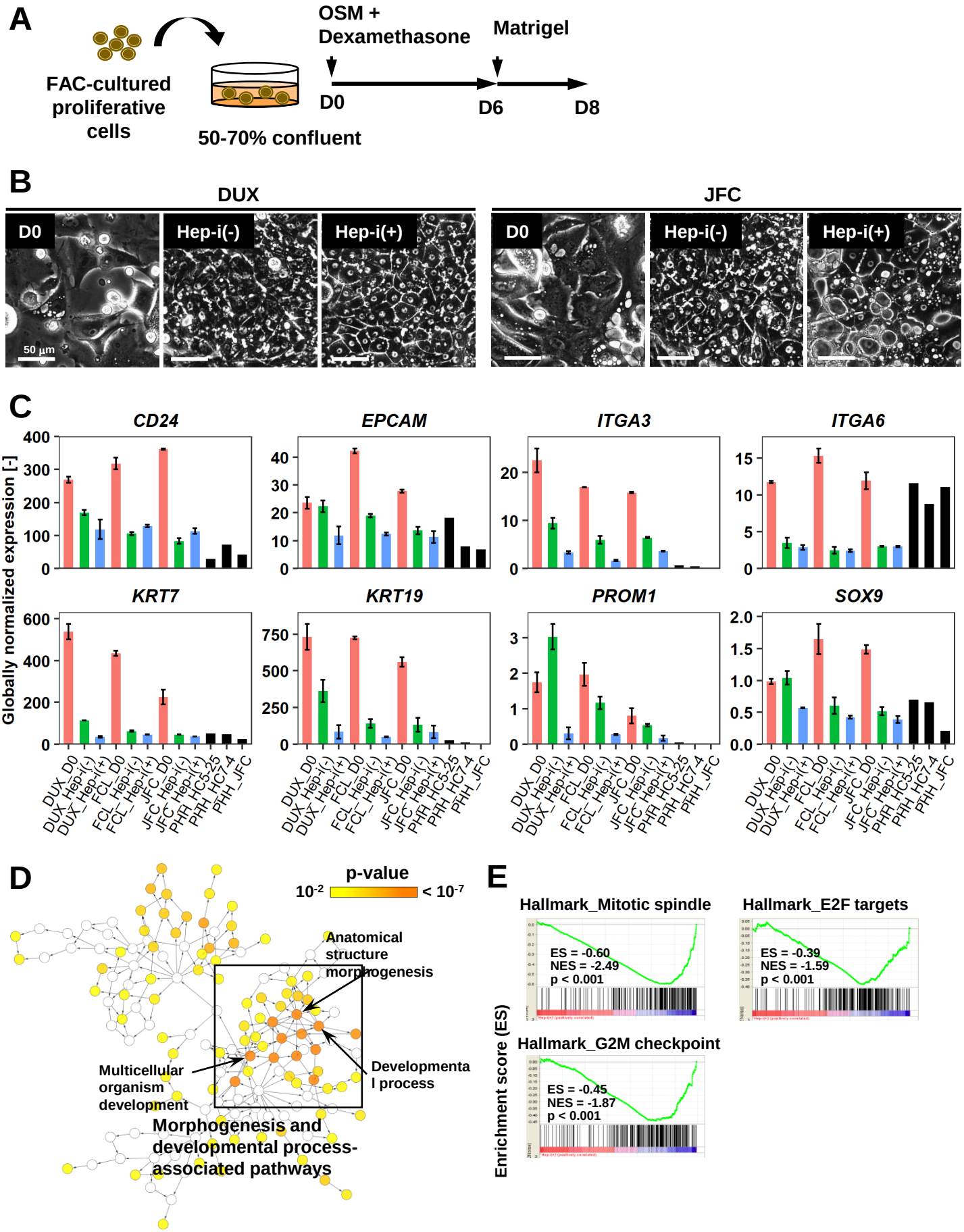

Figure 3-figure supplement 1

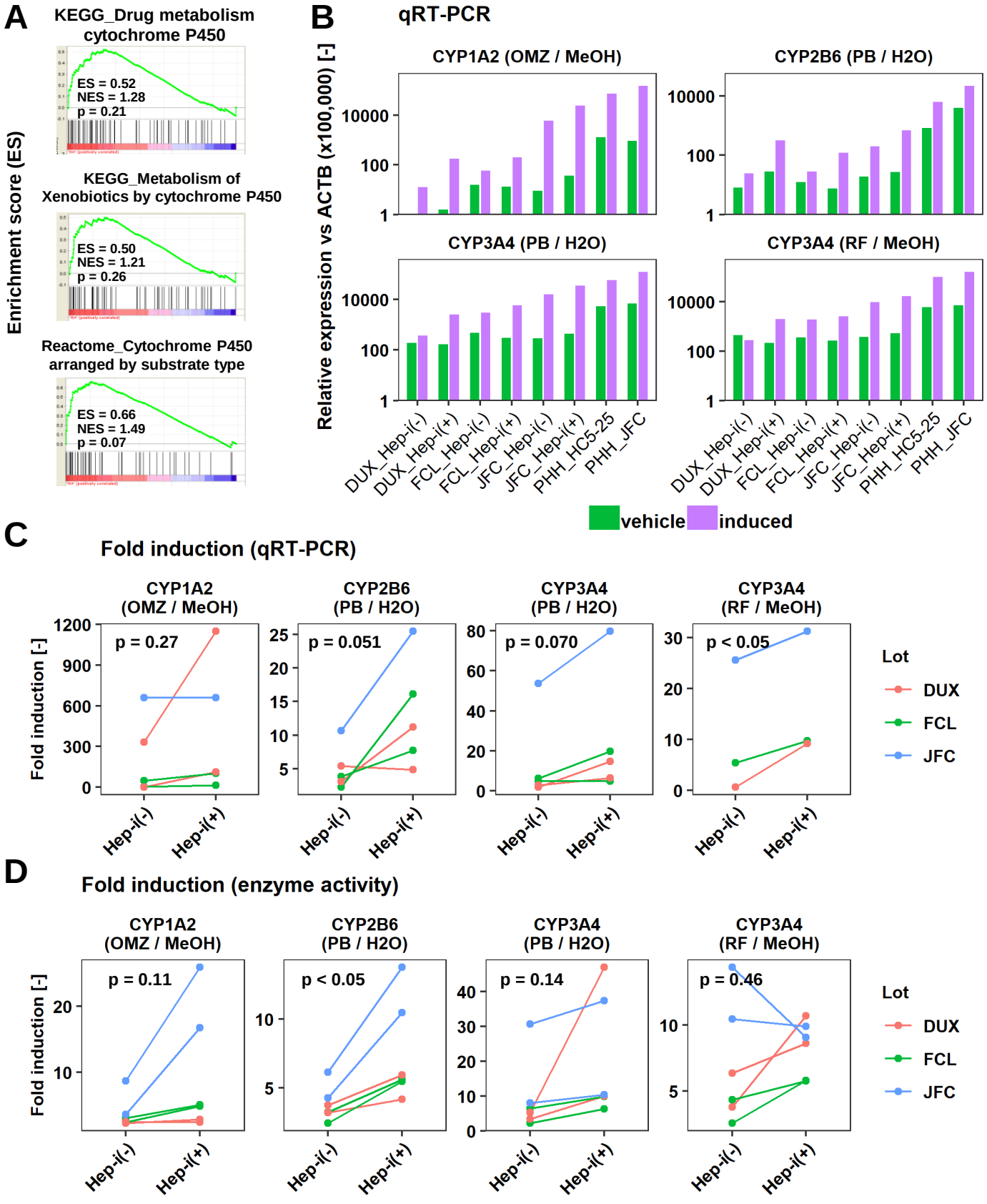

Figure 4-figure supplement 1

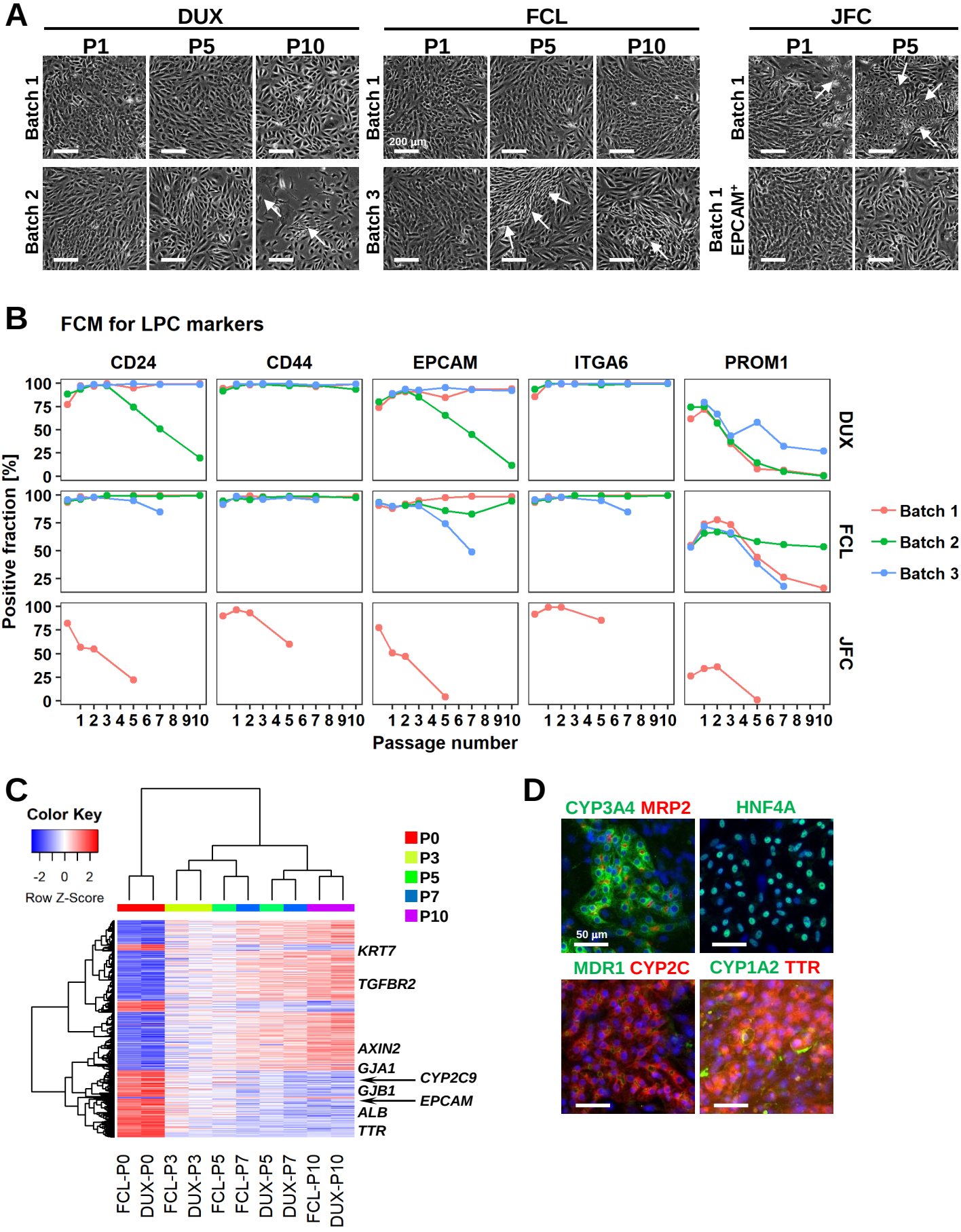

Figure 6-figure supplement 1

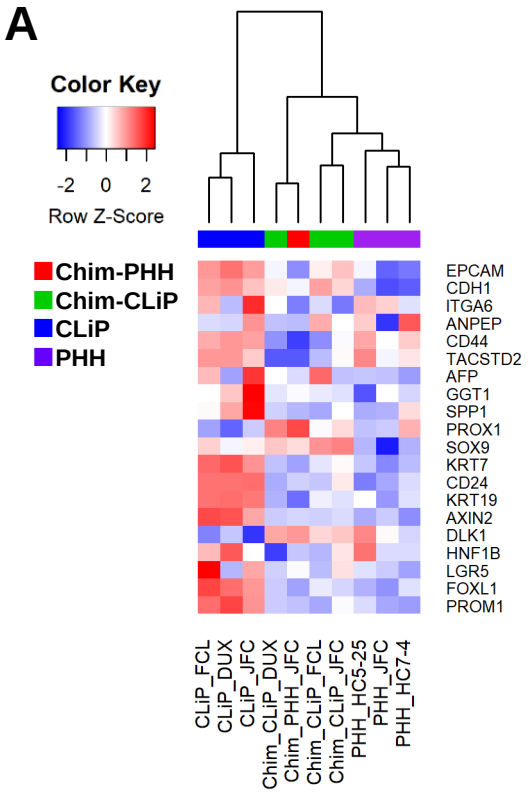

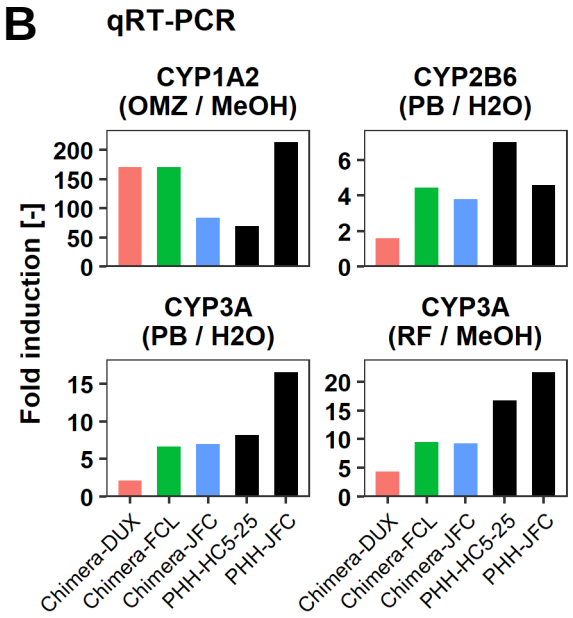

Supplemental material

Generation of human hepatic progenitor cells with regenerative and metabolic capacities from primary hepatocytes

Takeshi Katsuda,[1] Juntaro Matsuzaki,[1] Tomoko Yamaguchi,[1,2] Yasuhiro Yamada,[3] Kazunori Hosaka,[1] Atsuko Takeuchi,[4] Yoshimasa Saito,[2] Takahiro Ochiya[1]*

Supplemental Figure Legends

Figure 1-figure supplement 1. Morphological changes of hepatocytes in response to small molecule stimuli with/without FBS.

(A) Phase contrast images of APHHs cultured in the presence of YAC, which are used to obtain rat and mouse CLiPs. Insets indicate representative magnified images.

(B) Phase contrast images of rat CLiPs obtained by culture in the presence of YAC. The inset shows cells that spontaneously differentiated into mature hepatocyte (MH)-like cells in densely packed regions.

(C) Phase contrast images of mouse CLiPs obtained by culture in the presence of YAC. The inset shows cells that spontaneously differentiated into MH-like cells in densely packed regions.

(D) Phase contrast images of APHHs cultured in the presence of YAC and 10% FBS (FYAC). The inset shows cells that spontaneously differentiated into MH-like cells in densely packed regions.

(E) Phase contrast images of APHHs cultured in FAC. Insets show cells that spontaneously differentiated into MH-like cells in densely packed regions.

(F) Phase contrast images of PHHs obtained from infant donors (4 lots) and a juvenile donor (1 lot). Regions with spontaneous hepatic differentiation are magnified.

Figure 1-figure supplement 2. Characterization of FAC-cultured proliferative human hepatic cells, related to Figure 1.

(A) Flow cytometric analysis of surface expression of LPC markers in cells from lots DUX and JFC.

(B) GSEA demonstrating enrichment of cell cycle-related gene sets in cells cultured in FAC in comparison with cells cultured in the presence of FBS at D14.

(C) GSEA demonstrating enrichment of cell cycle-related gene sets in cells cultured in FAC at D14 in comparison with D1 hepatocytes.

(D) GSEA demonstrating enrichment of cell cycle-related gene sets in cells cultured in the presence of FBS at D14 in comparison with D1 hepatocytes.

(E) Time course of expression of hepatic (*GJB1* and *GJB2*) and NPC (*GJA1*) connexin genes as assessed by microarray analysis. Data are shown as mean ± SEM of three lots per time point (each value is determined as the mean of 2 repeated experiments for each lot). P-values were calculated by the linear mixed model to account for the covariance

structure due to repeated measures at different time points. The meanings of the various colors are described in the figure.

Figure 2-figure supplement 1. Characterization of proliferative human hepatic cells following hepatic maturation.

(A) Schematic of the hepatic maturation protocol.

(B) Phase contrast images showing the morphological changes of hCLiPs derived from lots DUX and JFC upon hepatic maturation.

(C) Quantified expression of BEC/LPC marker genes in hCLiPs derived from the three lots with or without hepatic maturation and in PHHs. Data are the mean ± SEM of two repeated experiments for each lot of hCLiPs and the results of one experiment for each lot of PHHs.

(A) Biological processes overrepresented in Hep-i(-) cells in comparison with Hep-i(+) cells, as identified using BiNGO, a Cytoscape plug-in. p-value is calculated by the default setting of the plug-in.

(D) GSEA demonstrating enrichment of cell cycle-related gene sets in Hep-i(-) cells in comparison with Hep-i(+) cells (see also Table S6).

Figure 3-figure supplement 1. Inducibility of CYP1A2 and CYP3A4 in Hep-i(+) cells.

(A) GSEA demonstrating enrichment of CYP-associated metabolic pathways in Hep-i(+) cells in comparison with Hep-i(-) cells.

(B) qRT-PCR analysis of the inducibility of *CYP1A2*, *CYP2B6*, and *CYP3A* mRNA expression. Gene expression levels were normalized against that of *ACTB*. Data are shown as one representative experiment.

(C) Summary of the inducibility of *CYP* mRNA expression in the individual experiments shown in (B). Data are obtained from one experiment for lot JFC and two repeated experiments for DUX and FCL except CYP3A4 (RF/MeOH) in which all data are obtained from one experiment.

(D) Summary of the inducibility of CYP enzymatic activities in the individual experiments shown in (Figure 3C). Data are obtained from two repeated experiments. P-values are obtained by paired student's t-test.

Figure 4-figure supplement 1. Characterization of hCLiPs upon long-term culture.

(A) Phase contrast images of hCLiPs upon serial passage. Arrows indicate cells with a fibroblast-like morphology.

(B) Surface marker profiling of hCLiPs upon serial passage. Data are from three repeated experiments for cells derived from lots FCL and DUX and from one experiment for cells derived from lot JFC.

(C) Hierarchical clustering based on Euclidean distance of genes that were differentially expressed between hCLiPs at P10 and those at P0. Probes were ranked by the weighted average difference method [1], and the top 5% (2445 probes) were defined as differentially expressed genes.

(D) Immunocytochemistry of hepatic function-related proteins in hCLiPs at P3 after hepatic maturation.

Figure 6-figure supplement 1. Characterization of human cells isolated from chimeric livers of mice transplanted with hCLiPs.

(A) Heatmap showing expression of BEC/LPC marker genes, as assessed by microarray analysis. Each element represents normalized (log2) expression, as indicated by the color scale. Hierarchical clustering was performed based on Euclidean distance.

(B) qRT-PCR analysis of the inducibility of *CYP1A2*, *CYP2B6*, and *CYP3A* mRNA expression. Gene expression levels were normalized against that of *ACTB*. Each value is determined by one experiment with two replicate cultures.

Table S1. All the gene sets enriched in FAC cells compared with FBS cells at D14 of culture (assessed by GSEA)

NAME	Data base	NOM p-val	FDR q-val	FWER p-val
HALLMARK_OXIDATIVE_PHOSPHORYLATION	HALLMARK	0	0.033297755	0.021
HALLMARK_FATTY_ACID_METABOLISM	HALLMARK	0.001968504	0.05551136	0.08
HALLMARK_MYC_TARGETS_V1	HALLMARK	0.03245436	0.101371616	0.176
HALLMARK_PANCREAS_BETA_CELLS	HALLMARK	0.037254903	0.3406712	0.74
HALLMARK_MYC_TARGETS_V2	HALLMARK	0.04684318	0.14761625	0.336
HALLMARK_INTERFERON_ALPHA_RESPONSE	HALLMARK	0.058939096	0.17794499	0.324
HALLMARK_GLYCOLYSIS	HALLMARK	0.06854839	0.27987996	0.828
HALLMARK_INTERFERON_GAMMA_RESPONSE	HALLMARK	0.09919028	0.31133965	0.751
HALLMARK_CHOLESTEROL_HOMEOSTASIS	HALLMARK	0.12252964	0.2770364	0.782
HALLMARK_ESTROGEN_RESPONSE_LATE	HALLMARK	0.13052209	0.27335626	0.868
HALLMARK_PEROXISOME	HALLMARK	0.1392157	0.3680212	0.667
HALLMARK_REACTIVE_OXIGEN_SPECIES_PATHWAY	HALLMARK	0.15031315	0.35984033	0.715
HALLMARK_BILE_ACID_METABOLISM	HALLMARK	0.16338582	0.2828164	0.818
HALLMARK_ADIPOGENESIS	HALLMARK	0.18	0.28598496	0.859
HALLMARK_UV_RESPONSE_UP	HALLMARK	0.2254902	0.34318617	0.965
HALLMARK_E2F_TARGETS	HALLMARK	0.2296748	0.29983094	0.774
HALLMARK_PI3K_AKT_MTOR_SIGNALING	HALLMARK	0.2309237	0.3209314	0.968
HALLMARK_XENOBIOTIC_METABOLISM	HALLMARK	0.25330812	0.29413024	0.889
HALLMARK_DNA_REPAIR	HALLMARK	0.2661448	0.32270163	0.93
HALLMARK_MTORC1_SIGNALING	HALLMARK	0.28033474	0.32892236	0.951
HALLMARK_G2M_CHECKPOINT	HALLMARK	0.39139345	0.33453783	0.968
HALLMARK_IL6_JAK_STAT3_SIGNALING	HALLMARK	0.44624746	0.4894568	0.995
HALLMARK_PROTEIN_SECRETION	HALLMARK	0.53235906	0.56213456	0.996
HALLMARK_SPERMATOGENESIS	HALLMARK	0.54789275	0.568492	0.996
KEGG_MATURITY_ONSET_DIABETES_OF_THE_YOUNG	KEGG	0	0.42114097	0.314
KEGG_GLYCOSPHINGOLIPID_BIOSYNTHESIS_LACTO_AND_NEOLACTO_SERIES	KEGG	0	0.09390438	0.581
KEGG_RIBOSOME	KEGG	0	0.10131376	0.708
KEGG_GLUTATHIONE_METABOLISM	KEGG	0.002	0.16022365	0.386
KEGG_FRUCTOSE_AND_MANNOSE_METABOLISM	KEGG	0.004115226	0.18038498	0.331
KEGG_TYROSINE_METABOLISM	KEGG	0.006097561	0.21838278	0.322
KEGG_PENTOSE_AND_GLUCURONATE_INTERCONVERSIONS	KEGG	0.00610998	0.10780261	0.455
KEGG_ASCORBATE_AND_ALDARATE_METABOLISM	KEGG	0.00814664	0.17743629	0.372
KEGG_PHENYLALANINE_METABOLISM	KEGG	0.010121457	0.28240538	0.317
KEGG_HISTIDINE_METABOLISM	KEGG	0.012	0.14469703	0.396
KEGG_VALINE_LEUCINE_AND_ISOLEUCINE_DEGRADATION	KEGG	0.012121212	0.8295114	0.311
KEGG_PORPHYRIN_AND_CHLOROPHYLL_METABOLISM	KEGG	0.012219959	0.13135943	0.401
KEGG_GLYOXYLATE_AND_DICARBOXYLATE_METABOLISM	KEGG	0.014373717	0.09476113	0.732
KEGG_LYSINE_DEGRADATION	KEGG	0.01778656	0.10249406	0.65
KEGG_RETINOL_METABOLISM	KEGG	0.018442623	0.1021333	0.473
KEGG_BASE_EXCISION_REPAIR	KEGG	0.01984127	0.093926735	0.515
KEGG_PROTEIN_EXPORT	KEGG	0.02008032	0.09562029	0.571

KEGG_PROPANOATE_METABOLISM	KEGG	0.02020202	0.11166452	0.411
KEGG_CITRATE_CYCLE_TCA_CYCLE	KEGG	0.021186441	0.097672336	0.481
KEGG_ALANINE_ASPARTATE_AND_GLUTAMATE_METABOLISM	KEGG	0.024340771	0.118603535	0.402
KEGG_TRYPTOPHAN_METABOLISM	KEGG	0.024640657	0.10244247	0.411
KEGG_METABOLISM_OF_XENOBIOTICS_BY_CYTOCHROME_P450	KEGG	0.026	0.096876964	0.54
KEGG_LINOLEIC_ACID_METABOLISM	KEGG	0.034274194	0.10892883	0.472
KEGG_PEROXISOME	KEGG	0.040983606	0.09460963	0.484
KEGG_DRUG_METABOLISM_CYTOCHROME_P450	KEGG	0.042596348	0.098331206	0.708
KEGG_ONE_CARBON_POOL_BY_FOLATE	KEGG	0.043659043	0.10397924	0.708
KEGG_SELENOAMINO_ACID_METABOLISM	KEGG	0.04517454	0.10162141	0.66
KEGG_NITROGEN_METABOLISM	KEGG	0.046653144	0.09837711	0.715
KEGG_AMINOACYL_TRNA_BIOSYNTHESIS	KEGG	0.046747968	0.10707487	0.701
KEGG_ARGININE_AND_PROLINE_METABOLISM	KEGG	0.04742268	0.103417106	0.701
KEGG_PYRUVATE_METABOLISM	KEGG	0.054166667	0.09788826	0.56
KEGG_PROXIMAL_TUBULE_BICARBONATE_RECLAMATION	KEGG	0.05427975	0.10104043	0.635
KEGG_GLYCINE_SERINE_AND_THREONINE_METABOLISM	KEGG	0.057142857	0.093402795	0.752
KEGG_STARCH_AND_SUCROSE_METABOLISM	KEGG	0.057259712	0.09463301	0.717
KEGG_BUTANOATE_METABOLISM	KEGG	0.06212425	0.10109947	0.619
KEGG_APOPTOSIS	KEGG	0.06517312	0.19443636	0.952
KEGG_BIOSYNTHESIS_OF_UNSATURATED_FATTY_ACIDS	KEGG	0.06567796	0.10622653	0.773
KEGG_PENTOSE_PHOSPHATE_PATHWAY	KEGG	0.06779661	0.096578725	0.715
KEGG_AMINO_SUGAR_AND_NUCLEOTIDE_SUGAR_METABOLISM	KEGG	0.07438017	0.114621975	0.803
KEGG_TERPENOID_BACKBONE_BIOSYNTHESIS	KEGG	0.07444668	0.09565625	0.752
KEGG_ETHER_LIPID_METABOLISM	KEGG	0.07676349	0.20346709	0.949
KEGG_GLYCOLYSIS_GLUCONEOGENESIS	KEGG	0.08097166	0.09815711	0.752
KEGG_THYROID_CANCER	KEGG	0.094262294	0.21395332	0.969
KEGG_ARACHIDONIC_ACID_METABOLISM	KEGG	0.09896907	0.16033487	0.895
KEGG_BETA_ALANINE_METABOLISM	KEGG	0.11812627	0.19656499	0.949
KEGG_CYSTEINE_AND_METHIONINE_METABOLISM	KEGG	0.1197479	0.20013466	0.958
KEGG_PANTOTHENATE_AND_COA_BIOSYNTHESIS	KEGG	0.12778905	0.19398184	0.94
KEGG_DRUG_METABOLISM_OTHER_ENZYMES	KEGG	0.12830958	0.15904222	0.887
KEGG_OXIDATIVE_PHOSPHORYLATION	KEGG	0.13017751	0.09054735	0.486
KEGG_STEROID_HORMONE_BIOSYNTHESIS	KEGG	0.13590264	0.20540762	0.958
KEGG_RENIN_ANGIOTENSIN_SYSTEM	KEGG	0.136	0.19953288	0.949
KEGG_PRIMARY_BILE_ACID_BIOSYNTHESIS	KEGG	0.13609467	0.16525279	0.901
KEGG_HUNTINGTONS_DISEASE	KEGG	0.15694165	0.27817953	0.982
KEGG_MISMATCH_REPAIR	KEGG	0.15904573	0.17480947	0.923
KEGG_FATTY_ACID_METABOLISM	KEGG	0.16869919	0.21870798	0.969
KEGG_SPLICEOSOME	KEGG	0.17004049	0.11633167	0.803
KEGG_PARKINSONS_DISEASE	KEGG	0.17922607	0.21483758	0.969
KEGG_GLYCEROPHOSPHOLIPID_METABOLISM	KEGG	0.18376069	0.3553235	0.997
KEGG_AMYOTROPHIC_LATERAL_SCLEROSIS_ALS	KEGG	0.18410853	0.35618344	0.997
KEGG_DNA_REPLICATION	KEGG	0.2016129	0.19814041	0.943

KEGG_BASAL_TRANSCRIPTION_FACTORS	KEGG	0.22626263	0.24280594	0.981
KEGG_ABC_TRANSPORTERS	KEGG	0.232	0.3579789	0.997
KEGG_CELL_CYCLE	KEGG	0.24404761	0.24309377	0.981
KEGG_GLYCOSYLPHOSPHATIDYLINOSITOL_GPI_ANCHOR_BIOSYNTHESIS	KEGG	0.2454361	0.3450071	0.994
KEGG_NUCLEOTIDE_EXCISION_REPAIR	KEGG	0.25462013	0.27620378	0.982
KEGG_PURINE_METABOLISM	KEGG	0.25976562	0.38422567	0.997
KEGG_O_GLYCAN_BIOSYNTHESIS	KEGG	0.26078433	0.37363204	0.997
KEGG_SPHINGOLIPID_METABOLISM	KEGG	0.278826	0.38488546	0.997
KEGG_ALPHA_LINOLENIC_ACID_METABOLISM	KEGG	0.28834355	0.38759118	0.997
KEGG_HOMOLOGOUS_RECOMBINATION	KEGG	0.29258516	0.29465127	0.988
KEGG_PRION_DISEASES	KEGG	0.3088803	0.41691926	0.998
KEGG_VASOPRESSIN_REGULATED_WATER_REABSORPTION	KEGG	0.31212723	0.4143397	0.998
KEGG_OOCYTE_MEIOSIS	KEGG	0.32938856	0.38119608	0.997
KEGG_NOD_LIKE_RECEPTOR_SIGNALING_PATHWAY	KEGG	0.33133733	0.4092224	0.998
KEGG_RNA_DEGRADATION	KEGG	0.34081632	0.40992564	0.998
KEGG_PROTEASOME	KEGG	0.3429752	0.38648933	0.998
KEGG_P53_SIGNALING_PATHWAY	KEGG	0.37181997	0.4313007	0.998
KEGG_COMPLEMENT_AND_COAGULATION_CASCADES	KEGG	0.38832998	0.41505232	0.998
KEGG_PYRIMIDINE_METABOLISM	KEGG	0.4106776	0.42677966	0.998
KEGG_RNA_POLYMERASE	KEGG	0.43486974	0.42597297	0.998
KEGG_STEROID_BIOSYNTHESIS	KEGG	0.45	0.49446833	1
KEGG_OTHER_GLYCAN_DEGRADATION	KEGG	0.45180723	0.47365963	1
KEGG_PROGESTERONE_MEDIATED_OOCYTE_MATURATION	KEGG	0.4814815	0.52019024	1
KEGG_N_GLYCAN_BIOSYNTHESIS	KEGG	0.5089109	0.5434582	1
KEGG_UBIQUITIN_MEDIATED_PROTEOLYSIS	KEGG	0.53358924	0.5898931	1
KEGG_GALACTOSE_METABOLISM	KEGG	0.5544355	0.5546186	1
KEGG_PPAR_SIGNALING_PATHWAY	KEGG	0.5882353	0.62858367	1
KEGG_ANTIGEN_PROCESSING_AND_PRESENTATION	KEGG	0.72121215	0.69641936	1
KEGG_SYSTEMIC_LUPUS_ERYTHEMATOSUS	KEGG	0.7373541	0.7425112	1
KEGG_CYTOSOLIC_DNA_SENSING_PATHWAY	KEGG	0.7887324	0.7792399	1
REACTOME_NONSENSE_MEDIATED_DECAY_ENHANCED_BY_THE_EXON_JUNCTION_COMPLEX	REACTOME	0	0.14834431	0.059
REACTOME_METABOLISM_OF_AMINO_ACIDS_AND_DERIVATIVES	REACTOME	0	0.30487517	0.2
REACTOME_3_UTR_MEDIATED_TRANSLATIONAL_REGULATION	REACTOME	0	0.3373143	0.332
REACTOME_INFLUENZA_VIRAL_RNA_TRANSCRIPTION_AND_REPLICATION	REACTOME	0	0.27887484	0.337
REACTOME_FORMATION_OF_THE_TERNARY_COMPLEX_AND_SUBSEQUENTLY_THE_43S_COMPLEX	REACTOME	0	0.21587852	0.353
REACTOME_ACTIVATION_OF_THE_MRNA_UPON_BINDING_OF_THE_CAP_BINDING_COMPLEX_AND_EIFS_AND_SUBSEQUENT_BINDING_TO_43S	REACTOME	0	0.20656125	0.373
REACTOME_SULFUR_AMINO_ACID_METABOLISM	REACTOME	0	0.24895614	0.546
REACTOME_CITRIC_ACID_CYCLE_TCA_CYCLE	REACTOME	0	0.23977095	0.626
REACTOME_PEPTIDE_CHAIN_ELONGATION	REACTOME	0	0.24481517	0.713
REACTOME_PHASE_II_CONJUGATION	REACTOME	0.001934236	0.25005826	0.573
REACTOME_MITOCHONDRIAL_TRNA_AMINOACYLATION	REACTOME	0.004237288	0.24431722	0.765
REACTOME_MITOCHONDRIAL_PROTEIN_IMPORT	REACTOME	0.00811359	0.23821583	0.642
REACTOME_BASE_EXCISION_REPAIR	REACTOME	0.012121212	0.24084394	0.828

REACTOME_FORMATION_OF_ATP_BY_CHEMIOSMOTIC_COUPLING	REACTOME	0.014767933	0.3934549	1
REACTOME_AMINE_DERIVED_HORMONES	REACTOME	0.01509434	0.24970664	0.592
REACTOME_GLUTATHIONE_CONJUGATION	REACTOME	0.015686275	0.2529925	0.745
REACTOME_TRANSLATION	REACTOME	0.016064256	0.39436933	0.299
REACTOME_RESOLUTION_OF_AP_SITES_VIA_THE_MULTIPLE_NUCLEOTIDE_PATCH_REPLACEMENT_PATHWAY	REACTOME	0.018480493	0.29105932	0.917
REACTOME_ANTIGEN_PRESENTATION_FOLDING_ASSEMBLY_AND_PEPTIDE_LOADING_OF_CLASS_I_MHC	REACTOME	0.019607844	0.24925458	0.737
REACTOME_PYRUVATE_METABOLISM_AND_CITRIC_ACID_TCA_CYCLE	REACTOME	0.021097047	0.2538807	0.821
REACTOME_TRNA_AMINOACYLATION	REACTOME	0.023655914	0.24221212	0.838
REACTOME_AMINO_ACID_AND_OLIGOPEPTIDE_SLC_TRANSPORTERS	REACTOME	0.024	0.34270996	0.997
REACTOME_BIOLOGICAL_OXIDATIONS	REACTOME	0.029069768	0.2282533	0.838
REACTOME_APOPTOTIC_CLEAVAGE_OF_CELLULAR_PROTEINS	REACTOME	0.03353057	0.3114458	0.976
REACTOME_TRIGLYCERIDE_BIOSYNTHESIS	REACTOME	0.037656903	0.3344046	0.993
REACTOME_NEF_MEDIATES_DOWN_MODULATION_OF_CELL_SURFACE_RECEPTORS_BY_RECRUITING_THEM_TO_CLATHRIN_ADAPTERS	REACTOME	0.03815261	0.24935777	0.828
REACTOME_TCA_CYCLE_AND_RESPIRATORY_ELECTRON_TRANSPORT	REACTOME	0.040339705	0.24183914	0.346
REACTOME_ENOS_ACTIVATION_AND_REGULATION	REACTOME	0.043137256	0.3198371	0.969
REACTOME_REGULATORY_RNA_PATHWAYS	REACTOME	0.044176705	0.28821295	0.927
REACTOME_REGULATION_OF_BETA_CELL_DEVELOPMENT	REACTOME	0.044487428	0.3211166	0.975
REACTOME_SRP_DEPENDENT_COTRANSLATIONAL_PROTEIN_TARGETING_TO_MEMBRANE	REACTOME	0.044660196	0.24903613	0.792
REACTOME_BIOSYNTHESIS_OF_THE_N_GLYCAN_PRECURSOR_DOLICHOL_LIPID_LINKED_OLIGOSACCHARIDE_LLO_AND_TRANSFER_TO_A_NASCENT_PROTEIN	REACTOME	0.04477612	0.28959754	0.953
REACTOME_ASSEMBLY_OF_THE_PRE_REPLICATIVE_COMPLEX	REACTOME	0.04897959	0.2413453	0.795
REACTOME_P53_INDEPENDENT_G1_S_DNA_DAMAGE_CHECKPOINT	REACTOME	0.050980393	0.24885343	0.68
REACTOME_MRNA_SPLICING	REACTOME	0.052313883	0.20725952	0.404
REACTOME_METABOLISM_OF_PROTEINS	REACTOME	0.05532787	0.32176888	0.985
REACTOME_PEROXISOMAL_LIPID_METABOLISM	REACTOME	0.061143983	0.31028682	0.962
REACTOME_CDT1_ASSOCIATION_WITH_THE_CDC6_ORC_ORIGIN_COMPLEX	REACTOME	0.06122449	0.22336264	0.839
REACTOME_LYSOSOME_VESICLE_BIOGENESIS	REACTOME	0.061440676	0.32084963	0.969
REACTOME_THE_ROLE_OF_NEF_IN_HIV1_REPLICATION_AND_DISEASE_PATHOGENESIS	REACTOME	0.061507937	0.3402293	0.993
REACTOME_METABOLISM_OF_MRNA	REACTOME	0.06313646	0.21606305	0.455
REACTOME_METABOLISM_OF_NUCLEOTIDES	REACTOME	0.06734694	0.31543422	0.973
REACTOME_RESPIRATORY_ELECTRON_TRANSPORT	REACTOME	0.06736842	0.2954439	0.955
REACTOME_APOPTOSIS	REACTOME	0.07116105	0.3880915	1
REACTOME_CELL_CYCLE_CHECKPOINTS	REACTOME	0.071428575	0.2504129	0.759
REACTOME_PHASE1_FUNCTIONALIZATION_OF_COMPOUNDS	REACTOME	0.07212476	0.3070894	0.976
REACTOME_BRANCHED_CHAIN_AMINO_ACID_CATABOLISM	REACTOME	0.07594936	0.3118364	0.975
REACTOME_AMINE_COMPOUND_SLC_TRANSPORTERS	REACTOME	0.078277886	0.40185714	1
REACTOME_ACTIVATION_OF_ATR_IN_RESPONSE_TO_REPLICATION_STRESS	REACTOME	0.08085106	0.32599536	0.969
REACTOME_METABOLISM_OF_RNA	REACTOME	0.082474224	0.24040431	0.598
REACTOME_MRNA_SPLICING_MINOR_PATHWAY	REACTOME	0.08281574	0.22691908	0.85
REACTOME_MRNA_3_END_PROCESSING	REACTOME	0.08350305	0.2720691	0.945
REACTOME_SYNTHESIS_OF_BILE_ACIDS_AND_BILE_SALTS	REACTOME	0.08396947	0.31590834	0.966
REACTOME_METABOLISM_OF_VITAMINS_AND_COFACTORS	REACTOME	0.08416834	0.3227702	0.995
REACTOME_P53_DEPENDENT_G1_DNA_DAMAGE_RESPONSE	REACTOME	0.084337346	0.2843147	0.917
REACTOME_FATTY_ACID_TRIACYLGLYCEROL_AND_KETONE_BODY_METABOLISM	REACTOME	0.08553971	0.38260165	1

REACTOME_RESPIRATORY_ELECTRON_TRANSPORT_ATP_SYNTHESIS_BY_CHEMIOSMOTIC_COUPLING_AND_HEAT_PRODUCTION_BY_UNCOUPLING_PROTEINS_	REACTOME	0.08559499	0.3127628	0.978
REACTOME_SYNTHESIS_OF_GLYCOSYLPHOSPHATIDYLINOSITOL_GPI	REACTOME	0.08695652	0.34805772	0.993
REACTOME_PROCESSING_OF_CAPPED_INTRON_CONTAINING_PRE_MRNA	REACTOME	0.08739837	0.24772395	0.703
REACTOME_CYTOCHROME_P450_ARRANGED_BY_SUBSTRATE_TYPE	REACTOME	0.09266409	0.32305565	0.983
REACTOME_APC_C_CDH1_MEDIATED_DEGRADATION_OF_CDC20_AND_OTHER_APC_C_CDH1_TARGETED_PROTEINS_IN_LATE_MITOSIS_EARLY_G1	REACTOME	0.093361	0.23568027	0.838
REACTOME_APOPTOTIC_EXECUTION_PHASE	REACTOME	0.09607843	0.39112645	1
REACTOME_EXTENSION_OF_TELOMERES	REACTOME	0.09670782	0.31750166	0.971
REACTOME_M_G1_TRANSITION	REACTOME	0.10559006	0.26549974	0.932
REACTOME_INTRINSIC_PATHWAY_FOR_APOPTOSIS	REACTOME	0.10638298	0.39149815	1
REACTOME_APC_C_CDC20_MEDIATED_DEGRADATION_OF_MITOTIC_PROTEINS	REACTOME	0.1085595	0.2707705	0.932
REACTOME_G2_M_CHECKPOINTS	REACTOME	0.10897436	0.32522154	0.969
REACTOME_REGULATION_OF_GENE_EXPRESSION_IN_BETA_CELLS	REACTOME	0.10980392	0.4004948	1
REACTOME_MICRORNA_MIRNA_BIOGENESIS	REACTOME	0.114519425	0.32574916	0.995
REACTOME_DNA_STRAND_ELONGATION	REACTOME	0.11618257	0.32391858	0.983
REACTOME_MRNA_PROCESSING	REACTOME	0.11666667	0.27966005	0.932
REACTOME_PKB_MEDIATED_EVENTS	REACTOME	0.124236256	0.39890435	1
REACTOME_LAGGING_STRAND_SYNTHESIS	REACTOME	0.125	0.3142302	0.979
REACTOME_NUCLEOTIDE_BINDING_DOMAIN_LEUCINE_RICH_REPEAT_CONTAINING_RECEPTOR_NLR_SIGNALING_PATHWAYS	REACTOME	0.1283525	0.4208231	1
REACTOME_TRANSMEMBRANE_TRANSPORT_OF_SMALL_MOLECULES	REACTOME	0.13118279	0.41568133	1
REACTOME_TRAF6_MEDIATED_IRF7_ACTIVATION	REACTOME	0.13319239	0.36600792	0.997
REACTOME_ACTIVATION_OF_THE_PRE_REPLICATIVE_COMPLEX	REACTOME	0.13541667	0.32180044	0.978
REACTOME_AUTODEGRADATION_OF_CDH1_BY_CDH1_APC_C	REACTOME	0.13963039	0.3222069	0.966
REACTOME_PHOSPHORYLATION_OF_THE_APC_C	REACTOME	0.14004377	0.33151585	0.995
REACTOME_SYNTHESIS_OF_BILE_ACIDS_AND_BILE_SALTS_VIA_7ALPHA_HYDROXYCHOLESTEROL	REACTOME	0.14203455	0.34211674	0.993
REACTOME_ORC1_REMOVAL_FROM_CHROMATIN	REACTOME	0.14285715	0.28295502	0.932
REACTOME_SYNTHESIS_OF_DNA	REACTOME	0.14344262	0.29000065	0.926
REACTOME_PURINE_METABOLISM	REACTOME	0.14396887	0.34014896	0.997
REACTOME_HIV_INFECTION	REACTOME	0.14741036	0.34548202	0.993
REACTOME_CLEAVAGE_OF_GROWING_TRANSCRIPT_IN_THE_TERMINATION_REGION_	REACTOME	0.14784394	0.3181305	0.971
REACTOME_APC_C_CDC20_MEDIATED_DEGRADATION_OF_CYCLIN_B	REACTOME	0.14945056	0.33415526	0.995
REACTOME_ACTIVATED_AMPK_STIMULATES_FATTY_ACID_OXIDATION_IN_MUSCLE	REACTOME	0.15079366	0.39681834	0.999
REACTOME_REGULATION_OF_KIT_SIGNALING	REACTOME	0.15109344	0.41736206	1
REACTOME_FATTY_ACYL_COA_BIOSYNTHESIS	REACTOME	0.15546219	0.39659685	1
REACTOME_INFLUENZA_LIFE_CYCLE	REACTOME	0.15592515	0.32271433	0.967
REACTOME_O_LINKED_GLYCOSYLATION_OF_MUCINS	REACTOME	0.1565762	0.41684753	1
REACTOME_HOST_INTERACTIONS_OF_HIV_FACTORS	REACTOME	0.15778689	0.34061125	0.997
REACTOME_S_PHASE	REACTOME	0.16322315	0.27616024	0.932
REACTOME_NOD1_2_SIGNALING_PATHWAY	REACTOME	0.16796875	0.41957736	1
REACTOME_PROCESSIVE_SYNTHESIS_ON_THE_LAGGING_STRAND	REACTOME	0.16904277	0.3303481	0.995
REACTOME_ANTIGEN_PROCESSING_UBIQUITINATION_PROTEASOME_DEGRADATION	REACTOME	0.16904277	0.4173632	1
REACTOME_TRANSPORT_OF_MATURE_TRANSCRIPT_TO_CYTOPLASM	REACTOME	0.17083333	0.31652805	0.975
REACTOME_RNA_POL_II_TRANSCRIPTION	REACTOME	0.17107943	0.33187097	0.995
REACTOME_VIF_MEDIATED_DEGRADATION_OF_APOBEC3G	REACTOME	0.17291667	0.33752167	0.993

REACTOME_ABC_FAMILY_PROTEINS_MEDIATED_TRANSPORT	REACTOME	0.17624521	0.39111936	1
REACTOME_AUTODEGRADATION_OF_THE_E3_UBIQUITIN_LIGASE_COP1	REACTOME	0.17751479	0.31758365	0.978
REACTOME_GLOBAL_GENOMIC_NER_GG_NER	REACTOME	0.1779661	0.34567192	0.993
REACTOME_GLUCOSE_METABOLISM	REACTOME	0.18326694	0.38544968	1
REACTOME_METABOLISM_OF_LIPIDS_AND_LIPOPROTEINS	REACTOME	0.18650794	0.42375132	1
REACTOME_FORMATION_OF_FIBRIN_CLOT_CLOTTING_CASCADE	REACTOME	0.1875	0.38072369	1
REACTOME_PPARA_ACTIVATES_GENE_EXPRESSION	REACTOME	0.19057377	0.45388272	1
REACTOME_INHIBITION_OF_THE_PROTEOLYTIC_ACTIVITY_OF_APC_C_REQUIRED_FOR_THE_ONSET_OF_ANAPHASE_BY_MITOTIC_SPINDLE_CHECKPOINT_COMPONENT	REACTOME	0.19739696	0.34430528	0.997
REACTOME_DNA_REPAIR	REACTOME	0.1987315	0.3321673	0.993
REACTOME_POST_TRANSLATIONAL_MODIFICATION_SYNTHESIS_OF_GPI_ANCHORED_PROTEINS	REACTOME	0.19917865	0.37931195	1
REACTOME_SYNTHESIS_OF_PA	REACTOME	0.20289855	0.42702937	1
REACTOME_PEPTIDE_LIGAND_BINDING_RECEPTORS	REACTOME	0.20507812	0.4588391	1
REACTOME_CDK_MEDIATED_PHOSPHORYLATION_AND_REMOVAL_OF_CDC6	REACTOME	0.20547946	0.3291922	0.995
REACTOME_HIV_LIFE_CYCLE	REACTOME	0.20724346	0.34142005	0.997
REACTOME_CHEMOKINE_RECEPTORS_BIND_CHEMOKINES	REACTOME	0.20784314	0.38121614	0.997
REACTOME_CHYLOMICRON_MEDIATED_LIPID_TRANSPORT	REACTOME	0.20990099	0.40005317	1
REACTOME_APC_CDC20_MEDIATED_DEGRADATION_OF_NEK2A	REACTOME	0.21199143	0.34560078	0.997
REACTOME_POST_TRANSLATIONAL_PROTEIN_MODIFICATION	REACTOME	0.21398304	0.44705743	1
REACTOME_TIGHT_JUNCTION_INTERACTIONS	REACTOME	0.21900827	0.3931931	1
REACTOME_SYNTHESIS_AND_INTERCONVERSION_OF_NUCLEOTIDE_DI_AND_TRIPHOSPHATES	REACTOME	0.2193159	0.3864641	1
REACTOME_DNA_REPLICATION	REACTOME	0.21966527	0.3329332	0.989
REACTOME_REGULATION_OF_ORNITHINE_DECARBOXYLASE_ODC	REACTOME	0.22460938	0.34196997	0.997
REACTOME_G_ALPHA_I_SIGNALLING_EVENTS	REACTOME	0.2248996	0.46085224	1
REACTOME_TRANSPORT_OF_INORGANIC_CATIONS_ANIONS_AND_AMINO_ACIDS_OLIGOPEPTIDES	REACTOME	0.2281059	0.4677785	1
REACTOME_GLUCOSE_TRANSPORT	REACTOME	0.23125	0.40926257	1
REACTOME_TRAFFICKING_OF_GLUR2_CONTAINING_AMPA_RECEPTORS	REACTOME	0.23308271	0.4104767	1
REACTOME_BILE_ACID_AND_BILE_SALT_METABOLISM	REACTOME	0.23346303	0.40115365	1
REACTOME_METABOLISM_OF_NON_CODING_RNA	REACTOME	0.23430963	0.32900137	0.995
REACTOME_MITOTIC_M_M_G1_PHASES	REACTOME	0.23480085	0.33544847	0.993
REACTOME_RIG_I_MDA5_MEDIATED_INDUCTION_OF_IFN_ALPHA_BETA_PATHWAYS	REACTOME	0.23619048	0.42684433	1
REACTOME_RNA_POL_II_PRE_TRANSCRIPTION_EVENTS	REACTOME	0.23684211	0.3809569	1
REACTOME_CYTOSOLIC_TRNA_AMINOACYLATION	REACTOME	0.23940678	0.38256228	1
REACTOME_DEADENYLATION_DEPENDENT_MRNA_DECAY	REACTOME	0.23952095	0.38925996	1
REACTOME_SPHINGOLIPID_METABOLISM	REACTOME	0.24340771	0.44991434	1
REACTOME_G1_S_TRANSITION	REACTOME	0.24430642	0.3336314	0.995
REACTOME_CONVERSION_FROM_APC_C_CDC20_TO_APC_C_CDH1_IN_LATE_ANAPHASE	REACTOME	0.2451193	0.3890782	1
REACTOME_NUCLEAR_RECEPTOR_TRANSCRIPTION_PATHWAY	REACTOME	0.24654832	0.45051867	1
REACTOME_SLC_MEDIATED_TRANSMEMBRANE_TRANSPORT	REACTOME	0.25	0.45891866	1
REACTOME_SCFSKP2_MEDIATED_DEGRADATION_OF_P27_P21	REACTOME	0.252588	0.38746932	1
REACTOME_CELL_CYCLE	REACTOME	0.25732216	0.3714769	0.997
REACTOME_DESTABILIZATION_OF_MRNA_BY_AUF1_HNRNP_D0	REACTOME	0.26078433	0.3986547	0.999
REACTOME_TELOMERE_MAINTENANCE	REACTOME	0.26215646	0.41380584	1
REACTOME_CLASS_I_MHC_MEDIATED_ANTIGEN_PROCESSING_PRESENTATION	REACTOME	0.2632653	0.47124398	1

REACTOME_LATE_PHASE_OF_HIV_LIFE_CYCLE	REACTOME	0.26337448	0.37904	1
REACTOME_MEIOTIC_RECOMBINATION	REACTOME	0.26666668	0.38613245	1
REACTOME_TRANSPORT_OF_MATURE_MRNA_DERIVED_FROM_AN_INTRONLESS_TRANSCRIPT	REACTOME	0.26709402	0.39647242	0.999
REACTOME_CELL_CYCLE_MITOTIC	REACTOME	0.26736844	0.38002416	0.999
REACTOME_REGULATION_OF_MITOTIC_CELL_CYCLE	REACTOME	0.26849896	0.400388	0.999
REACTOME_INTERFERON_ALPHA_BETA_SIGNALING	REACTOME	0.27037773	0.4261867	1
REACTOME_ASPARAGINE_N_LINKED_GLYCOSYLATION	REACTOME	0.2704918	0.45721033	1
REACTOME_MRNA_CAPPING	REACTOME	0.27272728	0.41190708	1
REACTOME_RNA_POL_III_TRANSCRIPTION_INITIATION_FROM_TYPE_2_PROMOTER	REACTOME	0.27326733	0.4113757	1
REACTOME_KINESINS	REACTOME	0.2746781	0.39012966	1
REACTOME_PHOSPHOLIPID_METABOLISM	REACTOME	0.2747934	0.48552188	1
REACTOME_RNA_POL_II_TRANSCRIPTION_PRE_INITIATION_AND_PROMOTER_OPENING	REACTOME	0.275	0.3831219	1
REACTOME_SPHINGOLIPID_DE_NOVO_BIOSYNTHESIS	REACTOME	0.28244275	0.4548656	1
REACTOME_NUCLEOTIDE_EXCISION_REPAIR	REACTOME	0.28423238	0.39946163	1
REACTOME_DEADENYLATION_OF_MRNA	REACTOME	0.28601253	0.47237924	1
REACTOME_MITOTIC_G1_G1_S_PHASES	REACTOME	0.2892562	0.38394	1
REACTOME_PROCESSING_OF_CAPPED_INTRONLESS_PRE_MRNA	REACTOME	0.29132232	0.4155147	1
REACTOME_MITOTIC_PROMETAPHASE	REACTOME	0.29621848	0.4012425	1
REACTOME_COMPLEMENT_CASCADE	REACTOME	0.2994129	0.45295823	1
REACTOME_GOLGI_ASSOCIATED_VESICLE_BIOGENESIS	REACTOME	0.30043858	0.45651188	1
REACTOME_GLYCOSPHINGOLIPID_METABOLISM	REACTOME	0.30128205	0.4664604	1
REACTOME_FANCONI_ANEMIA_PATHWAY	REACTOME	0.30172414	0.4112565	1
REACTOME_CELL_CELL_JUNCTION_ORGANIZATION	REACTOME	0.30214426	0.47493532	1
REACTOME_CHROMOSOME_MAINTENANCE	REACTOME	0.30543932	0.41349512	1
REACTOME_TRANSCRIPTION	REACTOME	0.3114754	0.454661	1
REACTOME_GLUCONEOGENESIS	REACTOME	0.31546393	0.45287386	1
REACTOME_TRANSCRIPTION_COUPLED_NER_TC_NER	REACTOME	0.31622177	0.41472828	1
REACTOME_FORMATION_OF_INCISION_COMPLEX_IN_GG_NER	REACTOME	0.31790745	0.4548806	1
REACTOME_ENDOGENOUS_STEROLS	REACTOME	0.3201581	0.45566493	1
REACTOME_ER_PHAGOSOME_PATHWAY	REACTOME	0.32108316	0.42281845	1
REACTOME_CYCLIN_E_ASSOCIATED_EVENTS_DURING_G1_S_TRANSITION_	REACTOME	0.32415253	0.42661408	1
REACTOME_GLYCEROPHOSPHOLIPID_BIOSYNTHESIS	REACTOME	0.33056134	0.51064956	1
REACTOME_MEIOSIS	REACTOME	0.33333334	0.45214424	1
REACTOME_FORMATION_OF_RNA_POL_II_ELONGATION_COMPLEX_	REACTOME	0.33333334	0.45881116	1
REACTOME_SCF_BETA_TRCP_MEDIATED_DEGRADATION_OF_EMI1	REACTOME	0.33734939	0.45346054	1
REACTOME_NA_CL_DEPENDENT_NEUROTRANSMITTER_TRANSPORTERS	REACTOME	0.33734939	0.5014261	1
REACTOME_AMINO_ACID_SYNTHESIS_AND_INTERCONVERSION_TRANSAMINATION	REACTOME	0.3407258	0.4548132	1
REACTOME_REGULATION_OF_WATER_BALANCE_BY_RENAL_AQUAPORINS	REACTOME	0.3438155	0.53250974	1
REACTOME_FORMATION_OF_THE_HIV1_EARLY_ELONGATION_COMPLEX	REACTOME	0.34489796	0.48445484	1
REACTOME_AQUAPORIN_MEDIATED_TRANSPORT	REACTOME	0.3478261	0.5342746	1
REACTOME_RECYCLING_PATHWAY_OF_L1	REACTOME	0.34979424	0.50857395	1
REACTOME_DOUBLE_STRAND_BREAK_REPAIR	REACTOME	0.35157895	0.4615434	1
REACTOME_SYNTHESIS_OF_PC	REACTOME	0.35892117	0.506885	1

REACTOME_NEP_NS2_INTERACTS_WITH_THE_CELLULAR_EXPORT_MACHINERY	REACTOME	0.35908142	0.4259943	1
REACTOME_RECRUITMENT_OF_MITOTIC_CENTROSOME_PROTEINS_AND_COMPLEXES	REACTOME	0.36210525	0.48352095	1
REACTOME_TRAF6_MEDIATED_NFKB_ACTIVATION	REACTOME	0.36345777	0.48138395	1
REACTOME_E2F_MEDIATED_REGULATION_OF_DNA_REPLICATION	REACTOME	0.36401674	0.4247335	1
REACTOME_TRANSPORT_OF_VITAMINS_NUCLEOSIDES_AND_RELATED_MOLECULES	REACTOME	0.36565655	0.48103687	1
REACTOME_RNA_POL_I_TRANSCRIPTION_TERMINATION	REACTOME	0.36666667	0.45379722	1
REACTOME_MITOTIC_G2_G2_M_PHASES	REACTOME	0.36673775	0.47165075	1
REACTOME_INTERFERON_SIGNALING	REACTOME	0.3783784	0.54333705	1
REACTOME_CLASS_A1_RHODOPSIN_LIKE_RECEPTORS	REACTOME	0.3809524	0.56051135	1
REACTOME_REGULATION_OF_GLUCOKINASE_BY_GLUCOKINASE_REGULATORY_PROTEIN	REACTOME	0.38414633	0.4618469	1
REACTOME_DEPOSITION_OF_NEW_CENPA_CONTAINING_NUCLEOSOMES_AT_THE_CENTROMERE	REACTOME	0.3866944	0.5005811	1
REACTOME_G1_S_SPECIFIC_TRANSCRIPTION	REACTOME	0.4	0.46111745	1
REACTOME_RNA_POL_I_TRANSCRIPTION_INITIATION	REACTOME	0.40980393	0.5133242	1
REACTOME_REGULATION_OF_MRNA_STABILITY_BY_PROTEINS_THAT_BIND_AU_RICH_ELEMENTS	REACTOME	0.4107143	0.52621585	1
REACTOME_LOSS_OF_NLP_FROM_MITOTIC_CENTROSOMES	REACTOME	0.4121339	0.5193209	1
REACTOME_CYCLIN_A_B1_ASSOCIATED_EVENTS_DURING_G2_M_TRANSITION	REACTOME	0.41525424	0.48213312	1
REACTOME_ENDOSOMAL_SORTING_COMPLEX_REQUIRED_FOR_TRANSPORT_ESCRT	REACTOME	0.42028984	0.56217843	1
REACTOME_INNATE_IMMUNE_SYSTEM	REACTOME	0.42307693	0.5641727	1
REACTOME_HOMOLOGOUS_RECOMBINATION_REPAIR_OF_REPLICATION_INDEPENDENT_DOUBLE_STRAND_BREAKS	REACTOME	0.4231579	0.48362187	1
REACTOME_MHC_CLASS_II_ANTIGEN_PRESENTATION	REACTOME	0.42887932	0.56559366	1
REACTOME_METAL_ION_SLC_TRANSPORTERS	REACTOME	0.4364754	0.5357536	1
REACTOME_TRANSFERRIN_ENDOCYTOSIS_AND_RECYCLING	REACTOME	0.44111776	0.55913264	1
REACTOME_CROSS_PRESENTATION_OF_SOLUBLE_EXOGENOUS_ANTIGENS_ENDOSOMES	REACTOME	0.44930416	0.593185	1
REACTOME_INTERACTIONS_OF_VPR_WITH_HOST_CELLULAR_PROTEINS	REACTOME	0.45884773	0.52784324	1
REACTOME_GENERIC_TRANSCRIPTION_PATHWAY	REACTOME	0.462845	0.6106658	1
REACTOME_GAP_JUNCTION_ASSEMBLY	REACTOME	0.46450305	0.58301556	1
REACTOME_ANTIVIRAL_MECHANISM_BY_IFN_STIMULATED_GENES	REACTOME	0.46707818	0.5623559	1
REACTOME_AMINO_ACID_TRANSPORT_ACROSS_THE_PLASMA_MEMBRANE	REACTOME	0.47010309	0.5824264	1
REACTOME_PRE_NOTCH_TRANSCRIPTION_AND_TRANSLATION	REACTOME	0.47843942	0.57754576	1
REACTOME_ABORTIVE_ELONGATION_OF_HIV1_TRANSCRIPT_IN_THE_ABSENCE_OF_TAT	REACTOME	0.4826176	0.62806636	1
REACTOME_G0_AND_EARLY_G1	REACTOME	0.4957265	0.5769924	1
REACTOME_METABOLISM_OF_STEROID_HORMONES_AND_VITAMINS_A_AND_D	REACTOME	0.49906543	0.58763456	1
REACTOME_RNA_POL_III_CHAIN_ELONGATION	REACTOME	0.50701404	0.6135092	1
REACTOME_REGULATION_OF_APOPTOSIS	REACTOME	0.5152672	0.6568452	1
REACTOME_TRANSPORT_OF_RIBONUCLEOPROTEINS_INTO_THE_HOST_NUCLEUS	REACTOME	0.51619434	0.6159706	1
REACTOME_NUCLEOTIDE_LIKE_PURINERGIC_RECEPTORS	REACTOME	0.51827955	0.62653494	1
REACTOME_ABCA_TRANSPORTERS_IN_LIPID_HOMEOSTASIS	REACTOME	0.5217391	0.6165913	1
REACTOME_RNA_POL_I_RNA_POL_III_AND_MITOCHONDRIAL_TRANSCRIPTION	REACTOME	0.5394191	0.63438565	1
REACTOME_STEROID_HORMONES	REACTOME	0.5485714	0.6274575	1
REACTOME_REGULATION_OF_INSULIN_SECRETION_BY_GLUCAGON_LIKE_PEPTIDE1	REACTOME	0.55193484	0.6294302	1
REACTOME_IRON_UPTAKE_AND_TRANSPORT	REACTOME	0.55666006	0.6361149	1
REACTOME_INTERFERON_GAMMA_SIGNALING	REACTOME	0.55836576	0.6387037	1
REACTOME_TRANS_GOLGI_NETWORK_VESICLE_BUDDING	REACTOME	0.5588235	0.6404874	1

REACTOME_RNA_POL_I_TRANSCRIPTION	REACTOME	0.565762	0.63537836	1
REACTOME_ACTIVATED_TAK1_MEDIATES_P38_MAPK_ACTIVATION	REACTOME	0.5658153	0.66276973	1
REACTOME_GLYCOLYSIS	REACTOME	0.56646216	0.63272005	1
REACTOME_SIGNALLING_TO_P38_VIA_RIT_AND_RIN	REACTOME	0.57349896	0.6638823	1
REACTOME_ELONGATION_ARREST_AND_RECOVERY	REACTOME	0.5767635	0.6828649	1
REACTOME_SIGNALING_BY_WNT	REACTOME	0.5803922	0.67282784	1
REACTOME_LIPID_DIGESTION_MOBILIZATION_AND_TRANSPORT	REACTOME	0.5812133	0.68031454	1
REACTOME_ACYL_CHAIN_REMODELLING_OF_PG	REACTOME	0.5825427	0.63826406	1
REACTOME_ENERGY_DEPENDENT_REGULATION_OF_MTOR_BY_LKB1_AMPK	REACTOME	0.59591836	0.6750794	1
REACTOME_AMINE_LIGAND_BINDING_RECEPTORS	REACTOME	0.6069959	0.66685146	1
REACTOME_RNA_POL_III_TRANSCRIPTION	REACTOME	0.6163022	0.6803079	1
REACTOME_ION_TRANSPORT_BY_P_TYPE_ATPASES	REACTOME	0.61935484	0.66180366	1
REACTOME_ZINC_TRANSPORTERS	REACTOME	0.6265306	0.6783707	1
REACTOME_GLYCOGEN_BREAKDOWN_GLYCOGENOLYSIS	REACTOME	0.62818	0.6715496	1
REACTOME_RNA_POL_III_TRANSCRIPTION_TERMINATION	REACTOME	0.6539235	0.79426503	1
REACTOME_RNA_POL_III_TRANSCRIPTION_INITIATION_FROM_TYPE_3_PROMOTER	REACTOME	0.6888454	0.7745008	1
REACTOME_INTRINSIC_PATHWAY	REACTOME	0.71456313	0.79761237	1
REACTOME_PERK_REGULATED_GENE_EXPRESSION	REACTOME	0.71568626	0.7728441	1
REACTOME_AMYLOIDS	REACTOME	0.7244898	0.83438134	1
REACTOME_CHOLESTEROL_BIOSYNTHESIS	REACTOME	0.75374734	0.8593017	1
REACTOME_RNA_POL_I_PROMOTER_OPENING	REACTOME	0.7870564	0.895438	1
REACTOME_PYRUVATE_METABOLISM	REACTOME	0.8015564	0.7980452	1
REACTOME_TRAFFICKING_OF_AMPA_RECEPTORS	REACTOME	0.805501	0.79619396	1
REACTOME_MEIOTIC_SYNAPSIS	REACTOME	0.8088235	0.88057816	1
REACTOME_ION_CHANNEL_TRANSPORT	REACTOME	0.8269231	0.8372439	1
REACTOME_DESTABILIZATION_OF_MRNA_BY_KSRP	REACTOME	0.83625734	0.8988807	1
REACTOME_DESTABILIZATION_OF_MRNA_BY_TRISTETRAPROLIN_TTP	REACTOME	0.85742575	0.9298458	1
REACTOME_DARPP_32_EVENTS	REACTOME	0.87603307	0.8618352	1
REACTOME_PACKAGING_OF_TELOMERE_ENDS	REACTOME	0.8773006	0.9328822	1
REACTOME_FORMATION_OF_TRANSCRIPTION_COUPLED_NER_TC_NER_REPAIR_COMPLEX	REACTOME	0.888668	0.9220794	1
REACTOME_DESTABILIZATION_OF_MRNA_BY_BRF1	REACTOME	0.8922764	0.9434982	1
REACTOME_TAK1_ACTIVATES_NFKB_BY_PHOSPHORYLATION_AND_ACTIVATION_OF_IKKS_COMPLEX	REACTOME	0.89463603	0.8910266	1

Table S2. All the gene sets enriched in FBS cells compared with FAC cells at D14 of culture (assessed by GSEA)

NAME	Data base	NOM p-val	FDR q-val	FWER p-val
HALLMARK_TGF_BETA_SIGNALING	HALLMARK	0	0.009140522	0.005
HALLMARK_MYOGENESIS	HALLMARK	0	0.069657445	0.105
HALLMARK_NOTCH_SIGNALING	HALLMARK	0	0.059325222	0.131
HALLMARK_HYPOXIA	HALLMARK	0	0.045752253	0.132
HALLMARK_ANDROGEN_RESPONSE	HALLMARK	0	0.048646573	0.15
HALLMARK_IL2_STAT5_SIGNALING	HALLMARK	0	0.12665664	0.46
HALLMARK_UV_RESPONSE_DN	HALLMARK	0.004	0.050967343	0.202
HALLMARK_EPITHELIAL_MESENCHYMAL_TRANSITION	HALLMARK	0.004032258	0.040872145	0.15
HALLMARK_APICAL_JUNCTION	HALLMARK	0.008080808	0.064334035	0.26
HALLMARK_TNFA_SIGNALING_VIA_NFKB	HALLMARK	0.04710921	0.23871371	0.678
HALLMARK_ESTROGEN_RESPONSE_EARLY	HALLMARK	0.068041235	0.39715317	0.848
HALLMARK_KRAS_SIGNALING_UP	HALLMARK	0.08595388	0.3668031	0.873
HALLMARK_INFLAMMATORY_RESPONSE	HALLMARK	0.104166664	0.3623399	0.884
HALLMARK_HEME_METABOLISM	HALLMARK	0.10735586	0.37135115	0.856
HALLMARK_APOPTOSIS	HALLMARK	0.20162933	0.3912459	0.925
HALLMARK_ALLOGRAFT_REJECTION	HALLMARK	0.20654397	0.40170398	0.971
HALLMARK_KRAS_SIGNALING_DN	HALLMARK	0.23695652	0.44194546	0.971
HALLMARK_COMPLEMENT	HALLMARK	0.25995806	0.40901086	0.979
HALLMARK_WNT_BETA_CATENIN_SIGNALING	HALLMARK	0.27145708	0.39942184	0.985
HALLMARK_ANGIOGENESIS	HALLMARK	0.276	0.3740405	0.935
HALLMARK_HEDGEHOG_SIGNALING	HALLMARK	0.29218107	0.417504	0.971
HALLMARK_COAGULATION	HALLMARK	0.3668033	0.4653472	0.994
HALLMARK_APICAL_SURFACE	HALLMARK	0.49266246	0.5583202	0.996
HALLMARK_P53_PATHWAY	HALLMARK	0.562	0.6015378	0.996
HALLMARK_MITOTIC_SPINDLE	HALLMARK	0.634981	0.6962988	0.999
HALLMARK_UNFOLDED_PROTEIN_RESPONSE	HALLMARK	0.6608187	0.7113714	0.999
KEGG_REGULATION_OF_ACTIN_CYTOSKELETON	KEGG	0	0.26748475	0.135
KEGG_RENAL_CELL_CARCINOMA	KEGG	0	0.14733337	0.145
KEGG_FOCAL_ADHESION	KEGG	0	0.11863231	0.177
KEGG_GAP_JUNCTION	KEGG	0	0.090973504	0.181
KEGG_PANCREATIC_CANCER	KEGG	0	0.07751717	0.191
KEGG_GLYCOSAMINOGLYCAN_BIOSYNTHESIS_CHONDROITIN_SULFATE	KEGG	0	0.072336674	0.238
KEGG_GLIOMA	KEGG	0	0.07472582	0.303
KEGG_PATHWAYS_IN_CANCER	KEGG	0	0.08921946	0.356
KEGG_GNRH_SIGNALING_PATHWAY	KEGG	0	0.08600339	0.471
KEGG_MELANOGENESIS	KEGG	0	0.083558686	0.499

KEGG_NEUROTROPHIN_SIGNALING_PATHWAY	KEGG	0	0.08406236	0.513
KEGG_MELANOMA	KEGG	0	0.07987432	0.526
KEGG_MTOR_SIGNALING_PATHWAY	KEGG	0.001984127	0.08965724	0.404
KEGG_ADHERENS_JUNCTION	KEGG	0.002	0.14376044	0.792
KEGG_HEDGEHOG_SIGNALING_PATHWAY	KEGG	0.00203252	0.08200651	0.3
KEGG_DILATED_CARDIOMYOPATHY	KEGG	0.00203666	0.08499132	0.412
KEGG_MAPK_SIGNALING_PATHWAY	KEGG	0.004016064	0.11455426	0.723
KEGG_TGF_BETA_SIGNALING_PATHWAY	KEGG	0.006048387	0.07543207	0.218
KEGG_WNT_SIGNALING_PATHWAY	KEGG	0.006072875	0.10199339	0.654
KEGG_AXON_GUIDANCE	KEGG	0.00610998	0.08408259	0.561
KEGG_ECM_RECEPTOR_INTERACTION	KEGG	0.006134969	0.08696964	0.457
KEGG_ARRHYTHMOGENIC_RIGHT_VENTRICULAR_CARDIOMYOPATHY_ARVC	KEGG	0.008048289	0.09411278	0.396
KEGG_CALCIUM_SIGNALING_PATHWAY	KEGG	0.008048289	0.118434206	0.72
KEGG_ERBB_SIGNALING_PATHWAY	KEGG	0.011560693	0.1067723	0.69
KEGG_NATURAL_KILLER_CELL_MEDIATED_CYTOTOXICITY	KEGG	0.011695907	0.18083973	0.893
KEGG_PHOSPHATIDYLINOSITOL_SIGNALING_SYSTEM	KEGG	0.012	0.15729877	0.811
KEGG_HYPERTROPHIC_CARDIOMYOPATHY_HCM	KEGG	0.012121212	0.087504394	0.496
KEGG_GLYCOSAMINOGLYCAN_BIOSYNTHESIS_HEPARAN_SULFATE	KEGG	0.012371134	0.092803225	0.457
KEGG_EPITHELIAL_CELL_SIGNALING_IN_HELICOBACTER_PYLORI_INFECTION	KEGG	0.013752456	0.108081	0.686
KEGG_CHRONIC_MYELOID_LEUKEMIA	KEGG	0.014141414	0.08300006	0.525
KEGG_PATHOGENIC_ESCHERICHIA_COLI_INFECTION	KEGG	0.017681729	0.11683933	0.737
KEGG_BASAL_CELL_CARCINOMA	KEGG	0.017716536	0.09833793	0.624
KEGG_T_CELL_RECEPTOR_SIGNALING_PATHWAY	KEGG	0.023529412	0.16331795	0.837
KEGG_ENDOCYTOSIS	KEGG	0.02414487	0.17571844	0.86
KEGG_LEUKOCYTE_TRANSENDOTHELIAL_MIGRATION	KEGG	0.024193548	0.14368884	0.796
KEGG_TIGHT_JUNCTION	KEGG	0.025742574	0.21947087	0.954
KEGG_DORSO_VENTRAL_AXIS_FORMATION	KEGG	0.028	0.12896602	0.765
KEGG_SMALL_CELL_LUNG_CANCER	KEGG	0.030303031	0.22385934	0.954
KEGG_COLORECTAL_CANCER	KEGG	0.031007752	0.18293922	0.887
KEGG_JAK_STAT_SIGNALING_PATHWAY	KEGG	0.032388665	0.22420412	0.951
KEGG_LONG_TERM_DEPRESSION	KEGG	0.039014373	0.18600619	0.906
KEGG_INOSITOL_PHOSPHATE_METABOLISM	KEGG	0.03984064	0.22847301	0.95
KEGG_LONG_TERM_POTENTIATION	KEGG	0.04106776	0.1794217	0.876
KEGG_PROSTATE_CANCER	KEGG	0.051181104	0.20984371	0.94
KEGG_VEGF_SIGNALING_PATHWAY	KEGG	0.051587302	0.18688232	0.887
KEGG_REGULATION_OF_AUTOPHAGY	KEGG	0.057613168	0.18491682	0.908
KEGG_NEUROACTIVE_LIGAND_RECEPTOR_INTERACTION	KEGG	0.06560636	0.22859918	0.969
KEGG_GLYCOSPHINGOLIPID_BIOSYNTHESIS_GANGLIO_SERIES	KEGG	0.06732673	0.17187776	0.851

KEGG_LEISHMANIA_INFECTION	KEGG	0.07350097	0.17480563	0.863
KEGG_TYPE_II_DIABETES_MELLITUS	KEGG	0.07535642	0.22229297	0.962
KEGG_ALDOSTERONE_REGULATED_SODIUM_REABSORPTION	KEGG	0.079766534	0.2695417	0.982
KEGG_ACUTE_MYELOID_LEUKEMIA	KEGG	0.083984375	0.18182568	0.891
KEGG_NOTCH_SIGNALING_PATHWAY	KEGG	0.0945674	0.2062194	0.937
KEGG_BLADDER_CANCER	KEGG	0.09475806	0.2211357	0.962
KEGG_VASCULAR_SMOOTH_MUSCLE_CONTRACTION	KEGG	0.09775967	0.26839873	0.985
KEGG_RIG_I_LIKE_RECEPTOR_SIGNALING_PATHWAY	KEGG	0.098076925	0.22352594	0.956
KEGG_ALZHEIMERS_DISEASE	KEGG	0.111561865	0.227249	0.969
KEGG_NON_SMALL_CELL_LUNG_CANCER	KEGG	0.115686275	0.26617536	0.982
KEGG_VIRAL_MYOCARDITIS	KEGG	0.11585366	0.27478614	0.991
KEGG_TOLL_LIKE_RECEPTOR_SIGNALING_PATHWAY	KEGG	0.1391129	0.32056734	0.995
KEGG_CELL_ADHESION_MOLECULES_CAMS	KEGG	0.14137214	0.27759257	0.991
KEGG_HEMATOPOIETIC_CELL_LINEAGE	KEGG	0.15132925	0.27026564	0.985
KEGG_B_CELL_RECEPTOR_SIGNALING_PATHWAY	KEGG	0.17358491	0.31436855	0.995
KEGG_CYTOKINE_CYTOKINE_RECEPTOR_INTERACTION	KEGG	0.2248996	0.38231078	1
KEGG_SNARE_INTERACTIONS_IN_VESICULAR_TRANSPORT	KEGG	0.238921	0.34350556	0.996
KEGG_GLYCEROLIPID_METABOLISM	KEGG	0.2446184	0.39567888	1
KEGG_FC_EPSILON_RI_SIGNALING_PATHWAY	KEGG	0.27272728	0.4235654	1
KEGG_CARDIAC_MUSCLE_CONTRACTION	KEGG	0.28629032	0.36679903	0.996
KEGG_INSULIN_SIGNALING_PATHWAY	KEGG	0.28962818	0.4352693	1
KEGG_TYPE_I_DIABETES_MELLITUS	KEGG	0.29531568	0.36894542	0.996
KEGG_TASTE_TRANSDUCTION	KEGG	0.3149284	0.44023284	1
KEGG_CHEMOKINE_SIGNALING_PATHWAY	KEGG	0.32515338	0.44404286	1
KEGG_ALLOGRAFT_REJECTION	KEGG	0.34653464	0.43249342	1
KEGG_ENDOMETRIAL_CANCER	KEGG	0.37356323	0.4635634	1
KEGG_FC_GAMMA_R_MEDIATED_PHAGOCYTOSIS	KEGG	0.37821782	0.46541697	1
KEGG_GLYCOSAMINOGLYCAN_DEGRADATION	KEGG	0.38431373	0.45974267	1
KEGG_OLFACTORY_TRANSDUCTION	KEGG	0.40243903	0.4683876	1
KEGG_ASTHMA	KEGG	0.4251497	0.5052454	1
KEGG_ADIPOCYTOKINE_SIGNALING_PATHWAY	KEGG	0.4389313	0.50958693	1
KEGG_RIBOFLAVIN_METABOLISM	KEGG	0.53521127	0.58716464	1
KEGG_GRAFT_VERSUS_HOST_DISEASE	KEGG	0.55040324	0.6123126	1
KEGG_INTESTINAL_IMMUNE_NETWORK_FOR_IGA_PRODUCTION	KEGG	0.5691383	0.6504817	1
KEGG_LYSOSOME	KEGG	0.5777778	0.6579626	1
KEGG_AUTOIMMUNE_THYROID_DISEASE	KEGG	0.5922921	0.6494898	1
KEGG_VIBRIO_CHOLERAE_INFECTION	KEGG	0.60465115	0.6276522	1
KEGG_NICOTINATE_AND_NICOTINAMIDE_METABOLISM	KEGG	0.66041666	0.71129733	1

KEGG_PRIMARY_IMMUNODEFICIENCY	KEGG	0.76811594	0.71775633	1
REACTOME_SIGNALING_BY_TGF_BETA_RECEPTOR_COMPLEX	REACTOME	0	0.00867238	0.004
REACTOME_TGF_BETA_RECEPTOR_SIGNALING_ACTIVATES_SMADS	REACTOME	0	0.0321095	0.032
REACTOME_TRANSCRIPTIONAL_ACTIVITY_OF_SMAD2_SMAD3_SMAD4_HETEROTRIMER	REACTOME	0	0.07693706	0.107
REACTOME_DOWNREGULATION_OF_SMAD2_3_SMAD4_TRANSCRIPTIONAL_ACTIVITY	REACTOME	0	0.06992341	0.115
REACTOME_AXON_GUIDANCE	REACTOME	0	0.35091195	0.49
REACTOME_INTEGRIN_CELL_SURFACE_INTERACTIONS	REACTOME	0	0.3494062	0.577
REACTOME_MUSCLE_CONTRACTION	REACTOME	0	0.33231696	0.597
REACTOME_YAP1_AND_WWTR1_TAZ_STIMULATED_GENE_EXPRESSION	REACTOME	0	0.2804547	0.601
REACTOME_DEVELOPMENTAL_BIOLOGY	REACTOME	0	0.23259923	0.795
REACTOME_PLATELET_CALCIUM_HOMEOSTASIS	REACTOME	0	0.20971842	0.831
REACTOME_PLATELET_ACTIVATION_SIGNALING_AND_AGGREGATION	REACTOME	0	0.24093941	0.87
REACTOME_SIGNALLING_BY_NGF	REACTOME	0	0.2461391	0.93
REACTOME_DOWNREGULATION_OF_TGF_BETA_RECEPTOR_SIGNALING	REACTOME	0.001953125	0.041110802	0.055
REACTOME_CD28_CO_STIMULATION	REACTOME	0.001968504	0.2805215	0.634
REACTOME_SIGNALING_BY_NOTCH	REACTOME	0.002012072	0.24262534	0.976
REACTOME_L1CAM_INTERACTIONS	REACTOME	0.00204918	0.21195865	0.817
REACTOME_PRE_NOTCH_PROCESSING_IN_GOLGI	REACTOME	0.002061856	0.24514043	0.739
REACTOME_SIGNALING_BY_BMP	REACTOME	0.002150538	0.24930373	0.703
REACTOME_GENERATION_OF_SECOND_MESSENGER_MOLECULES	REACTOME	0.003968254	0.2305382	0.758
REACTOME_SIGNALLING_TO_RAS	REACTOME	0.003968254	0.23967251	0.877
REACTOME_CELL_SURFACE_INTERACTIONS_AT_THE_VASCULAR_WALL	REACTOME	0.004024145	0.23225863	0.96
REACTOME_SIGNALING_BY_FGFR1_MUTANTS	REACTOME	0.00407332	0.23080613	0.744
REACTOME_COSTIMULATION_BY_THE_CD28_FAMILY	REACTOME	0.004106776	0.23217085	0.893
REACTOME_DOWNSTREAM_SIGNAL_TRANSDUCTION	REACTOME	0.004149378	0.23200437	0.966
REACTOME_CD28_DEPENDENT_PI3K_AKT_SIGNALING	REACTOME	0.004166667	0.25671923	0.679
REACTOME_CLASS_B_2_SECRETIN_FAMILY_RECEPTORS	REACTOME	0.00422833	0.24751215	0.791
REACTOME_P75_NTR_RECEPTOR_MEDIATED_SIGNALLING	REACTOME	0.005964215	0.23963746	0.793
REACTOME_INTEGRIN_ALPHAIIB_BETA3_SIGNALING	REACTOME	0.006024096	0.22004622	0.813
REACTOME_SIGNALING_BY_PDGF	REACTOME	0.006048387	0.26569343	0.668
REACTOME_SIGNAL_TRANSDUCTION_BY_L1	REACTOME	0.006048387	0.24925639	0.929
REACTOME_SMOOTH_MUSCLE_CONTRACTION	REACTOME	0.00631579	0.32470444	0.513
REACTOME_METABOLISM_OF_CARBOHYDRATES	REACTOME	0.007797271	0.3127157	0.998
REACTOME_SIGNALLING_TO_ERKS	REACTOME	0.007968128	0.26005664	0.988
REACTOME_HS_GAG_BIOSYNTHESIS	REACTOME	0.008048289	0.21591046	0.817
REACTOME_GASTRIN_CREB_SIGNALLING_PATHWAY_VIA_PKC_AND_MAPK	REACTOME	0.008298756	0.27300233	0.991
REACTOME_SEMAPHORIN_INTERACTIONS	REACTOME	0.00990099	0.23250946	0.809
REACTOME_NOTCH1_INTRACELLULAR_DOMAIN_REGULATES_TRANSCRIPTION	REACTOME	0.012244898	0.25205648	0.981

REACTOME_P130CAS_LINKAGE_TO_MAPK_SIGNALING_FOR_INTEGRINS	REACTOME	0.012371134	0.2632364	0.703
REACTOME_GRB2_SOS_PROVIDES_LINKAGE_TO_MAPK_SIGNALING_FOR_INTERGRINS_	REACTOME	0.012371134	0.21779336	0.831
REACTOME_PI_METABOLISM	REACTOME	0.012474013	0.25229868	0.929
REACTOME_PLATELET_AGGREGATION_PLUG_FORMATION	REACTOME	0.014028057	0.2576922	0.988
REACTOME_HEMOSTASIS	REACTOME	0.014198783	0.28338233	0.997
REACTOME_RESPONSE_TO_ELEVATED_PLATELET_CYTOSOLIC_CA2_	REACTOME	0.015625	0.2240701	0.851
REACTOME_SEMA4D_IN_SEMAPHORIN_SIGNALING	REACTOME	0.015748031	0.21119988	0.831
REACTOME_DOWNSTREAM_TCR_SIGNALING	REACTOME	0.016129032	0.24868692	0.949
REACTOME_SEMA4D_INDUCED_CELL_MIGRATION_AND_GROWTH_CONE_COLLAPSE	REACTOME	0.016161617	0.23207392	0.886
REACTOME_OTHER_SEMAPHORIN_INTERACTIONS	REACTOME	0.018	0.24003094	0.952
REACTOME_TRANSMISSION_ACROSS_CHEMICAL_SYNAPSES	REACTOME	0.01814516	0.2539283	0.988
REACTOME_NUCLEAR_SIGNALING_BY_ERBB4	REACTOME	0.01814516	0.27369186	0.991
REACTOME_NCAM_SIGNALING_FOR_NEURITE_OUT_GROWTH	REACTOME	0.01863354	0.30494705	0.599
REACTOME_EXTRACELLULAR_MATRIX_ORGANIZATION	REACTOME	0.018828452	0.2749102	0.656
REACTOME_ACYL_CHAIN_REMODELLING_OF_PE	REACTOME	0.018947368	0.26741624	0.988
REACTOME_SIGNALING_BY_FGFR_MUTANTS	REACTOME	0.01980198	0.25468048	0.988
REACTOME_DIABETES_PATHWAYS	REACTOME	0.021611001	0.25085908	0.951
REACTOME_MYOGENESIS	REACTOME	0.021956088	0.2474796	0.911
REACTOME_RAP1_SIGNALLING	REACTOME	0.022312373	0.22653966	0.813
REACTOME_CELL_DEATH_SIGNALLING_VIA_NRAGE_NRIF_AND_NADE	REACTOME	0.022403259	0.24449967	0.952
REACTOME_CIRCADIAN_CLOCK	REACTOME	0.022403259	0.28052288	0.997
REACTOME_G_ALPHA_Q_SIGNALLING_EVENTS	REACTOME	0.022821577	0.28192982	0.998
REACTOME_NEURONAL_SYSTEM	REACTOME	0.024193548	0.28348413	0.997
REACTOME_GLYCOSAMINOGLYCAN_METABOLISM	REACTOME	0.024390243	0.25490764	0.929
REACTOME_ACTIVATED_POINT_MUTANTS_OF_FGFR2	REACTOME	0.024390243	0.24852021	0.944
REACTOME_DOWNSTREAM_SIGNALING_OF_ACTIVATED_FGFR	REACTOME	0.025242718	0.3339532	1
REACTOME_SIGNALING_BY_ERBB4	REACTOME	0.026748972	0.24671023	0.976
REACTOME_TRANSCRIPTIONAL_REGULATION_OF_WHITE_ADIPOCYTE_DIFFERENTIATION	REACTOME	0.028957529	0.32913035	1
REACTOME_RAS_ACTIVATION_UOPN_CA2_INFUX_THROUGH_NMDA_RECEPTOR	REACTOME	0.03006012	0.23558456	0.877
REACTOME_NGF_SIGNALLING_VIA_TRKA_FROM_THE_PLASMA_MEMBRANE	REACTOME	0.030487806	0.30239654	0.998
REACTOME_COLLAGEN_FORMATION	REACTOME	0.031712472	0.25439405	0.733
REACTOME_CELL_CELL_COMMUNICATION	REACTOME	0.033464566	0.29693905	0.998
REACTOME_SIGNALING_BY_EGFR_IN_CANCER	REACTOME	0.03353057	0.32806626	1
REACTOME_SIGNALING_BY_FGFR	REACTOME	0.03508772	0.3287987	1
REACTOME_CHONDROITIN_SULFATE_DERMATAN_SULFATE_METABOLISM	REACTOME	0.036363635	0.23524624	0.956
REACTOME_SIGNALING_BY_ROBO_RECEPTOR	REACTOME	0.036363635	0.2828244	0.997
REACTOME_STRIATED_MUSCLE_CONTRACTION	REACTOME	0.037190083	0.23630208	0.954
REACTOME_NCAM1_INTERACTIONS	REACTOME	0.03757829	0.23719299	0.739

REACTOME_SIGNALING_BY_FGFR_IN_DISEASE	REACTOME	0.03815261	0.33262077	1
REACTOME_SIGNALING_BY_ERBB2	REACTOME	0.038854804	0.3314266	1
REACTOME_G_ALPHA1213_SIGNALLING_EVENTS	REACTOME	0.04158004	0.27109525	0.992
REACTOME_UNBLOCKING_OF_NMDA_RECEPTOR_GLUTAMATE_BINDING_AND_ACTIVATION	REACTOME	0.042462844	0.25614145	0.988
REACTOME_MYD88_MAL_CASCADE_INITIATED_ON_PLASMA_MEMBRANE	REACTOME	0.043659043	0.3283036	1
REACTOME_SIGNALING_BY_NOTCH1	REACTOME	0.044088177	0.3268648	0.998
REACTOME_SMAD2_SMAD3_SMAD4_HETEROTRIMER_REGULATES_TRANSCRIPTION	REACTOME	0.04519774	0.28565967	0.997
REACTOME_HEPARAN_SULFATE_HEPARIN_HS_GAG_METABOLISM	REACTOME	0.047808766	0.25139165	0.936
REACTOME_CTLA4_INHIBITORY_SIGNALING	REACTOME	0.053169735	0.28500253	0.998
REACTOME_SHC_RELATED_EVENTS	REACTOME	0.05367793	0.26087067	0.985
REACTOME_SYNTHESIS_OF_PIPS_AT_THE_PLASMA_MEMBRANE	REACTOME	0.05383023	0.28497827	0.997
REACTOME_NRAGE_SIGNALS_DEATH_THROUGH_JNK	REACTOME	0.055555556	0.2853004	0.996
REACTOME_PLC_BETA_MEDIATED_EVENTS	REACTOME	0.055555556	0.28691858	0.998
REACTOME_DEGRADATION_OF_THE_EXTRACELLULAR_MATRIX	REACTOME	0.055670105	0.24722461	0.951
REACTOME_EFFECTS_OF_PIP2_HYDROLYSIS	REACTOME	0.056338027	0.29976577	0.998
REACTOME_TCR_SIGNALING	REACTOME	0.056862745	0.2794434	0.997
REACTOME_SIGNALING_BY_CONSTITUTIVELY_ACTIVE_EGFR	REACTOME	0.059760958	0.23002647	0.966
REACTOME_NEUROTRANSMITTER_RECEPTOR_BINDING_AND_DOWNSTREAM_TRANSMISSION_IN_THE_POSTSYNAPTIC_CELL	REACTOME	0.061143983	0.299749	0.998
REACTOME_PI_3K_CASCADE	REACTOME	0.06418219	0.32761446	1
REACTOME_OPIOID_SIGNALLING	REACTOME	0.06464647	0.29923415	0.998
REACTOME_SIGNAL_AMPLIFICATION	REACTOME	0.06465517	0.283984	0.997
REACTOME_PRE_NOTCH_EXPRESSION_AND_PROCESSING	REACTOME	0.06827309	0.2988784	0.998
REACTOME_CIRCADIAN_REPRESSION_OF_EXPRESSION_BY_REV_ERBA	REACTOME	0.07064018	0.31410003	0.998
REACTOME_POST_CHAPERONIN_TUBULIN_FOLDING_PATHWAY	REACTOME	0.07185629	0.24711274	0.936
REACTOME_NEUROTRANSMITTER_RELEASE_CYCLE	REACTOME	0.073469386	0.2788295	0.993
REACTOME_A_TETRASACCHARIDE_LINKER_SEQUENCE_IS_REQUIRED_FOR_GAG_SYNTHESIS	REACTOME	0.07355865	0.24500555	0.977
REACTOME_ACTIVATED_TLR4_SIGNALLING	REACTOME	0.073619634	0.32829455	1
REACTOME_TIE2_SIGNALING	REACTOME	0.07378641	0.3233947	1
REACTOME_ACTIVATION_OF_NMDA_RECEPTOR_UPON_GLUTAMATE_BINDING_AND_POSTSYNAPTIC_EVENTS	REACTOME	0.076612905	0.32168338	1
REACTOME_TOLL_RECEPTOR_CASCADES	REACTOME	0.077689245	0.32870877	1
REACTOME_INTEGRATION_OF_ENERGY_METABOLISM	REACTOME	0.07936508	0.32500213	1
REACTOME_CHONDROITIN_SULFATE_BIOSYNTHESIS	REACTOME	0.08384458	0.280959	0.997
REACTOME_SIGNALING_BY_NODAL	REACTOME	0.084980235	0.27994627	0.998
REACTOME_SHC1_EVENTS_IN_EGFR_SIGNALING	REACTOME	0.08634538	0.28288525	0.998
REACTOME_REGULATION_OF_INSULIN_LIKE_GROWTH_FACTOR_IGF_ACTIVITY_BY_INSULIN_LIKE_GROWTH_FACTOR_BINDING_PROTEINS_IGFBI	REACTOME	0.0882353	0.28480482	0.997
REACTOME_REGULATION_OF_INSULIN_SECRETION	REACTOME	0.09202454	0.32412344	1
REACTOME_G_ALPHA_Z_SIGNALLING_EVENTS	REACTOME	0.093495935	0.3244087	1
REACTOME_NETRIN1_SIGNALING	REACTOME	0.09356725	0.30178303	0.998

REACTOME_PI3K_EVENTS_IN_ERBB2_SIGNALING	REACTOME	0.0960334	0.3284108	1
REACTOME_SYNTHESIS_OF_PIPS_AT_THE_GOLGI_MEMBRANE	REACTOME	0.0970297	0.2798374	0.997
REACTOME_BMAL1_CLOCK_NPAS2_ACTIVATES_CIRCADIAN_EXPRESSION	REACTOME	0.09775967	0.3219142	1
REACTOME_INSULIN_SYNTHESIS_AND_PROCESSING	REACTOME	0.09861933	0.2962775	0.998
REACTOME_POTASSIUM_CHANNELS	REACTOME	0.10220441	0.3258145	1
REACTOME_INTERACTION_BETWEEN_L1_AND_ANKYRINS	REACTOME	0.103375524	0.32748824	0.998
REACTOME_IMMUNOREGULATORY_INTERACTIONS_BETWEEN_A_LYMPHOID_AND_A_NON_LYMPHOID_CELL	REACTOME	0.10927835	0.33035788	1
REACTOME_SIGNALING_BY_HIPPO	REACTOME	0.115530305	0.30865756	0.998
REACTOME_ADP_SIGNALLING_THROUGH_P2RY1	REACTOME	0.11940298	0.3161717	0.998
REACTOME_IL_2_SIGNALING	REACTOME	0.123203285	0.32519415	1
REACTOME_GRB2_EVENTS_IN_ERBB2_SIGNALING	REACTOME	0.12450593	0.32897526	1
REACTOME_ACYL_CHAIN_REMODELLING_OF_PC	REACTOME	0.13347457	0.32896888	1
REACTOME_SHC_MEDIATED_SIGNALLING	REACTOME	0.13872832	0.3229409	1
REACTOME_PI3K_EVENTS_IN_ERBB4_SIGNALING	REACTOME	0.14257029	0.34992045	1
REACTOME_GLUTAMATE_NEUROTRANSMITTER_RELEASE_CYCLE	REACTOME	0.14728682	0.32513803	1
REACTOME_THROMBIN_SIGNALLING_THROUGH_PROTEINASE_ACTIVATED_RECEPTORS_PARS	REACTOME	0.14822547	0.32844713	1
REACTOME_SIGNALING_BY_FGFR1_FUSION_MUTANTS	REACTOME	0.14928426	0.32928428	1
REACTOME_GAB1_SIGNALOSOME	REACTOME	0.15212981	0.33141497	1
REACTOME_PD1_SIGNALING	REACTOME	0.1557377	0.32983807	1
REACTOME_GABA_RECEPTOR_ACTIVATION	REACTOME	0.15655577	0.3226219	1
REACTOME_PI3K_AKT_ACTIVATION	REACTOME	0.15690376	0.35738695	1
REACTOME_CREB_PHOSPHORYLATION_THROUGH_THE_ACTIVATION_OF_CAMKII	REACTOME	0.15809524	0.3295535	1
REACTOME_ADHERENS_JUNCTIONS_INTERACTIONS	REACTOME	0.1610338	0.329095	1
REACTOME_G_PROTEIN_BETA_GAMMA_SIGNALLING	REACTOME	0.16170213	0.33044824	1
REACTOME_GAP_JUNCTION_TRAFFICKING	REACTOME	0.1628866	0.36222064	1
REACTOME_PROTEIN_FOLDING	REACTOME	0.16441005	0.3270723	1
REACTOME_BASIGIN_INTERACTIONS	REACTOME	0.16496944	0.32799527	1
REACTOME_POST_NMDA_RECEPTOR_ACTIVATION_EVENTS	REACTOME	0.17137097	0.35828114	1
REACTOME_G_PROTEIN_ACTIVATION	REACTOME	0.17456897	0.35015082	1
REACTOME_SIGNALING_BY_RHO_GTPASES	REACTOME	0.1755424	0.37313068	1
REACTOME_TRANSPORT_TO_THE_GOLGI_AND_SUBSEQUENT_MODIFICATION	REACTOME	0.17922607	0.34853542	1
REACTOME_INSULIN_RECEPTOR_SIGNALLING_CASCADE	REACTOME	0.1799591	0.39856154	1
REACTOME_THROMBOXANE_SIGNALLING_THROUGH_TP_RECEPTOR	REACTOME	0.18025751	0.32612854	1
REACTOME_GPCR_LIGAND_BINDING	REACTOME	0.18219462	0.39871272	1
REACTOME_SIGNALING_BY_SCF_KIT	REACTOME	0.1827112	0.3726675	1
REACTOME_RORA_ACTIVATES_CIRCADIAN_EXPRESSION	REACTOME	0.18480493	0.34820315	1
REACTOME_CREB_PHOSPHORYLATION_THROUGH_THE_ACTIVATION_OF_RAS	REACTOME	0.18577075	0.35927606	1
REACTOME_GLUCAGON_TYPE_LIGAND_RECEPTORS	REACTOME	0.18589744	0.32380924	1

REACTOME_ANTIGEN_PROCESSING_CROSS_PRESENTATION	REACTOME	0.1875	0.33319962	1
REACTOME_GABA_B_RECEPTOR_ACTIVATION	REACTOME	0.18787879	0.34142375	1
REACTOME_KERATAN_SULFATE_KERATIN_METABOLISM	REACTOME	0.18997912	0.3308823	1
REACTOME_SIGNALING_BY_INSULIN_RECEPTOR	REACTOME	0.19560878	0.4002343	1
REACTOME_KERATAN_SULFATE_BIOSYNTHESIS	REACTOME	0.19668737	0.33144927	1
REACTOME_JNK_C_JUN_KINASES_PHOSPHORYLATION_AND_ACTIVATION_MEDIATED_BY_ACTIVATED_HUMAN_TAK1	REACTOME	0.19795918	0.34449878	1
REACTOME_HS_GAG_DEGRADATION	REACTOME	0.1979798	0.3489778	1
REACTOME_NEPHRIN_INTERACTIONS	REACTOME	0.20164609	0.3733181	1
REACTOME_IL_RECEPTOR_SHC_SIGNALING	REACTOME	0.20502092	0.36008283	1
REACTOME_HDL_MEDIATED_LIPID_TRANSPORT	REACTOME	0.20731707	0.32820785	1
REACTOME_G_BETA_GAMMA_SIGNALLING_THROUGH_PLC_BETA	REACTOME	0.20754717	0.32693923	1
REACTOME_CELL_JUNCTION_ORGANIZATION	REACTOME	0.21188119	0.37920493	1
REACTOME_IL1_SIGNALING	REACTOME	0.22109534	0.379856	1
REACTOME_TRAF6_MEDIATED_INDUCTION_OF_NFKB_AND_MAP_KINASES_UPON_TLR7_8_OR_9_ACTIVATION	REACTOME	0.22268908	0.41069278	1
REACTOME_N_GLYCAN_ANTENNAE_ELONGATION_IN_THE_MEDIAL_TRANS_GOLGI	REACTOME	0.22403258	0.36706555	1
REACTOME_G_ALPHA_S_SIGNALLING_EVENTS	REACTOME	0.2244898	0.39475402	1
REACTOME_UNFOLDED_PROTEIN_RESPONSE	REACTOME	0.22568093	0.38747323	1
REACTOME_SYNTHESIS_SECRETION_AND_DEACYLATION_OF_GHRELIN	REACTOME	0.22916667	0.39289185	1
REACTOME_SIGNALING_BY_THE_B_CELL_RECEPTOR_BCR	REACTOME	0.2296748	0.3978931	1
REACTOME_PLATELET_HOMEOSTASIS	REACTOME	0.2314225	0.4005247	1
REACTOME_CTNNB1_PHOSPHORYLATION_CASCADE	REACTOME	0.234714	0.3291482	1
REACTOME_NUCLEAR_EVENTS_KINASE_AND_TRANSCRIPTION_FACTOR_ACTIVATION	REACTOME	0.24081632	0.36574677	1
REACTOME_GROWTH_HORMONE_RECEPTOR_SIGNALING	REACTOME	0.24568966	0.36284536	1
REACTOME_FORMATION_OF_TUBULIN_FOLDING_INTERMEDIATES_BY_CCT_TRIC	REACTOME	0.24900399	0.36852872	1
REACTOME_DOWNSTREAM_SIGNALING_EVENTS_OF_B_CELL_RECEPTOR_BCR	REACTOME	0.25311205	0.39305526	1
REACTOME_SIGNALING_BY_ILS	REACTOME	0.25562373	0.43739653	1
REACTOME_PIP3_ACTIVATES_AKT_SIGNALING	REACTOME	0.2580645	0.39920583	1
REACTOME_G_BETA_GAMMA_SIGNALLING_THROUGH_PI3KGAMMA	REACTOME	0.25902337	0.37023848	1
REACTOME_NEGATIVE_REGULATORS_OF_RIG_I_MDA5_SIGNALING	REACTOME	0.26078027	0.38571507	1
REACTOME_IL_3_5_AND_GM_CSF_SIGNALING	REACTOME	0.26293996	0.40824696	1
REACTOME_INHIBITION_OF_VOLTAGE_GATED_CA2_CHANNELS_VIA_GBETA_GAMMA_SUBUNITS	REACTOME	0.26793247	0.37496087	1
REACTOME_MAP_KINASE_ACTIVATION_IN_TLR_CASCADE	REACTOME	0.27087575	0.424824	1
REACTOME_INHIBITION_OF_INSULIN_SECRETION_BY_ADRENALINE_NORADRENALINE	REACTOME	0.27310926	0.39240447	1
REACTOME_GLUCAGON_SIGNALING_IN_METABOLIC_REGULATION	REACTOME	0.27327934	0.42668998	1
REACTOME_VOLTAGE_GATED_POTASSIUM_CHANNELS	REACTOME	0.2761905	0.3777031	1
REACTOME_OLFACTORY_SIGNALING_PATHWAY	REACTOME	0.2782258	0.37659118	1
REACTOME_ACTIVATION_OF_BH3_ONLY_PROTEINS	REACTOME	0.27926078	0.37521905	1
REACTOME_NFKB_AND_MAP_KINASES_ACTIVATION_MEDIATED_BY_TLR4_SIGNALING_REPERTOIRE	REACTOME	0.27966103	0.4394963	1

REACTOME_PYRIMIDINE_METABOLISM	REACTOME	0.2805907	0.4261171	1
REACTOME_TRANSPORT_OF_GLUCOSE_AND_OTHER_SUGARS_BILE_SALTS_AND_ORGANIC_ACIDS_METAL_IONS_AND_AMINE_COMPOUNDS	REACTOME	0.28803244	0.42935404	1
REACTOME_ACTIVATION_OF_CHAPERONE_GENES_BY_XBP1S	REACTOME	0.29124236	0.37474626	1
REACTOME_CA_DEPENDENT_EVENTS	REACTOME	0.29501915	0.4521635	1
REACTOME_MAPK_TARGETS_NUCLEAR_EVENTS_MEDIATED_BY_MAP_KINASES	REACTOME	0.30040324	0.39665794	1
REACTOME_NEGATIVE_REGULATION_OF_FGFR_SIGNALING	REACTOME	0.30218688	0.45186204	1
REACTOME_PI3K_CASCADE	REACTOME	0.30497926	0.45263076	1
REACTOME_INCRETIN_SYNTHESIS_SECRETION_AND_INACTIVATION	REACTOME	0.3131991	0.40868554	1
REACTOME_ASSOCIATION_OF_TRIC_CCT_WITH_TARGET_PROTEINS_DURING_BIOSYNTHESIS	REACTOME	0.32007575	0.43748567	1
REACTOME_ADP_SIGNALLING_THROUGH_P2RY12	REACTOME	0.32484075	0.4343321	1
REACTOME_PLATELET_SENSITIZATION_BY_LDL	REACTOME	0.334004	0.4535328	1
REACTOME_ACTIVATION_OF_KAINATE_RECEPTORS_UPON_GLUTAMATE_BINDING	REACTOME	0.33887735	0.42012647	1
REACTOME_GPVI_MEDIATED_ACTIVATION_CASCADE	REACTOME	0.3472222	0.43783134	1
REACTOME_PHOSPHOLIPASE_C_MEDIATED_CASCADE	REACTOME	0.3488372	0.5029352	1
REACTOME_GABA_SYNTHESIS_RELEASE_REUPTAKE_AND_DEGRADATION	REACTOME	0.35341364	0.44305515	1
REACTOME_SYNTHESIS_SECRETION_AND_INACTIVATION_OF_GLP1	REACTOME	0.36147186	0.43114588	1
REACTOME_INWARDLY_RECTIFYING_K_CHANNELS	REACTOME	0.37894738	0.4501165	1
REACTOME_MEMBRANE_TRAFFICKING	REACTOME	0.3806706	0.47394824	1
REACTOME_INSULIN_RECEPTOR_RECYCLING	REACTOME	0.39059305	0.4918246	1
REACTOME_ERK_MAPK_TARGETS	REACTOME	0.40408164	0.45055467	1
REACTOME_OXYGEN_DEPENDENT_PROLINE_HYDROXYLATION_OF_HYPOXIA_INDUCIBLE_FACTOR_ALPHA	REACTOME	0.4265873	0.5013527	1
REACTOME_FRS2_MEDIATED_CASCADE	REACTOME	0.43460765	0.51945704	1
REACTOME_ACTIVATION_OF_NF_KAPPAB_IN_B_CELLS	REACTOME	0.43991855	0.52947336	1
REACTOME_TRIF_MEDIATED_TLR3_SIGNALING	REACTOME	0.44583333	0.536109	1
REACTOME_PREFOLDIN_MEDIATED_TRANSFER_OF_SUBSTRATE_TO_CCT_TRIC	REACTOME	0.45759368	0.5363732	1
REACTOME_SHC_MEDIATED_CASCADE	REACTOME	0.46558705	0.56682193	1
REACTOME_SHC1_EVENTS_IN_ERBB4_SIGNALING	REACTOME	0.47162426	0.56457573	1
REACTOME_PROSTACYCLIN_SIGNALLING_THROUGH_PROSTACYCLIN_RECEPTOR	REACTOME	0.48723406	0.5781133	1
REACTOME_REGULATION_OF_IFNA_SIGNALING	REACTOME	0.4979424	0.59973633	1
REACTOME_LATENT_INFECTION_OF_HOMO_SAPIENS_WITH_MYCOBACTERIUM_TUBERCULOSIS	REACTOME	0.4990099	0.5871416	1
REACTOME_DAG_AND_IP3_SIGNALING	REACTOME	0.5057915	0.5787475	1
REACTOME_LIGAND_GATED_ION_CHANNEL_TRANSPORT	REACTOME	0.50857145	0.59067005	1
REACTOME_CYTOKINE_SIGNALING_IN_IMMUNE_SYSTEM	REACTOME	0.52025586	0.583416	1
REACTOME_ACETYLCHOLINE_BINDING_AND_DOWNSTREAM_EVENTS	REACTOME	0.5234375	0.5931487	1
REACTOME_TERMINATION_OF_O_GLYCAN_BIOSYNTHESIS	REACTOME	0.5387597	0.58463204	1
REACTOME_DEFENSINS	REACTOME	0.5875	0.6639476	1
REACTOME_FGFR_LIGAND_BINDING_AND_ACTIVATION	REACTOME	0.58964145	0.63852566	1
REACTOME_PKA_MEDIATED_PHOSPHORYLATION_OF_CREB	REACTOME	0.6003788	0.6547844	1

REACTOME_BETA_DEFENSINS	REACTOME	0.60991377	0.6945276	1
REACTOME_ACTIVATION_OF_GENES_BY_ATF4	REACTOME	0.6184739	0.69640636	1
REACTOME_REGULATION_OF_SIGNALING_BY_CBL	REACTOME	0.6277228	0.65669465	1
REACTOME_REGULATION_OF_HYPOXIA_INDUCIBLE_FACTOR_HIF_BY_OXYGEN	REACTOME	0.642	0.6977118	1
REACTOME_ACYL_CHAIN_REMODELLING_OF_PS	REACTOME	0.64681727	0.68370587	1
REACTOME_PROLONGED_ERK_ACTIVATION_EVENTS	REACTOME	0.6487026	0.6829492	1
REACTOME_FACTORS_INVOLVED_IN_MEGAKARYOCYTE_DEVELOPMENT_AND_PLATELET_PRODUCTION	REACTOME	0.655706	0.7207404	1
REACTOME_PHOSPHORYLATION_OF_CD3_AND_TCR_ZETA_CHAINS	REACTOME	0.66262627	0.74118894	1
REACTOME_LIPOPROTEIN_METABOLISM	REACTOME	0.66735536	0.71920806	1
REACTOME_EGFR_DOWNREGULATION	REACTOME	0.7153996	0.698543	1
REACTOME_G1_PHASE	REACTOME	0.7247525	0.7448583	1
REACTOME_ANTIGEN_ACTIVATES_B_CELL_RECEPTOR_LEADING_TO_GENERATION_OF_SECOND_MESSENGERS	REACTOME	0.76953906	0.7667614	1
REACTOME_ARMS_MEDIATED_ACTIVATION	REACTOME	0.83430797	0.844075	1
REACTOME_PTM_GAMMA_CARBOXYLATION_HYPUSINE_FORMATION_AND_ARYLSULFATASE_ACTIVATION	REACTOME	0.84166664	0.8691274	1
REACTOME_INFLAMMASOMES	REACTOME	0.8441815	0.81469715	1
REACTOME_PROTEOLYTIC_CLEAVAGE_OF_SNARE_COMPLEX_PROTEINS	REACTOME	0.87866926	0.8793891	1
REACTOME_ACTIVATED_NOTCH1_TRANSMITS_SIGNAL_TO_THE_NUCLEUS	REACTOME	0.88293654	0.8689792	1
REACTOME_BOTULINUM_NEUROTOXICITY	REACTOME	0.9001957	0.8991205	1
REACTOME_ACYL_CHAIN_REMODELLING_OF_PI	REACTOME	0.91549295	0.8765289	1
REACTOME_CGMP_EFFECTS	REACTOME	0.92354125	0.8787303	1
REACTOME_NITRIC_OXIDE_STIMULATES_GUANYLATE_CYCLASE	REACTOME	0.92421055	0.8652372	1
REACTOME_RIP_MEDIATED_NFKB_ACTIVATION_VIA_DAI	REACTOME	0.9631902	0.976541	1

Table S3. All the gene sets enriched in FAC cells at D14 of culture compared with D1 hepatocytes (assessed by GSEA)

NAME	Data base	NOM p-val	FDR q-val	FWER p-val
HALLMARK_GLYCOLYSIS	HALLMARK	0	0.7723993	0.31
HALLMARK_MITOTIC_SPINDLE	HALLMARK	0	0.40886086	0.325
HALLMARK_ESTROGEN_RESPONSE_LATE	HALLMARK	0	0.28703052	0.337
HALLMARK_ESTROGEN_RESPONSE_EARLY	HALLMARK	0	0.30188328	0.513
HALLMARK_APICAL_JUNCTION	HALLMARK	0.00204918	0.22587866	0.345
HALLMARK_G2M_CHECKPOINT	HALLMARK	0.002079002	0.198052	0.365
HALLMARK_MYOGENESIS	HALLMARK	0.014736842	0.24096768	0.523
HALLMARK_E2F_TARGETS	HALLMARK	0.019067796	0.26477665	0.516
HALLMARK_SPERMATOGENESIS	HALLMARK	0.041501977	0.2996557	0.68
HALLMARK_P53_PATHWAY	HALLMARK	0.052301254	0.27523178	0.7
HALLMARK_WNT_BETA_CATENIN_SIGNALING	HALLMARK	0.055555556	0.2485178	0.715
HALLMARK_APOPTOSIS	HALLMARK	0.058467742	0.25779	0.713
HALLMARK_APICAL_SURFACE	HALLMARK	0.071428575	0.3019745	0.67
HALLMARK_EPITHELIAL_MESENCHYMAL_TRANSITION	HALLMARK	0.07707911	0.21365157	0.552
HALLMARK_IL2_STAT5_SIGNALING	HALLMARK	0.10865191	0.2975242	0.774
HALLMARK_PROTEIN_SECRETION	HALLMARK	0.11287129	0.21933454	0.531
HALLMARK_MTORC1_SIGNALING	HALLMARK	0.17479675	0.26067865	0.703
HALLMARK_ADIPOGENESIS	HALLMARK	0.18737672	0.30644655	0.772
HALLMARK_REACTIVE_OXIGEN_SPECIES_PATHWAY	HALLMARK	0.21518987	0.27716193	0.747
HALLMARK_OXIDATIVE_PHOSPHORYLATION	HALLMARK	0.21676892	0.2929448	0.697
HALLMARK_HEME_METABOLISM	HALLMARK	0.22244489	0.32734865	0.824
HALLMARK_NOTCH_SIGNALING	HALLMARK	0.23565574	0.35386723	0.862
HALLMARK_UV_RESPONSE_DN	HALLMARK	0.23935091	0.33959162	0.817
HALLMARK_CHOLESTEROL_HOMEOSTASIS	HALLMARK	0.29158512	0.33648738	0.84
HALLMARK_HYPOXIA	HALLMARK	0.30184805	0.42338282	0.916
HALLMARK_ALLOGRAFT_REJECTION	HALLMARK	0.31411532	0.44160774	0.927
HALLMARK_PANCREAS_BETA_CELLS	HALLMARK	0.32251522	0.37625432	0.887
HALLMARK_MYC_TARGETS_V1	HALLMARK	0.34215885	0.33057216	0.821
HALLMARK_ANGIOGENESIS	HALLMARK	0.3501048	0.33168286	0.835
HALLMARK_DNA_REPAIR	HALLMARK	0.38729507	0.38013265	0.887
HALLMARK_PEROXISOME	HALLMARK	0.3884462	0.42333442	0.918
HALLMARK_UNFOLDED_PROTEIN_RESPONSE	HALLMARK	0.43286574	0.44448406	0.927
HALLMARK_PI3K_AKT_MTOR_SIGNALING	HALLMARK	0.4871795	0.5088305	0.958
HALLMARK_FATTY_ACID_METABOLISM	HALLMARK	0.5149105	0.52106726	0.958
HALLMARK_HEDGEHOG_SIGNALING	HALLMARK	0.53166986	0.524049	0.963
HALLMARK_KRAS_SIGNALING_UP	HALLMARK	0.5697446	0.5549849	0.97
HALLMARK_ANDROGEN_RESPONSE	HALLMARK	0.614	0.5705363	0.973
HALLMARK_MYC_TARGETS_V2	HALLMARK	0.6204082	0.7148062	0.989
HALLMARK_INTERFERON_ALPHA_RESPONSE	HALLMARK	0.64908725	0.57167804	0.974
KEGG_CELL_CYCLE	KEGG	0	0	0
KEGG_LYSOSOME	KEGG	0	0	0

KEGG_OOCYTE_MEIOSIS	KEGG	0	0	0
KEGG_AMINOACYL_TRNA_BIOSYNTHESIS	KEGG	0	0	0
KEGG_DNA_REPLICATION	KEGG	0	0	0
KEGG_PROGESTERONE_MEDIATED_OOCYTE_MATURATION	KEGG	0	0	0
KEGG_GLUTATHIONE_METABOLISM	KEGG	0	0	0
KEGG_NUCLEOTIDE_EXCISION_REPAIR	KEGG	0	0	0
KEGG_REGULATION_OF_ACTIN_CYTOSKELETON	KEGG	0	0	0
KEGG_FOCAL_ADHESION	KEGG	0	0	0
KEGG_ECM_RECEPTOR_INTERACTION	KEGG	0	0	0
KEGG_PHOSPHATIDYLINOSITOL_SIGNALING_SYSTEM	KEGG	0	0	0
KEGG_SMALL_CELL_LUNG_CANCER	KEGG	0	0	0
KEGG_BASE_EXCISION_REPAIR	KEGG	0	0	0
KEGG_VASOPRESSIN_REGULATED_WATER_REABSORPTION	KEGG	0	0	0
KEGG_P53_SIGNALING_PATHWAY	KEGG	0	0	0
KEGG_VIBRIO_CHOLERAE_INFECTION	KEGG	0	0	0
KEGG_ADHERENS_JUNCTION	KEGG	0	0	0
KEGG_MISMATCH_REPAIR	KEGG	0	0	0
KEGG_UBIQUITIN_MEDIATED_PROTEOLYSIS	KEGG	0	0	0
KEGG_N_GLYCAN_BIOSYNTHESIS	KEGG	0	0	0
KEGG_OTHER_GLYCAN_DEGRADATION	KEGG	0	0	0
KEGG_PURINE_METABOLISM	KEGG	0	0	0
KEGG_AXON_GUIDANCE	KEGG	0	0	0
KEGG_AMINO_SUGAR_AND_NUCLEOTIDE_SUGAR_METABOLISM	KEGG	0	0	0
KEGG_RIBOSOME	KEGG	0	0	0
KEGG_GLYCOSYLPHOSPHATIDYLINOSITOL_GPI_ANCHOR_BIOSYNTHESIS	KEGG	0	6.62E-05	0.001
KEGG_O_GLYCAN_BIOSYNTHESIS	KEGG	0	6.38E-05	0.001
KEGG_HOMOLOGOUS_RECOMBINATION	KEGG	0	6.16E-05	0.001
KEGG_FRUCTOSE_AND_MANNOSE_METABOLISM	KEGG	0	1.69E-04	0.003
KEGG_GLYCOSAMINOGLYCAN_DEGRADATION	KEGG	0	1.64E-04	0.003
KEGG_GAP_JUNCTION	KEGG	0	2.62E-04	0.005
KEGG_ENDOCYTOSIS	KEGG	0	3.14E-04	0.006
KEGG_TIGHT_JUNCTION	KEGG	0	4.50E-04	0.009
KEGG_APOPTOSIS	KEGG	0	4.37E-04	0.009
KEGG_INOSITOL_PHOSPHATE_METABOLISM	KEGG	0	4.25E-04	0.009
KEGG_PANCREATIC_CANCER	KEGG	0	5.03E-04	0.011
KEGG_FC_GAMMA_R_MEDIATED_PHAGOCYTOSIS	KEGG	0	5.34E-04	0.012
KEGG_COLORECTAL_CANCER	KEGG	0	9.53E-04	0.022
KEGG_DILATED_CARDIOMYOPATHY	KEGG	0	0.001616864	0.038
KEGG_INSULIN_SIGNALING_PATHWAY	KEGG	0	0.001986736	0.046
KEGG_PATHWAYS_IN_CANCER	KEGG	0	0.003456226	0.084
KEGG_PYRIMIDINE_METABOLISM	KEGG	0	0.004266664	0.106
KEGG_ENDOMETRIAL_CANCER	KEGG	0	0.004352812	0.111
KEGG_LEUKOCYTE_TRANSENDOTHELIAL_MIGRATION	KEGG	0	0.004411798	0.114

KEGG_CHRONIC_MYELOID_LEUKEMIA	KEGG	0	0.007003753	0.178
KEGG_WNT_SIGNALING_PATHWAY	KEGG	0	0.01072876	0.271
KEGG_GLIOMA	KEGG	0	0.010621405	0.274
KEGG_MELANOGENESIS	KEGG	0	0.01156208	0.3
KEGG_ALZHEIMERS_DISEASE	KEGG	0	0.012936451	0.347
KEGG_HUNTINGTONS_DISEASE	KEGG	0	0.015376451	0.435
KEGG_CALCIUM_SIGNALING_PATHWAY	KEGG	0	0.01631627	0.47
KEGG_CHEMOKINE_SIGNALING_PATHWAY	KEGG	0	0.019824699	0.576
KEGG_MAPK_SIGNALING_PATHWAY	KEGG	0.002155172	0.067673706	0.984
KEGG_PROSTATE_CANCER	KEGG	0.002197802	0.01527281	0.426
KEGG_STARCH_AND_SUCROSE_METABOLISM	KEGG	0.002222222	0.014982908	0.41
KEGG_GNRH_SIGNALING_PATHWAY	KEGG	0.002222222	0.016675703	0.488
KEGG_ARRHYTHMOGENIC_RIGHT_VENTRICULAR_CARDIOMYOPATHY_ARVC	KEGG	0.002247191	0.018730922	0.552
KEGG_GALACTOSE_METABOLISM	KEGG	0.002288329	0.003202736	0.076
KEGG_ERBB_SIGNALING_PATHWAY	KEGG	0.002288329	0.015575612	0.446
KEGG_NEUROTROPHIN_SIGNALING_PATHWAY	KEGG	0.002298851	0.015015173	0.407
KEGG_LYSINE_DEGRADATION	KEGG	0.002358491	0.015358713	0.424
KEGG_LONG_TERM_POTENTIATION	KEGG	0.002415459	0.015616251	0.451
KEGG_AMYOTROPHIC_LATERAL_SCLEROSIS_ALS	KEGG	0.004405286	0.010494809	0.255
KEGG_NON_SMALL_CELL_LUNG_CANCER	KEGG	0.004474273	0.010810233	0.268
KEGG_GLYCEROPHOSPHOLIPID_METABOLISM	KEGG	0.004545454	0.013242764	0.364
KEGG_VALINE_LEUCINE_AND_ISOLEUCINE_DEGRADATION	KEGG	0.004739337	0.017759304	0.518
KEGG_GLYCOSPHINGOLIPID_BIOSYNTHESIS_GANGLIO_SERIES	KEGG	0.004938272	0.005373636	0.137
KEGG_VASCULAR_SMOOTH_MUSCLE_CONTRACTION	KEGG	0.008658009	0.040922906	0.869
KEGG_SPHINGOLIPID_METABOLISM	KEGG	0.008888889	0.013143363	0.346
KEGG_GLYCOSAMINOGLYCAN_BIOSYNTHESIS_CHONDROITIN_SULFATE	KEGG	0.009049774	0.014737287	0.41
KEGG_THYROID_CANCER	KEGG	0.009259259	0.01309296	0.355
KEGG_PATHOGENIC_ESCHERICHIA_COLI_INFECTION	KEGG	0.011389522	0.02432695	0.658
KEGG_ABC_TRANSPORTERS	KEGG	0.011655011	0.013329947	0.362
KEGG_GLYCOSPHINGOLIPID_BIOSYNTHESIS_LACTO_AND_NEOLACTO_SERIES	KEGG	0.011961723	0.016869238	0.487
KEGG_MTOR_SIGNALING_PATHWAY	KEGG	0.013636364	0.025632897	0.685
KEGG_GLYCOSAMINOGLYCAN_BIOSYNTHESIS_HEPARAN_SULFATE	KEGG	0.014018691	0.018549422	0.536
KEGG_BIOSYNTHESIS_OF_UNSATURATED_FATTY_ACIDS	KEGG	0.014319809	0.018474327	0.542
KEGG_MELANOMA	KEGG	0.017278617	0.033582814	0.797
KEGG_NOTCH_SIGNALING_PATHWAY	KEGG	0.018181818	0.027876204	0.716
KEGG_HYPERTROPHIC_CARDIOMYOPATHY_HCM	KEGG	0.018518519	0.05076178	0.937
KEGG_METABOLISM_OF_XENOBIOTICS_BY_CYTOCHROME_P450	KEGG	0.019607844	0.048371077	0.922
KEGG_GLYCEROLIPID_METABOLISM	KEGG	0.021413276	0.031003203	0.768
KEGG_BLADDER_CANCER	KEGG	0.025462963	0.052480165	0.949
KEGG_ETHER_LIPID_METABOLISM	KEGG	0.02764977	0.028341327	0.726
KEGG_SELENOAMINO_ACID_METABOLISM	KEGG	0.027713627	0.021582056	0.61
KEGG_PROPANOATE_METABOLISM	KEGG	0.032397408	0.03986285	0.857
KEGG_PYRUVATE_METABOLISM	KEGG	0.038297873	0.043947835	0.893

KEGG_FC_EPSILON_RI_SIGNALING_PATHWAY	KEGG	0.041284405	0.0717209	0.988
KEGG_VEGF_SIGNALING_PATHWAY	KEGG	0.045454547	0.08156346	0.992
KEGG_BUTANOATE_METABOLISM	KEGG	0.04793028	0.050346125	0.938
KEGG_RIBOFLAVIN_METABOLISM	KEGG	0.0520362	0.045024633	0.903
KEGG_PENTOSE_AND_GLUCURONATE_INTERCONVERSIONS	KEGG	0.055684455	0.0422941	0.879
KEGG_RENAL_CELL_CARCINOMA	KEGG	0.063318774	0.09984917	0.998
KEGG_EPITHELIAL_CELL_SIGNALING_IN_HELICOBACTER_PYLORI_INFECTION	KEGG	0.06864989	0.11024506	0.998
KEGG_LEISHMANIA_INFECTION	KEGG	0.06896552	0.11621386	0.998
KEGG_CITRATE_CYCLE_TCA_CYCLE	KEGG	0.07434053	0.048649922	0.919
KEGG_ARGININE_AND_PROLINE_METABOLISM	KEGG	0.08057851	0.094120145	0.996
KEGG_NOD_LIKE_RECEPTOR_SIGNALING_PATHWAY	KEGG	0.08658009	0.11733061	0.999
KEGG_CELL_ADHESION_MOLECULES_CAMS	KEGG	0.09803922	0.19722567	1
KEGG_PENTOSE_PHOSPHATE_PATHWAY	KEGG	0.10609481	0.09888695	0.998
KEGG_ASCORBATE_AND_ALDARATE_METABOLISM	KEGG	0.11590909	0.09826752	0.998
KEGG_OXIDATIVE_PHOSPHORYLATION	KEGG	0.12334802	0.19605072	1
KEGG_VIRAL_MYOCARDITIS	KEGG	0.12471655	0.18410188	1
KEGG_RNA_DEGRADATION	KEGG	0.12527964	0.18487182	1
KEGG_TGF_BETA_SIGNALING_PATHWAY	KEGG	0.13348417	0.18209364	1
KEGG_BASAL_TRANSCRIPTION_FACTORS	KEGG	0.13876653	0.13069779	1
KEGG_REGULATION_OF_AUTOPHAGY	KEGG	0.13943355	0.14972553	1
KEGG_PEROXISOME	KEGG	0.14732143	0.1817419	1
KEGG_PHENYLALANINE_METABOLISM	KEGG	0.15246637	0.15060557	1
KEGG_GLYCOLYSIS_GLUCONEOGENESIS	KEGG	0.15367965	0.19832751	1
KEGG_NATURAL_KILLER_CELL_MEDIATED_CYTOTOXICITY	KEGG	0.15418503	0.23342331	1
KEGG_PORPHYRIN_AND_CHLOROPHYLL_METABOLISM	KEGG	0.16216215	0.18325478	1
KEGG_HISTIDINE_METABOLISM	KEGG	0.19955157	0.20490012	1
KEGG_NICOTINATE_AND_NICOTINAMIDE_METABOLISM	KEGG	0.20941177	0.2125814	1
KEGG_CARDIAC_MUSCLE_CONTRACTION	KEGG	0.21158129	0.23373218	1
KEGG_ACUTE_MYELOID_LEUKEMIA	KEGG	0.23340471	0.2608107	1
KEGG_DORSO_VENTRAL_AXIS_FORMATION	KEGG	0.23515981	0.20635562	1
KEGG_CYTOSOLIC_DNA_SENSING_PATHWAY	KEGG	0.25	0.29340875	1
KEGG_TRYPTOPHAN_METABOLISM	KEGG	0.33566433	0.3560652	1
KEGG_T_CELL_RECEPTOR_SIGNALING_PATHWAY	KEGG	0.34151787	0.39606786	1
KEGG_TOLL_LIKE_RECEPTOR_SIGNALING_PATHWAY	KEGG	0.34597155	0.38018134	1
KEGG_PARKINSONS_DISEASE	KEGG	0.35729846	0.4223987	1
KEGG_HEDGEHOG_SIGNALING_PATHWAY	KEGG	0.35869566	0.39523086	1
KEGG_PROTEIN_EXPORT	KEGG	0.37938598	0.40231144	1
KEGG_ALDOSTERONE_REGULATED_SODIUM_REABSORPTION	KEGG	0.40950227	0.42508033	1
KEGG_CYSTEINE_AND_METHIONINE_METABOLISM	KEGG	0.4483568	0.48203516	1
KEGG_PANTOTHENATE_AND_COA_BIOSYNTHESIS	KEGG	0.504329	0.5433458	1
KEGG_BASAL_CELL_CARCINOMA	KEGG	0.53900707	0.5465684	1
KEGG_RIG_I_LIKE_RECEPTOR_SIGNALING_PATHWAY	KEGG	0.5409091	0.59091693	1
KEGG_TYPE_II_DIABETES_MELLITUS	KEGG	0.6143498	0.652293	1

KEGG_RNA_POLYMERASE	KEGG	0.70509976	0.7758138	1
KEGG_SNARE_INTERACTIONS_IN_VESICULAR_TRANSPORT	KEGG	0.73660713	0.73980784	1
KEGG_PROTEASOME	KEGG	0.77412283	0.78505254	1
REACTOME_THE_ROLE_OF_NEF_IN_HIV1_REPLICATION_AND_DISEASE_PATHOGENESIS	REACTOME	0	1	0.268
REACTOME_O_LINKED_GLYCOSYLATION_OF_MUCINS	REACTOME	0	0.8851604	0.351
REACTOME_NEF_MEDIATES_DOWN_MODULATION_OF_CELL_SURFACE_RECEPTORS_BY_RECRUITING_THEM_TO_CLATHRIN_ADAPTERS	REACTOME	0	0.6324703	0.362
REACTOME_NEUROTRANSMITTER_RECEPTOR_BINDING_AND_DOWNSTREAM_TRANSMISSION_IN_THE_POSTSYNAPTIC_CELL	REACTOME	0	0.83120763	0.511
REACTOME_TRAFFICKING_OF_AMPA_RECEPTORS	REACTOME	0	0.82879305	0.603
REACTOME_L1CAM_INTERACTIONS	REACTOME	0	0.7801215	0.618
REACTOME_AXON_GUIDANCE	REACTOME	0	0.695976	0.618
REACTOME_SEMAPHORIN_INTERACTIONS	REACTOME	0	0.65015167	0.624
REACTOME_FACTORS_INVOLVED_IN_MEGAKARYOCYTE_DEVELOPMENT_AND_PLATELET_PRODUCTION	REACTOME	0	0.60931796	0.66
REACTOME_MHC_CLASS_II_ANTIGEN_PRESENTATION	REACTOME	0	0.57284474	0.683
REACTOME_SIGNALING_BY_RHO_GTPASES	REACTOME	0	0.52456874	0.698
REACTOME_ERK_MAPK_TARGETS	REACTOME	0	0.50633156	0.736
REACTOME_ACTIVATION_OF_NMDA_RECEPTOR_UPON_GLUTAMATE_BINDING_AND_POSTSYNAPTIC_EVENTS	REACTOME	0	0.53220123	0.794
REACTOME_POST_NMDA_RECEPTOR_ACTIVATION_EVENTS	REACTOME	0	0.5318182	0.8
REACTOME_KINESINS	REACTOME	0	0.61455905	0.866
REACTOME_DEVELOPMENTAL_BIOLOGY	REACTOME	0	0.5425098	0.889
REACTOME_CREB_PHOSPHORYLATION_THROUGH_THE_ACTIVATION_OF_RAS	REACTOME	0	0.5038631	0.899
REACTOME_NUCLEAR_EVENTS_KINASE_AND_TRANSCRIPTION_FACTOR_ACTIVATION	REACTOME	0	0.40034893	0.93
REACTOME_PHOSPHOLIPASE_C_MEDIATED_CASCADE	REACTOME	0	0.39148378	0.96
REACTOME_LYSOSOME_VESICLE_BIOGENESIS	REACTOME	0.001968504	0.5226312	0.758
REACTOME_P75_NTR_RECEPTOR_MEDIATED_SIGNALLING	REACTOME	0.003861004	0.4140051	0.929
REACTOME_G1_PHASE	REACTOME	0.003868472	0.59802717	0.674
REACTOME_PYRUVATE_METABOLISM_AND_CITRIC_ACID_TCA_CYCLE	REACTOME	0.006	0.43935186	0.908
REACTOME_CYCLIN_A_B1_ASSOCIATED_EVENTS_DURING_G2_M_TRANSITION	REACTOME	0.006060606	0.5126904	0.709
REACTOME_RAS_ACTIVATION_UOPN_CA2_INFUX_THROUGH_NMDA_RECEPTOR	REACTOME	0.006329114	0.5272311	0.824
REACTOME_INTERACTION_BETWEEN_L1_AND_ANKYRINS	REACTOME	0.006410257	0.7468776	0.431
REACTOME_EFFECTS_OF_PIP2_HYDROLYSIS	REACTOME	0.00750469	0.48666987	0.899
REACTOME_CELL_CYCLE	REACTOME	0.008032128	0.51863986	0.816
REACTOME_REGULATION_OF_WATER_BALANCE_BY_RENAL_AQUAPORINS	REACTOME	0.008097166	0.40266946	0.935
REACTOME_POST_TRANSLATIONAL_PROTEIN_MODIFICATION	REACTOME	0.008196721	0.5253107	0.895
REACTOME_CELL_DEATH_SIGNALLING_VIA_NRAGE_NRIF_AND_NADE	REACTOME	0.009784736	0.39611223	0.93
REACTOME_MITOTIC_PROMETAPHASE	REACTOME	0.010141988	0.5161005	0.899
REACTOME_G_ALPHA_Z_SIGNALLING_EVENTS	REACTOME	0.01178782	0.5364289	0.895
REACTOME_SIGNALLING_BY_NGF	REACTOME	0.01183432	0.44375852	0.908
REACTOME_REGULATION_OF_KIT_SIGNALING	REACTOME	0.012170386	0.4785466	0.899
REACTOME_FATTY_ACYL_COA_BIOSYNTHESIS	REACTOME	0.012474013	0.62777346	0.864
REACTOME_E2F_MEDIATED_REGULATION_OF_DNA_REPLICATION	REACTOME	0.014084507	0.37932944	0.938
REACTOME_SIGNALING_BY_FGFR	REACTOME	0.015779093	0.4250233	0.927
REACTOME_METABOLISM_OF_CARBOHYDRATES	REACTOME	0.016064256	0.38940674	0.961
REACTOME_G_ALPHA1213_SIGNALLING_EVENTS	REACTOME	0.01814516	0.41490427	0.929

REACTOME_SEMA4D_IN_SEMAPHORIN_SIGNALING	REACTOME	0.019607844	0.59871024	0.866
REACTOME_SRP_DEPENDENT_COTRANSLATIONAL_PROTEIN_TARGETING_TO_MEMBRANE	REACTOME	0.01992032	0.6503028	0.652
REACTOME_SHC1_EVENTS_IN_ERBB4_SIGNALING	REACTOME	0.01996008	0.40467605	0.934
REACTOME_TRANSMISSION_ACROSS_CHEMICAL_SYNAPSES	REACTOME	0.020618556	0.5858371	0.875
REACTOME_CELL_JUNCTION_ORGANIZATION	REACTOME	0.02173913	0.4493058	0.903
REACTOME_GABA_RECEPTOR_ACTIVATION	REACTOME	0.023809524	0.7463928	0.533
REACTOME_DOWNSTREAM_SIGNALING_OF_ACTIVATED_FGFR	REACTOME	0.023809524	0.39704943	0.96
REACTOME_CHROMOSOME_MAINTENANCE	REACTOME	0.026369167	0.49423516	0.899
REACTOME_SIGNALING_BY_ERBB2	REACTOME	0.02739726	0.43366992	0.913
REACTOME_NGF_SIGNALLING_VIA_TRKA_FROM_THE_PLASMA_MEMBRANE	REACTOME	0.027613413	0.40752572	0.929
REACTOME_CELL_CELL_COMMUNICATION	REACTOME	0.027944112	0.38178933	0.941
REACTOME_CELL_CYCLE_MITOTIC	REACTOME	0.028571429	0.44978172	0.904
REACTOME_CREB_PHOSPHORYLATION_THROUGH_THE_ACTIVATION_OF_CAMKII	REACTOME	0.02886598	0.42404675	0.921
REACTOME_PYRUVATE_METABOLISM	REACTOME	0.03	0.4274575	0.908
REACTOME_CHONDROITIN_SULFATE_BIOSYNTHESIS	REACTOME	0.031055901	0.51261544	0.8
REACTOME_GRB2_EVENTS_IN_ERBB2_SIGNALING	REACTOME	0.03125	0.39221242	0.968
REACTOME_BIOSYNTHESIS_OF_THE_N_GLYCAN_PRECURSOR_DOLICHOL_LIPID_LINKED_OLIGOSACCHARIDE_LLO_AND_TRANSFER_TO_A_NASCENT_PROTEIN	REACTOME	0.03187251	0.46996012	0.9
REACTOME_DAG_AND_IP3_SIGNALING	REACTOME	0.032	0.40043262	0.957
REACTOME_HEMOSTASIS	REACTOME	0.03245436	0.37782547	0.973
REACTOME_AQUAPORIN_MEDIATED_TRANSPORT	REACTOME	0.034	0.38116404	0.97
REACTOME_SIGNALING_BY_EGFR_IN_CANCER	REACTOME	0.034615386	0.4588655	0.903
REACTOME_GLYCOSAMINOGLYCAN_METABOLISM	REACTOME	0.035051547	0.39384407	0.93
REACTOME_REGULATION_OF_INSULIN_SECRETION	REACTOME	0.03526971	0.38474652	0.97
REACTOME_MITOTIC_G2_G2_M_PHASES	REACTOME	0.035785288	0.40479413	0.93
REACTOME_EGFR_DOWNREGULATION	REACTOME	0.036	0.3924705	0.979
REACTOME_CHONDROITIN_SULFATE_DERMATAN_SULFATE_METABOLISM	REACTOME	0.0375	0.39847398	0.968
REACTOME_REGULATION_OF_INSULIN_SECRETION_BY_GLUCAGON_LIKE_PEPTIDE1	REACTOME	0.03757829	0.38335457	0.97
REACTOME_SIGNALLING_TO_RAS	REACTOME	0.04016064	0.3933041	0.961
REACTOME_TRAFFICKING_OF_GLUR2_CONTAINING_AMPA_RECEPTORS	REACTOME	0.04106776	0.39186966	0.96
REACTOME_GABA_B_RECEPTOR_ACTIVATION	REACTOME	0.04158004	0.525541	0.779
REACTOME_HS_GAG_DEGRADATION	REACTOME	0.041841004	0.43131557	0.908
REACTOME_DEPOSITION_OF_NEW_CENPA_CONTAINING_NUCLEOSOMES_AT_THE_CENTROMERE	REACTOME	0.043809526	0.54476666	0.777
REACTOME_KERATAN_SULFATE_KERATIN_METABOLISM	REACTOME	0.043912176	0.38281733	0.961
REACTOME_RECRUITMENT_OF_MITOTIC_CENTROSOME_PROTEINS_AND_COMPLEXES	REACTOME	0.044265594	0.38321716	0.938
REACTOME_NRAGE_SIGNALS_DEATH_THROUGH_JNK	REACTOME	0.044444446	0.39475164	0.96
REACTOME_ASPARAGINE_N_LINKED_GLYCOSYLATION	REACTOME	0.04509804	0.55457187	0.875
REACTOME_MEIOSIS	REACTOME	0.0455408	0.5207542	0.731
REACTOME_LOSS_OF_NLP_FROM_MITOTIC_CENTROSOMES	REACTOME	0.047808766	0.37895462	0.938
REACTOME_DNA_REPLICATION	REACTOME	0.04828974	0.6039341	0.875
REACTOME_CITRIC_ACID_CYCLE_TCA_CYCLE	REACTOME	0.05	0.3994328	0.955
REACTOME_INSULIN_SYNTHESIS_AND_PROCESSING	REACTOME	0.05068226	0.382607	0.97
REACTOME_RECYCLING_PATHWAY_OF_L1	REACTOME	0.05078125	0.3771852	0.941
REACTOME_BASIGIN_INTERACTIONS	REACTOME	0.051181104	0.3962499	0.968

REACTOME_MITOTIC_M_M_G1_PHASES	REACTOME	0.052738335	0.46293998	0.901
REACTOME_SIGNALING_BY_FGFR_IN_DISEASE	REACTOME	0.054263566	0.38632184	0.961
REACTOME_MAPK_TARGETS_NUCLEAR_EVENTS_MEDIATED_BY_MAP_KINASES	REACTOME	0.054474708	0.38700843	0.979
REACTOME_TRANSMEMBRANE_TRANSPORT_OF_SMALL_MOLECULES	REACTOME	0.055776894	0.4102343	1
REACTOME_ACTIVATION_OF_CHAPERONE_GENES_BY_XBP1S	REACTOME	0.056	0.4381816	0.913
REACTOME_PKA_MEDIATED_PHOSPHORYLATION_OF_CREB	REACTOME	0.056751467	0.40009403	0.96
REACTOME_KERATAN_SULFATE_BIOSYNTHESIS	REACTOME	0.057086613	0.40500292	0.957
REACTOME_NCAM_SIGNALING_FOR_NEURITE_OUT_GROWTH	REACTOME	0.061571125	0.5695607	0.875
REACTOME_NUCLEOTIDE_BINDING_DOMAIN_LEUCINE_RICH_REPEAT_CONTAINING_RECEPTOR_NLR_SIGNALING_PATHWAYS	REACTOME	0.06349207	0.41660777	1
REACTOME_MEIOTIC_RECOMBINATION	REACTOME	0.06500956	0.5587787	0.697
REACTOME_SEMA4D_INDUCED_CELL_MIGRATION_AND_GROWTH_CONE_COLLAPSE	REACTOME	0.06560636	0.3942077	0.97
REACTOME_G1_S_SPECIFIC_TRANSCRIPTION	REACTOME	0.06613226	0.39237642	0.968
REACTOME_APOPTOTIC_CLEAVAGE_OF_CELLULAR_PROTEINS	REACTOME	0.06692161	0.39483285	0.936
REACTOME_GLYCOSPHINGOLIPID_METABOLISM	REACTOME	0.068136275	0.39172095	0.936
REACTOME_SYNTHESIS_AND_INTERCONVERSION_OF_NUCLEOTIDE_DI_AND_TRIPHOSPHATES	REACTOME	0.068627454	0.3883507	0.938
REACTOME_SMOOTH_MUSCLE_CONTRACTION	REACTOME	0.07184466	0.41125813	0.954
REACTOME_CA_DEPENDENT_EVENTS	REACTOME	0.0734127	0.39407763	0.968
REACTOME_TCA_CYCLE_AND_RESPIRATORY_ELECTRON_TRANSPORT	REACTOME	0.0761523	0.3969876	0.935
REACTOME_APC_CDC20_MEDIATED_DEGRADATION_OF_NEK2A	REACTOME	0.078313254	0.39356983	0.957
REACTOME_OPIOID_SIGNALLING	REACTOME	0.08024691	0.38981414	0.979
REACTOME_MITOTIC_G1_G1_S_PHASES	REACTOME	0.08350305	0.4213248	0.929
REACTOME_SIGNALING_BY_PDGF	REACTOME	0.084	0.3871738	0.97
REACTOME_APC_C_CDC20_MEDIATED_DEGRADATION_OF_CYCLIN_B	REACTOME	0.08553971	0.3817681	0.97
REACTOME_POST_CHAPERONIN_TUBULIN_FOLDING_PATHWAY	REACTOME	0.08678501	0.3807575	0.973
REACTOME_REGULATION_OF_MITOTIC_CELL_CYCLE	REACTOME	0.09325397	0.5230971	0.897
REACTOME_FRS2_MEDIATED_CASCADE	REACTOME	0.09406953	0.3854793	0.979
REACTOME_PHOSPHORYLATION_OF_THE_APC_C	REACTOME	0.097165994	0.37874204	0.976
REACTOME_TELOMERE_MAINTENANCE	REACTOME	0.099029124	0.388413	0.938
REACTOME_FORMATION_OF_ATP_BY_CHEMIOSMOTIC_COUPLING	REACTOME	0.099403575	0.41686797	1
REACTOME_A_TETRASACCHARIDE_LINKER_SEQUENCE_IS_REQUIRED_FOR_GAG_SYNTHESIS	REACTOME	0.09978768	0.40270683	0.954
REACTOME_PLC_BETA_MEDIATED_EVENTS	REACTOME	0.09979633	0.38989168	0.985
REACTOME_G1_S_TRANSITION	REACTOME	0.10121457	0.3753401	0.945
REACTOME_INTEGRIN_CELL_SURFACE_INTERACTIONS	REACTOME	0.101626016	0.37805417	0.97
REACTOME_ABC_FAMILY_PROTEINS_MEDIATED_TRANSPORT	REACTOME	0.10176125	0.37173083	0.976
REACTOME_FORMATION_OF_INCISION_COMPLEX_IN_GG_NER	REACTOME	0.10412574	0.38361013	0.97
REACTOME_METABOLISM_OF_PROTEINS	REACTOME	0.10526316	0.40049005	0.953
REACTOME_TRANSPORT_OF_INORGANIC_CATIONS_ANIONS_AND_AMINO_ACIDS_OLIGOPEPTIDES	REACTOME	0.107421875	0.3962436	0.996
REACTOME_TRIGLYCERIDE_BIOSYNTHESIS	REACTOME	0.10934394	0.38961098	0.979
REACTOME_SIGNAL_TRANSDUCTION_BY_L1	REACTOME	0.1124031	0.39259705	0.968
REACTOME_INHIBITION_OF_VOLTAGE_GATED_CA2_CHANNELS_VIA_GBETA_GAMMA_SUBUNITS	REACTOME	0.11276596	0.4118742	0.929
REACTOME_COLLAGEN_FORMATION	REACTOME	0.11392405	0.5527623	0.883
REACTOME_PI3K_EVENTS_IN_ERBB4_SIGNALING	REACTOME	0.114119925	0.4067151	1
REACTOME_CELL_CYCLE_CHECKPOINTS	REACTOME	0.11585366	0.3766149	0.946

REACTOME_INTEGRATION_OF_ENERGY_METABOLISM	REACTOME	0.11812627	0.415283	1
REACTOME_PRE_NOTCH_EXPRESSION_AND_PROCESSING	REACTOME	0.118236475	0.38254505	0.977
REACTOME_GLOBAL_GENOMIC_NER_GG_NER	REACTOME	0.11919192	0.39467975	0.968
REACTOME_SPHINGOLIPID_METABOLISM	REACTOME	0.119760476	0.3766789	0.976
REACTOME_SIGNALING_BY_ROBO_RECEPTOR	REACTOME	0.12859885	0.39696637	0.982
REACTOME_MAP_KINASE_ACTIVATION_IN_TLR_CASCADE	REACTOME	0.13017751	0.39798453	0.985
REACTOME_DIABETES_PATHWAYS	REACTOME	0.13085938	0.41305438	1
REACTOME_G0_AND_EARLY_G1	REACTOME	0.13211381	0.3910634	0.979
REACTOME_POST_TRANSLATIONAL_MODIFICATION_SYNTHESIS_OF_GPI_ANCHORED_PROTEINS	REACTOME	0.13373253	0.37942657	0.961
REACTOME_PRE_NOTCH_TRANSCRIPTION_AND_TRANSLATION	REACTOME	0.13412228	0.3857857	0.97
REACTOME_CELL_SURFACE_INTERACTIONS_AT_THE_VASCULAR_WALL	REACTOME	0.13453816	0.40824386	1
REACTOME_NEURONAL_SYSTEM	REACTOME	0.13675214	0.39119446	0.985
REACTOME_SIGNALLING_TO_ERKS	REACTOME	0.13872832	0.3989197	0.994
REACTOME_TIGHT_JUNCTION_INTERACTIONS	REACTOME	0.1388889	0.39087278	0.979
REACTOME_RNA_POL_I_TRANSCRIPTION	REACTOME	0.14007781	0.39655754	0.968
REACTOME_ION_TRANSPORT_BY_P_TYPE_ATPASES	REACTOME	0.14081633	0.4105806	1
REACTOME_APOPTOTIC_EXECUTION_PHASE	REACTOME	0.14092664	0.37421197	0.976
REACTOME_RNA_POL_I_PROMOTER_OPENING	REACTOME	0.14257812	0.42878565	0.913
REACTOME_SIGNALING_BY_SCF_KIT	REACTOME	0.14285715	0.39500278	0.984
REACTOME_INHIBITION_OF_THE_PROTEOLYTIC_ACTIVITY_OF_APC_C_REQUIRED_FOR_THE_ONSET_OF_ANAPHASE_BY_MITOTIC_SPINDLE_CHECKPOINT_COMPONENT	REACTOME	0.14516129	0.37467924	0.976
REACTOME_GLUTATHIONE_CONJUGATION	REACTOME	0.146	0.397845	0.957
REACTOME_INHIBITION_OF_INSULIN_SECRETION_BY_ADRENALINE_NORADRENALINE	REACTOME	0.14644352	0.39705968	0.985
REACTOME_PEPTIDE_CHAIN_ELONGATION	REACTOME	0.148	0.40909272	1
REACTOME_ADHERENS_JUNCTIONS_INTERACTIONS	REACTOME	0.14876033	0.3909849	0.97
REACTOME_ADP_SIGNALLING_THROUGH_P2RY12	REACTOME	0.14928426	0.39914888	0.993
REACTOME_FORMATION_OF_TUBULIN_FOLDING_INTERMEDIATES_BY_CCT_TRIC	REACTOME	0.15145631	0.38218352	0.973
REACTOME_SYNTHESIS_OF_DNA	REACTOME	0.15430862	0.38476247	0.963
REACTOME_GLYCOGEN_BREAKDOWN_GLYCOGENOLYSIS	REACTOME	0.15655577	0.3948873	0.982
REACTOME_DARPP_32_EVENTS	REACTOME	0.15779093	0.4063622	0.954
REACTOME_G2_M_CHECKPOINTS	REACTOME	0.15959597	0.39037696	0.979
REACTOME_HS_GAG_BIOSYNTHESIS	REACTOME	0.16188525	0.3723651	0.976
REACTOME_PROCESSIVE_SYNTHESIS_ON_THE_LAGGING_STRAND	REACTOME	0.16297787	0.40037245	0.985
REACTOME_GLUCAGON_SIGNALING_IN_METABOLIC_REGULATION	REACTOME	0.16330644	0.40670067	1
REACTOME_ACTIVATION_OF_THE_PRE_REPLICATIVE_COMPLEX	REACTOME	0.16969697	0.39075407	0.985
REACTOME_NEPHRIN_INTERACTIONS	REACTOME	0.17004049	0.41325134	1
REACTOME_PHASE_II_CONJUGATION	REACTOME	0.17034069	0.38411835	0.97
REACTOME_DNA_STRAND_ELONGATION	REACTOME	0.17206478	0.3959296	0.99
REACTOME_THROMBIN_SIGNALLING_THROUGH_PROTEINASE_ACTIVATED_RECEPTORS_PARS	REACTOME	0.17254902	0.41522864	1
REACTOME_G_PROTEIN_ACTIVATION	REACTOME	0.1734694	0.41658682	1
REACTOME_TRAF6_MEDIATED_INDUCTION_OF_NFKB_AND_MAP_KINASES_UPON_TLR7_8_OR_9_ACTIVATION	REACTOME	0.17567568	0.41457486	1
REACTOME_MUSCLE_CONTRACTION	REACTOME	0.17575757	0.4252397	1
REACTOME_OTHER_SEMAPHORIN_INTERACTIONS	REACTOME	0.17879418	0.38080388	0.973
REACTOME_ACTIVATION_OF_ATR_IN_RESPONSE_TO_REPLICATION_STRESS	REACTOME	0.17886178	0.39445215	0.985

REACTOME_HEPARAN_SULFATE_HEPARIN_HS_GAG_METABOLISM	REACTOME	0.18295218	0.39014104	0.979
REACTOME_PI3K_EVENTS_IN_ERBB2_SIGNALING	REACTOME	0.18857142	0.41460118	1
REACTOME_EXTENSION_OF_TELOMERES	REACTOME	0.19	0.3929536	0.984
REACTOME_TRIF_MEDIATED_TLR3_SIGNALING	REACTOME	0.192607	0.4163476	1
REACTOME_MYD88_MAL_CASCADE_INITIATED_ON_PLASMA_MEMBRANE	REACTOME	0.1949807	0.43007055	1
REACTOME_NFKB_AND_MAP_KINASES_ACTIVATION_MEDIATED_BY_TLR4_SIGNALING_REPERTOIRE	REACTOME	0.19502868	0.42334357	1
REACTOME_ENOS_ACTIVATION_AND_REGULATION	REACTOME	0.19607843	0.40043715	0.99
REACTOME_CELL_CELL_JUNCTION_ORGANIZATION	REACTOME	0.1984127	0.38721308	0.985
REACTOME_RESOLUTION_OF_AP_SITES_VIA_THE_MULTIPLE_NUCLEOTIDE_PATCH_REPLACEMENT_PATHWAY	REACTOME	0.19959678	0.40172574	0.985
REACTOME_MEMBRANE_TRAFFICKING	REACTOME	0.20156556	0.39714947	0.995
REACTOME_SIGNALLING_TO_P38_VIA_RIT_AND_RIN	REACTOME	0.20338982	0.3952734	0.995
REACTOME_ACTIVATED_NOTCH1_TRANSMITS_SIGNAL_TO_THE_NUCLEUS	REACTOME	0.2035225	0.4116327	1
REACTOME_BRANCHED_CHAIN_AMINO_ACID_CATABOLISM	REACTOME	0.2041237	0.41041288	1
REACTOME_CONVERSION_FROM_APC_C_CDC20_TO_APC_C_CDH1_IN_LATE_ANAPHASE	REACTOME	0.20440882	0.39413565	0.985
REACTOME_GAB1_SIGNALOSOME	REACTOME	0.2046332	0.40201423	0.99
REACTOME_PIP3_ACTIVATES_AKT_SIGNALING	REACTOME	0.20498085	0.41232926	1
REACTOME_ABCA_TRANSPORTERS_IN_LIPID_HOMEOSTASIS	REACTOME	0.20594059	0.4109548	1
REACTOME_CTLA4_INHIBITORY_SIGNALING	REACTOME	0.20750988	0.41681367	1
REACTOME_APOPTOSIS	REACTOME	0.20769231	0.38835683	0.97
REACTOME_TERMINATION_OF_O_GLYCAN_BIOSYNTHESIS	REACTOME	0.20842105	0.41257992	1
REACTOME_SIGNAL_AMPLIFICATION	REACTOME	0.20977597	0.42697042	1
REACTOME_S_PHASE	REACTOME	0.2128514	0.37982127	0.973
REACTOME_GLYCEROPHOSPHOLIPID_BIOSYNTHESIS	REACTOME	0.21301775	0.4173784	1
REACTOME_SIGNALING_BY_INSULIN_RECEPTOR	REACTOME	0.21387284	0.41110358	1
REACTOME_MEIOTIC_SYNAPSIS	REACTOME	0.21470019	0.39621022	0.994
REACTOME_HOMOLOGOUS_RECOMBINATION_REPAIR_OF_REPLICATION_INDEPENDENT_DOUBLE_STRAND_BREAKS	REACTOME	0.2165992	0.39591026	0.982
REACTOME_NETRIN1_SIGNALING	REACTOME	0.21789883	0.4596214	1
REACTOME_SHC_MEDIATED_SIGNALLING	REACTOME	0.22047244	0.38437605	0.979
REACTOME_AMYLOIDS	REACTOME	0.22200392	0.38833344	0.985
REACTOME_PACKAGING_OF_TELOMERE_ENDS	REACTOME	0.22307692	0.39468333	0.995
REACTOME_MYOGENESIS	REACTOME	0.22494887	0.43130243	1
REACTOME_PLATELET_HOMEOSTASIS	REACTOME	0.22606924	0.44040203	1
REACTOME_DNA_REPAIR	REACTOME	0.22736418	0.385613	0.977
REACTOME_MITOCHONDRIAL_TRNA_AMINOACYLATION	REACTOME	0.22762646	0.38289326	0.979
REACTOME_PLATELET_ACTIVATION_SIGNALING_AND_AGGREGATION	REACTOME	0.22762646	0.47644565	1
REACTOME_BASE_EXCISION_REPAIR	REACTOME	0.22903885	0.39579573	0.985
REACTOME_ION_CHANNEL_TRANSPORT	REACTOME	0.22908367	0.41324213	1
REACTOME_EXTRACELLULAR_MATRIX_ORGANIZATION	REACTOME	0.22947368	0.39796183	0.982
REACTOME_DOUBLE_STRAND_BREAK_REPAIR	REACTOME	0.23469388	0.3927739	0.985
REACTOME_UNFOLDED_PROTEIN_RESPONSE	REACTOME	0.2370518	0.4143571	1
REACTOME_PHOSPHOLIPID_METABOLISM	REACTOME	0.2407045	0.3975199	0.994
REACTOME_ACTIVATION_OF_KAINATE_RECEPTORS_UPON_GLUTAMATE_BINDING	REACTOME	0.24223602	0.42952272	1
REACTOME_IL_2_SIGNALING	REACTOME	0.24266145	0.47090816	1

REACTOME_LAGGING_STRAND_SYNTHESIS	REACTOME	0.24346076	0.40332192	1
REACTOME_GABA_SYNTHESIS_RELEASE_REUPTAKE_AND_DEGRADATION	REACTOME	0.24842106	0.42833132	1
REACTOME_FANCONI_ANEMIA_PATHWAY	REACTOME	0.25	0.38749287	0.985
REACTOME_NEGATIVE_REGULATION_OF_FGFR_SIGNALING	REACTOME	0.25	0.48545644	1
REACTOME_TRNA_AMINOACYLATION	REACTOME	0.25146198	0.38943264	0.979
REACTOME_SHC_RELATED_EVENTS	REACTOME	0.25646123	0.4135579	1
REACTOME_PREFOLDIN_MEDIATED_TRANSFER_OF_SUBSTRATE_TO_CCT_TRIC	REACTOME	0.2581262	0.4102672	1
REACTOME_GAP_JUNCTION_TRAFFICKING	REACTOME	0.2653846	0.47247592	1
REACTOME_NITRIC_OXIDE_STIMULATES_GUANYLATE_CYCLASE	REACTOME	0.26652893	0.4410526	1
REACTOME_SYNTHESIS_OF_GLYCOSYLPHOSPHATIDYLINOSITOL_GPI	REACTOME	0.26706827	0.39806297	0.994
REACTOME_NUCLEOTIDE_EXCISION_REPAIR	REACTOME	0.26907632	0.40049168	0.99
REACTOME_ORC1_REMOVAL_FROM_CHROMATIN	REACTOME	0.26984128	0.40019473	0.985
REACTOME_ACTIVATED_TLR4_SIGNALLING	REACTOME	0.2706334	0.49710628	1
REACTOME_GASTRIN_CREB_SIGNALLING_PATHWAY_VIA_PKC_AND_MAPK	REACTOME	0.27663934	0.4977732	1
REACTOME_PI_3K_CASCADE	REACTOME	0.2776699	0.4985531	1
REACTOME_DOWNSTREAM_SIGNAL_TRANSDUCTION	REACTOME	0.2782101	0.41314906	1
REACTOME_CGMP_EFFECTS	REACTOME	0.27920792	0.47571832	1
REACTOME_ADP_SIGNALLING_THROUGH_P2RY1	REACTOME	0.27935222	0.48178342	1
REACTOME_SHC1_EVENTS_IN_EGFR_SIGNALING	REACTOME	0.29056603	0.4189004	1
REACTOME_GPVI_MEDIATED_ACTIVATION_CASCADE	REACTOME	0.29577464	0.4727983	1
REACTOME_INSULIN_RECEPTOR_RECYCLING	REACTOME	0.29745597	0.4386842	1
REACTOME_SIGNALING_BY_ERBB4	REACTOME	0.29865125	0.48565835	1
REACTOME_APC_C_CDH1_MEDIATED_DEGRADATION_OF_CDC20_AND_OTHER_APC_C_CDH1_TARGETED_PROTEINS_IN_LATE_MITOSIS_EARLY_G1	REACTOME	0.30214426	0.40860397	1
REACTOME_APC_C_CDC20_MEDIATED_DEGRADATION_OF_MITOTIC_PROTEINS	REACTOME	0.30255404	0.39817518	0.996
REACTOME_INWARDLY_RECTIFYING_K_CHANNELS	REACTOME	0.30406854	0.482639	1
REACTOME_NUCLEOTIDE_LIKE_PURINERGIC_RECEPTORS	REACTOME	0.30722892	0.47393575	1
REACTOME_INSULIN_RECEPTOR_SIGNALLING_CASCADE	REACTOME	0.30753967	0.46407533	1
REACTOME_PROTEIN_FOLDING	REACTOME	0.31060606	0.43639275	1
REACTOME_G_BETA_GAMMA_SIGNALLING_THROUGH_PI3KGAMMA	REACTOME	0.31111112	0.49730146	1
REACTOME_HOST_INTERACTIONS_OF_HIV_FACTORS	REACTOME	0.3148515	0.40537477	1
REACTOME_INTRINSIC_PATHWAY_FOR_APOPTOSIS	REACTOME	0.31558186	0.44312698	1
REACTOME_ANTIGEN_ACTIVATES_B_CELL_RECEPTOR_LEADING_TO_GENERATION_OF_SECOND_MESSENGERS	REACTOME	0.32046333	0.49772078	1
REACTOME_RNA_POL_I_RNA_POL_III_AND_MITOCHONDRIAL_TRANSCRIPTION	REACTOME	0.32086614	0.43049237	1
REACTOME_SIGNALING_BY_NOTCH	REACTOME	0.32301742	0.43580106	1
REACTOME_RESPIRATORY_ELECTRON_TRANSPORT_ATP_SYNTHESIS_BY_CHEMIOSMOTIC_COUPLING_AND_HEAT_PRODUCTION_BY_UNCOUPLING_PROTEINS_	REACTOME	0.33003953	0.4833378	1
REACTOME_MRNA_CAPPING	REACTOME	0.33139536	0.4147052	1
REACTOME_YAP1_AND_WWTR1_TAZ_STIMULATED_GENE_EXPRESSION	REACTOME	0.33398438	0.47356662	1
REACTOME_M_G1_TRANSITION	REACTOME	0.33737373	0.4092618	1
REACTOME_TRANSCRIPTION_COUPLED_NER_TC_NER	REACTOME	0.33794466	0.4164459	1
REACTOME_CYTOSOLIC_TRNA_AMINOACYLATION	REACTOME	0.34	0.43001503	1
REACTOME_SLC_MEDIATED_TRANSMEMBRANE_TRANSPORT	REACTOME	0.34502923	0.5472944	1
REACTOME_INFLUENZA_VIRAL_RNA_TRANSCRIPTION_AND_REPLICATION	REACTOME	0.34791252	0.48294798	1
REACTOME_NCAM1_INTERACTIONS	REACTOME	0.34989202	0.47750407	1

REACTOME_METABOLISM_OF_NUCLEOTIDES	REACTOME	0.3501006	0.41223186	1
REACTOME_CLASS_I_MHC_MEDIATED_ANTIGEN_PROCESSING_PRESENTATION	REACTOME	0.35823753	0.43720365	1
REACTOME_LATENT_INFECTION_OF_HOMO_SAPIENS_WITH_MYCOBACTERIUM_TUBERCULOSIS	REACTOME	0.36	0.5184213	1
REACTOME_ANTIVIRAL_MECHANISM_BY_IFN_STIMULATED_GENES	REACTOME	0.36692014	0.4134197	1
REACTOME_UNBLOCKING_OF_NMDA_RECEPTOR_GLUTAMATE_BINDING_AND_ACTIVATION	REACTOME	0.36865342	0.5496919	1
REACTOME_PEROXISOMAL_LIPID_METABOLISM	REACTOME	0.3687375	0.4753319	1
REACTOME_ARMS_MEDIATED_ACTIVATION	REACTOME	0.37072244	0.5467539	1
REACTOME_ANTIGEN_PROCESSING_UBIQUITINATION_PROTEASOME_DEGRADATION	REACTOME	0.3716475	0.44203612	1
REACTOME_GOLGI_ASSOCIATED_VESICLE_BIOGENESIS	REACTOME	0.37254903	0.41160405	1
REACTOME_NOD1_2_SIGNALING_PATHWAY	REACTOME	0.37475345	0.5171495	1
REACTOME_GLUCOSE_METABOLISM	REACTOME	0.37695312	0.49020493	1
REACTOME_TRANS_GOLGI_NETWORK_VESICLE_BUDDING	REACTOME	0.390625	0.41196147	1
REACTOME_SYNTHESIS_OF_PA	REACTOME	0.396	0.5650456	1
REACTOME_ASSEMBLY_OF_THE_PRE_REPLICATIVE_COMPLEX	REACTOME	0.39679357	0.44381833	1
REACTOME_PI3K_AKT_ACTIVATION	REACTOME	0.40194175	0.5268161	1
REACTOME_SYNTHESIS_OF_PC	REACTOME	0.4034749	0.5484345	1
REACTOME_GLUCOSE_TRANSPORT	REACTOME	0.408	0.48417166	1
REACTOME_PI3K_CASCADE	REACTOME	0.4138614	0.5634793	1
REACTOME_ACYL_CHAIN_REMODELLING_OF_PC	REACTOME	0.41535434	0.59645736	1
REACTOME_SCFSKP2_MEDIATED_DEGRADATION_OF_P27_P21	REACTOME	0.41873804	0.50149244	1
REACTOME_PROSTACYCLIN_SIGNALLING_THROUGH_PROSTACYCLIN_RECEPTOR	REACTOME	0.42028984	0.57865626	1
REACTOME_METABOLISM_OF_LIPIDS_AND_LIPOPROTEINS	REACTOME	0.42147118	0.57166183	1
REACTOME_INTEGRIN_ALPHAIIB_BETA3_SIGNALING	REACTOME	0.4266145	0.5813633	1
REACTOME_IL_RECEPTOR_SHC_SIGNALING	REACTOME	0.4269006	0.58314604	1
REACTOME_P53_DEPENDENT_G1_DNA_DAMAGE_RESPONSE	REACTOME	0.42720306	0.55534893	1
REACTOME_TOLL_RECEPTOR_CASCADES	REACTOME	0.42857143	0.60189146	1
REACTOME_SYNTHESIS_OF_PIPS_AT_THE_PLASMA_MEMBRANE	REACTOME	0.42967245	0.54962206	1
REACTOME_HIV_INFECTION	REACTOME	0.43110237	0.48508114	1
REACTOME_G_BETA_GAMMA_SIGNALLING_THROUGH_PLC_BETA	REACTOME	0.43209878	0.5984986	1
REACTOME_THROMBOXANE_SIGNALLING_THROUGH_TP_RECEPTOR	REACTOME	0.43897638	0.6288117	1
REACTOME_SPHINGOLIPID_DE_NOVO_BIOSYNTHESIS	REACTOME	0.4396887	0.5740745	1
REACTOME_PKB_MEDIATED_EVENTS	REACTOME	0.44573644	0.5002726	1
REACTOME_PURINE_METABOLISM	REACTOME	0.4471058	0.44231677	1
REACTOME_NEUROTRANSMITTER_RELEASE_CYCLE	REACTOME	0.45	0.62423605	1
REACTOME_TRANSFERRIN_ENDOCYTOSIS_AND_RECYCLING	REACTOME	0.45039684	0.5483698	1
REACTOME_G_PROTEIN_BETA_GAMMA_SIGNALLING	REACTOME	0.451417	0.58632654	1
REACTOME_RESPIRATORY_ELECTRON_TRANSPORT	REACTOME	0.45596868	0.5717473	1
REACTOME_INFLAMMASOMES	REACTOME	0.46060607	0.59913534	1
REACTOME_P130CAS_LINKAGE_TO_MAPK_SIGNALING_FOR_INTEGRINS	REACTOME	0.46257198	0.5897685	1
REACTOME_PI_METABOLISM	REACTOME	0.46360153	0.51577127	1
REACTOME_PROLONGED_ERK_ACTIVATION_EVENTS	REACTOME	0.4718045	0.60680455	1
REACTOME_3_UTR_MEDIATED_TRANSLATIONAL_REGULATION	REACTOME	0.4749499	0.57604086	1
REACTOME_TRANSPORT_OF_MATURE_MRNA_DERIVED_FROM_AN_INTRONLESS_TRANSCRIPT	REACTOME	0.4781746	0.5197905	1

REACTOME_REGULATORY_RNA_PATHWAYS	REACTOME	0.47928995	0.5261053	1
REACTOME_CYCLIN_E_ASSOCIATED_EVENTS_DURING_G1_S_TRANSITION_	REACTOME	0.47953215	0.5808663	1
REACTOME_G_ALPHA_Q_SIGNALLING_EVENTS	REACTOME	0.47959185	0.63256544	1
REACTOME_TRANSPORT_TO_THE_GOLGI_AND_SUBSEQUENT_MODIFICATION	REACTOME	0.481409	0.58573663	1
REACTOME_PROTEOLYTIC_CLEAVAGE_OF_SNARE_COMPLEX_PROTEINS	REACTOME	0.48183557	0.598016	1
REACTOME_REGULATION_OF_APOPTOSIS	REACTOME	0.4837476	0.57464826	1
REACTOME_NONSENSE_MEDIATED_DECAY_ENHANCED_BY_THE_EXON_JUNCTION_COMPLEX	REACTOME	0.49112427	0.5988018	1
REACTOME_NEP_NS2_INTERACTS_WITH_THE_CELLULAR_EXPORT_MACHINERY	REACTOME	0.49224806	0.527021	1
REACTOME_FORMATION_OF_THE_HIV1_EARLY_ELONGATION_COMPLEX	REACTOME	0.49607843	0.57424474	1
REACTOME_AMINO_ACID_TRANSPORT_ACROSS_THE_PLASMA_MEMBRANE	REACTOME	0.49707603	0.6144028	1
REACTOME_SIGNALING_BY_ILS	REACTOME	0.5028791	0.6281965	1
REACTOME_INTERFERON_SIGNALING	REACTOME	0.50392157	0.63395095	1
REACTOME_GLUTAMATE_NEUROTRANSMITTER_RELEASE_CYCLE	REACTOME	0.5040486	0.65772176	1
REACTOME_INTERACTIONS_OF_VPR_WITH_HOST_CELLULAR_PROTEINS	REACTOME	0.5070422	0.5251864	1
REACTOME_CD28_CO_STIMULATION	REACTOME	0.5226824	0.6558214	1
REACTOME_PRE_NOTCH_PROCESSING_IN_GOLGI	REACTOME	0.5239044	0.6329253	1
REACTOME_MRNA_SPLICING_MINOR_PATHWAY	REACTOME	0.5290581	0.6699236	1
REACTOME_TRANSCRIPTION	REACTOME	0.52917504	0.65507454	1
REACTOME_GLUCAGON_TYPE_LIGAND_RECEPTORS	REACTOME	0.53149605	0.6614401	1
REACTOME_N_GLYCAN_ANTENNAE_ELONGATION_IN_THE_MEDIAL_TRANS_GOLGI	REACTOME	0.5362035	0.6250948	1
REACTOME_TRANSPORT_OF_RIBONUCLEOPROTEINS_INTO_THE_HOST_NUCLEUS	REACTOME	0.546875	0.57454634	1
REACTOME_CDT1_ASSOCIATION_WITH_THE_CDC6_ORC_ORIGIN_COMPLEX	REACTOME	0.5481336	0.6278814	1
REACTOME_ACTIVATED_AMPK_STIMULATES_FATTY_ACID_OXIDATION_IN_MUSCLE	REACTOME	0.55069584	0.6306855	1
REACTOME_REGULATION_OF_GLUCOKINASE_BY_GLUCOKINASE_REGULATORY_PROTEIN	REACTOME	0.55490196	0.6309231	1
REACTOME_PLATELET_SENSITIZATION_BY_LDL	REACTOME	0.55510205	0.6510041	1
REACTOME_P53_INDEPENDENT_G1_S_DNA_DAMAGE_CHECKPOINT	REACTOME	0.5553398	0.6595463	1
REACTOME_SULFUR_AMINO_ACID_METABOLISM	REACTOME	0.558	0.6530451	1
REACTOME_ACTIVATION_OF_THE_MRNA_UPON_BINDING_OF_THE_CAP_BINDING_COMPLEX_AND_EIFS_AND_SUBSEQUENT_BINDING_TO_43S	REACTOME	0.55938697	0.64726657	1
REACTOME_SCF_BETA_TRCP_MEDIATED_DEGRADATION_OF_EMI1	REACTOME	0.5596869	0.6514012	1
REACTOME_PLATELET_AGGREGATION_PLUG_FORMATION	REACTOME	0.5632184	0.636558	1
REACTOME_G_ALPHA_I_SIGNALLING_EVENTS	REACTOME	0.5670103	0.6611055	1
REACTOME_COSTIMULATION_BY_THE_CD28_FAMILY	REACTOME	0.56772906	0.6558719	1
REACTOME_ENERGY_DEPENDENT_REGULATION_OF_MTOR_BY_LKB1_AMPK	REACTOME	0.5697674	0.659588	1
REACTOME_FATTY_ACID_TRIACYLGLYCEROL_AND_KETONE_BODY_METABOLISM	REACTOME	0.57	0.65129155	1
REACTOME_FORMATION_OF_THE_TERNARY_COMPLEX_AND_SUBSEQUENTLY_THE_43S_COMPLEX	REACTOME	0.5725646	0.6582405	1
REACTOME_GRB2_SOS_PROVIDES_LINKAGE_TO_MAPK_SIGNALING_FOR_INTERGRINS_	REACTOME	0.57471263	0.6574912	1
REACTOME_TRANSLATION	REACTOME	0.5748032	0.6580678	1
REACTOME_SIGNALING_BY_NOTCH1	REACTOME	0.5761719	0.65233994	1
REACTOME_ZINC_TRANSPORTERS	REACTOME	0.5761719	0.67145264	1
REACTOME_INFLUENZA_LIFE_CYCLE	REACTOME	0.5768463	0.6532684	1
REACTOME_ACTIVATION_OF_BH3_ONLY_PROTEINS	REACTOME	0.5779093	0.65446746	1
REACTOME_HIV_LIFE_CYCLE	REACTOME	0.5796813	0.66856635	1
REACTOME_METABOLISM_OF_NON_CODING_RNA	REACTOME	0.5808967	0.6597082	1

REACTOME_TRANSPORT_OF_MATURE_TRANSCRIPT_TO_CYTOPLASM	REACTOME	0.5813492	0.6646683	1
REACTOME_CYTOKINE_SIGNALING_IN_IMMUNE_SYSTEM	REACTOME	0.5872093	0.67201287	1
REACTOME_RNA_POL_II_TRANSCRIPTION_PRE_INITIATION_AND_PROMOTER_OPENING	REACTOME	0.588694	0.67691565	1
REACTOME_MITOCHONDRIAL_PROTEIN_IMPORT	REACTOME	0.59607846	0.7107834	1
REACTOME_ASSOCIATION_OF_TRIC_CCT_WITH_TARGET_PROTEINS_DURING_BIOSYNTHESIS	REACTOME	0.5961165	0.6617224	1
REACTOME_ER_PHAGOSOME_PATHWAY	REACTOME	0.60341555	0.6719121	1
REACTOME_FORMATION_OF_TRANSCRIPTION_COUPLED_NER_TC_NER_REPAIR_COMPLEX	REACTOME	0.6046065	0.6967116	1
REACTOME_MICRORNA_MIRNA_BIOGENESIS	REACTOME	0.6130952	0.68457764	1
REACTOME_SIGNALING_BY_THE_B_CELL_RECEPTOR_BCR	REACTOME	0.6156788	0.69850504	1
REACTOME_IRON_UPTAKE_AND_TRANSPORT	REACTOME	0.6156863	0.707968	1
REACTOME_AUTODEGRADATION_OF_CDH1_BY_CDH1_APC_C	REACTOME	0.6171875	0.6973698	1
REACTOME_REGULATION_OF_ORNITHINE_DECARBOXYLASE_ODC	REACTOME	0.61742425	0.6985509	1
REACTOME_ACYL_CHAIN_REMODELLING_OF_PG	REACTOME	0.6184739	0.69997597	1
REACTOME_DEADENYLATION_OF_MRNA	REACTOME	0.6315789	0.7265882	1
REACTOME_TRANSPORT_OF_VITAMINS_NUCLEOSIDES_AND_RELATED_MOLECULES	REACTOME	0.6340509	0.7086435	1
REACTOME_SYNTHESIS_OF_PIPS_AT_THE_GOLGI_MEMBRANE	REACTOME	0.6400778	0.67692393	1
REACTOME_MRNA_PROCESSING	REACTOME	0.6464844	0.7357486	1
REACTOME_GLYCOLYSIS	REACTOME	0.6527197	0.6941115	1
REACTOME_IL_3_5_AND_GM_CSF_SIGNALING	REACTOME	0.66732675	0.7125085	1
REACTOME_NUCLEAR_SIGNALING_BY_ERBB4	REACTOME	0.6727273	0.709619	1
REACTOME_ACTIVATED_TAK1_MEDIATES_P38_MAPK_ACTIVATION	REACTOME	0.6742857	0.70873433	1
REACTOME_CROSS_PRESENTATION_OF_SOLUBLE_EXOGENOUS_ANTIGENS_ENDOSOMES	REACTOME	0.67898834	0.8289077	1
REACTOME_SIGNALING_BY_HIPPO	REACTOME	0.68241966	0.7471256	1
REACTOME_METABOLISM_OF_RNA	REACTOME	0.6829746	0.80239934	1
REACTOME_PROCESSING_OF_CAPPED_INTRON_CONTAINING_PRE_MRNA	REACTOME	0.6843137	0.7932807	1
REACTOME_VIF_MEDIATED_DEGRADATION_OF_APOBEC3G	REACTOME	0.6853282	0.7415259	1
REACTOME_ANTIGEN_PROCESSING_CROSS_PRESENTATION	REACTOME	0.68798447	0.76797783	1
REACTOME_AUTODEGRADATION_OF_THE_E3_UBIQUITIN_LIGASE_COP1	REACTOME	0.68880457	0.77596533	1
REACTOME_CDK_MEDIATED_PHOSPHORYLATION_AND_REMOVAL_OF_CDC6	REACTOME	0.6893204	0.74198365	1
REACTOME_TRANSCRIPTIONAL_REGULATION_OF_WHITE_ADIPOCYTE_DIFFERENTIATION	REACTOME	0.6923077	0.71260464	1
REACTOME_LATE_PHASE_OF_HIV_LIFE_CYCLE	REACTOME	0.6968504	0.80989	1
REACTOME_ANTIGEN_PRESENTATION_FOLDING_ASSEMBLY_AND_PEPTIDE_LOADING_OF_CLASS_I_MHC	REACTOME	0.6978131	0.8019022	1
REACTOME_RAP1_SIGNALLING	REACTOME	0.7	0.7130784	1
REACTOME_MRNA_SPLICING	REACTOME	0.7029703	0.8734247	1
REACTOME_METAL_ION_SLC_TRANSPORTERS	REACTOME	0.703125	0.765433	1
REACTOME_STRIATED_MUSCLE_CONTRACTION	REACTOME	0.71456313	0.7100167	1
REACTOME_ABORTIVE_ELONGATION_OF_HIV1_TRANSCRIPT_IN_THE_ABSENCE_OF_TAT	REACTOME	0.71734893	0.7773761	1
REACTOME_GAP_JUNCTION_ASSEMBLY	REACTOME	0.72745097	0.73580307	1
REACTOME_METABOLISM_OF_MRNA	REACTOME	0.729249	0.82917374	1
REACTOME_OXYGEN_DEPENDENT_PROLINE_HYDROXYLATION_OF_HYPOXIA_INDUCIBLE_FACTOR_ALPHA	REACTOME	0.7305503	0.7757375	1
REACTOME_REGULATION_OF_IFNA_SIGNALING	REACTOME	0.73733586	0.7694927	1
REACTOME_BOTULINUM_NEUROTOXICITY	REACTOME	0.74224806	0.7269335	1
REACTOME_METABOLISM_OF_VITAMINS_AND_COFACTORS	REACTOME	0.74552685	0.7653011	1

REACTOME_TIE2_SIGNALING	REACTOME	0.749499	0.71127254	1
REACTOME_RNA_POL_I_TRANSCRIPTION_INITIATION	REACTOME	0.756	0.83178324	1
REACTOME_SIGNALING_BY_WNT	REACTOME	0.756705	0.8778114	1
REACTOME_G_ALPHA_S_SIGNALLING_EVENTS	REACTOME	0.76844263	0.76427364	1
REACTOME_CIRCADIAN_REPRESSION_OF_EXPRESSION_BY_REV_ERBA	REACTOME	0.7684825	0.83742017	1
REACTOME_RNA_POL_III_TRANSCRIPTION_TERMINATION	REACTOME	0.78063244	0.8328324	1
REACTOME_DOWNSTREAM_SIGNALING_EVENTS_OF_B_CELL_RECEPTOR_BCR	REACTOME	0.7855787	0.84651625	1
REACTOME_CTNNB1_PHOSPHORYLATION_CASCADE	REACTOME	0.786	0.8235646	1
REACTOME_RORA_ACTIVATES_CIRCADIAN_EXPRESSION	REACTOME	0.7891683	0.8737765	1
REACTOME_AMINO_ACID_AND_OLIGOPEPTIDE_SLC_TRANSPORTERS	REACTOME	0.7899628	0.77381307	1
REACTOME_POTASSIUM_CHANNELS	REACTOME	0.7919192	0.77755594	1
REACTOME_DOWNREGULATION_OF_TGF_BETA_RECEPTOR_SIGNALING	REACTOME	0.8109162	0.8253485	1
REACTOME_DEADENYLATION_DEPENDENT_MRNA_DECAY	REACTOME	0.81349206	0.8905033	1
REACTOME_SIGNALING_BY_FGFR1_FUSION_MUTANTS	REACTOME	0.85048544	0.87164664	1
REACTOME_PYRIMIDINE_METABOLISM	REACTOME	0.86570245	0.81224537	1
REACTOME_SIGNALING_BY_CONSTITUTIVELY_ACTIVE_EGFR	REACTOME	0.8700565	0.9023749	1
REACTOME_DESTABILIZATION_OF_MRNA_BY_AUF1_HNRNP_D0	REACTOME	0.88235295	0.9651095	1
REACTOME_AMINE_COMPOUND_SLC_TRANSPORTERS	REACTOME	0.89641434	0.81328887	1
REACTOME_SIGNALING_BY_FGFR1_MUTANTS	REACTOME	0.9040307	0.8290558	1
REACTOME_ACETYLCHOLINE_BINDING_AND_DOWNSTREAM_EVENTS	REACTOME	0.9099617	0.90889	1
REACTOME_REGULATION_OF_SIGNALING_BY_CBL	REACTOME	0.94140625	0.8729694	1
REACTOME_FGFR_LIGAND_BINDING_AND_ACTIVATION	REACTOME	0.94255316	0.9218341	1
REACTOME_TRAF6_MEDIATED_NFKB_ACTIVATION	REACTOME	0.96007985	0.92219126	1
REACTOME_SHC_MEDIATED_CASCADE	REACTOME	0.97131145	0.93056417	1
REACTOME_RNA_POL_III_TRANSCRIPTION_INITIATION_FROM_TYPE_2_PROMOTER	REACTOME	0.9802371	0.9705219	1
REACTOME_SIGNALING_BY_FGFR_MUTANTS	REACTOME	0.98035365	0.9323336	1

Table S4. All the gene sets enriched in FBS cells at D14 of culture compared with D1 hepatocytes (assessed by GSEA)

NAME	Data base	NOM p-val	FDR q-val	FWER p-val
HALLMARK_MYOGENESIS	HALLMARK	0	0.14730352	0.079
HALLMARK_APICAL_SURFACE	HALLMARK	0	0.09853713	0.105
HALLMARK_APICAL_JUNCTION	HALLMARK	0	0.07615069	0.113
HALLMARK_EPITHELIAL_MESENCHYMAL_TRANSITION	HALLMARK	0.001972387	0.08726127	0.157
HALLMARK_GLYCOLYSIS	HALLMARK	0.00203252	0.16894755	0.293
HALLMARK_APOPTOSIS	HALLMARK	0.004282655	0.16553766	0.45
HALLMARK_ESTROGEN_RESPONSE_EARLY	HALLMARK	0.004329004	0.14200172	0.376
HALLMARK_WNT_BETA_CATENIN_SIGNALING	HALLMARK	0.007984032	0.23145741	0.667
HALLMARK_SPERMATOGENESIS	HALLMARK	0.00856531	0.2221453	0.62
HALLMARK_UV_RESPONSE_DN	HALLMARK	0.020449897	0.14861557	0.473
HALLMARK_TGF_BETA_SIGNALING	HALLMARK	0.021052632	0.14467469	0.34
HALLMARK_NOTCH_SIGNALING	HALLMARK	0.025263159	0.15411514	0.455
HALLMARK_MITOTIC_SPINDLE	HALLMARK	0.025948104	0.16412668	0.333
HALLMARK_P53_PATHWAY	HALLMARK	0.03164557	0.21310273	0.739
HALLMARK_IL2_STAT5_SIGNALING	HALLMARK	0.038297873	0.24038444	0.66
HALLMARK_HEME_METABOLISM	HALLMARK	0.049568966	0.2288018	0.694
HALLMARK_ESTROGEN_RESPONSE_LATE	HALLMARK	0.081196584	0.22756888	0.704
HALLMARK_HYPOXIA	HALLMARK	0.102970295	0.22310638	0.726
HALLMARK_G2M_CHECKPOINT	HALLMARK	0.11264822	0.18801047	0.562
HALLMARK_REACTIVE_OXIGEN_SPECIES_PATHWAY	HALLMARK	0.13598326	0.27202892	0.82
HALLMARK_ANGIOGENESIS	HALLMARK	0.14092664	0.21681286	0.705
HALLMARK_HEDGEHOG_SIGNALING	HALLMARK	0.1431624	0.29210445	0.819
HALLMARK_PROTEIN_SECRETION	HALLMARK	0.15	0.22699594	0.68
HALLMARK_ANDROGEN_RESPONSE	HALLMARK	0.16458334	0.2814426	0.819
HALLMARK_ALLOGRAFT_REJECTION	HALLMARK	0.20930232	0.37116182	0.906
HALLMARK_E2F_TARGETS	HALLMARK	0.21825397	0.21651524	0.731
HALLMARK_KRAS_SIGNALING_UP	HALLMARK	0.25240847	0.3832338	0.905
HALLMARK_ADIPOGENESIS	HALLMARK	0.25518674	0.3352233	0.883
HALLMARK_MTORC1_SIGNALING	HALLMARK	0.36325678	0.4023514	0.92
HALLMARK_PANCREAS_BETA_CELLS	HALLMARK	0.37281552	0.4749836	0.954
HALLMARK_CHOLESTEROL_HOMEOSTASIS	HALLMARK	0.42008197	0.5189852	0.968
HALLMARK_INFLAMMATORY_RESPONSE	HALLMARK	0.4731801	0.50717777	0.969
HALLMARK_DNA_REPAIR	HALLMARK	0.5020747	0.5112673	0.966
HALLMARK_UNFOLDED_PROTEIN_RESPONSE	HALLMARK	0.5177453	0.52676517	0.982
HALLMARK_COMPLEMENT	HALLMARK	0.5242915	0.5216831	0.981
HALLMARK_PEROXISOME	HALLMARK	0.68666667	0.6795607	0.996
HALLMARK_PI3K_AKT_MTOR_SIGNALING	HALLMARK	0.68937874	0.71274674	0.996
HALLMARK_KRAS_SIGNALING_DN	HALLMARK	0.6973415	0.69501626	0.996
HALLMARK_OXIDATIVE_PHOSPHORYLATION	HALLMARK	0.74012476	0.8970353	1
HALLMARK_MYC_TARGETS_V1	HALLMARK	0.77272725	0.9044862	1
KEGG_DILATED_CARDIOMYOPATHY	KEGG	0	0.25345153	0.119

KEGG_ECM_RECEPTOR_INTERACTION	KEGG	0	0.1343037	0.126
KEGG_ARRHYTHMOGENIC_RIGHT_VENTRICULAR_CARDIOMYOPATHY_ARVC	KEGG	0	0.2761134	0.297
KEGG_HYPERTROPHIC_CARDIOMYOPATHY_HCM	KEGG	0	0.2143639	0.307
KEGG_AXON_GUIDANCE	KEGG	0	0.18423094	0.324
KEGG_REGULATION_OF_ACTIN_CYTOSKELETON	KEGG	0	0.20594056	0.417
KEGG_FOCAL_ADHESION	KEGG	0	0.1871146	0.424
KEGG_P53_SIGNALING_PATHWAY	KEGG	0	0.18791685	0.489
KEGG_TIGHT_JUNCTION	KEGG	0	0.18172808	0.506
KEGG_VIBRIO_CHOLERAE_INFECTION	KEGG	0	0.1734608	0.545
KEGG_GAP_JUNCTION	KEGG	0	0.17016828	0.567
KEGG_HEDGEHOG_SIGNALING_PATHWAY	KEGG	0	0.16351056	0.573
KEGG_SMALL_CELL_LUNG_CANCER	KEGG	0	0.20655596	0.678
KEGG_MELANOGENESIS	KEGG	0	0.1952891	0.695
KEGG_MAPK_SIGNALING_PATHWAY	KEGG	0	0.2002625	0.731
KEGG_PATHWAYS_IN_CANCER	KEGG	0	0.19432552	0.731
KEGG_GLYCOSAMINOGLYCAN_BIOSYNTHESIS_CHONDROITIN_SULFATE	KEGG	0	0.18551813	0.753
KEGG_AMYOTROPHIC_LATERAL_SCLEROSIS_ALS	KEGG	0	0.18108751	0.757
KEGG_PROGESTERONE_MEDIATED_OOCYTE_MATURATION	KEGG	0	0.17099173	0.759
KEGG_COLORECTAL_CANCER	KEGG	0	0.17438845	0.774
KEGG_WNT_SIGNALING_PATHWAY	KEGG	0	0.1710808	0.786
KEGG_LONG_TERM_POTENTIATION	KEGG	0	0.17390785	0.804
KEGG_GNRH_SIGNALING_PATHWAY	KEGG	0	0.18236607	0.836
KEGG_CALCIUM_SIGNALING_PATHWAY	KEGG	0.002024292	0.15432021	0.575
KEGG_LEUKOCYTE_TRANSENDOTHELIAL_MIGRATION	KEGG	0.004140787	0.16351232	0.601
KEGG_ENDOCYTOSIS	KEGG	0.004264392	0.19572893	0.752
KEGG_OOCYTE_MEIOSIS	KEGG	0.006237006	0.17566079	0.801
KEGG_ADHERENS_JUNCTION	KEGG	0.008130081	0.19180676	0.753
KEGG_O_GLYCAN_BIOSYNTHESIS	KEGG	0.010204081	0.18710051	0.695
KEGG_MELANOMA	KEGG	0.010460251	0.17285359	0.807
KEGG_GLUTATHIONE_METABOLISM	KEGG	0.01048218	0.17627273	0.439
KEGG_ALZHEIMERS_DISEASE	KEGG	0.014522822	0.17202672	0.518
KEGG_GALACTOSE_METABOLISM	KEGG	0.016701462	0.18024631	0.362
KEGG_GLIOMA	KEGG	0.016985139	0.18871851	0.871
KEGG_FC_GAMMA_R_MEDIATED_PHAGOCYTOSIS	KEGG	0.021008404	0.18928348	0.875
KEGG_PHOSPHATIDYLINOSITOL_SIGNALING_SYSTEM	KEGG	0.023012552	0.1755819	0.757
KEGG_CHEMOKINE_SIGNALING_PATHWAY	KEGG	0.027196653	0.21314964	0.906
KEGG_GLYCOSAMINOGLYCAN_BIOSYNTHESIS_HEPARAN_SULFATE	KEGG	0.027777778	0.1912097	0.881
KEGG_TGF_BETA_SIGNALING_PATHWAY	KEGG	0.030172413	0.19194467	0.871
KEGG_VASOPRESSIN_REGULATED_WATER_REABSORPTION	KEGG	0.033472802	0.21128161	0.909
KEGG_GLYCOSPHINGOLIPID_BIOSYNTHESIS_LACTO_AND_NEOLACTO_SERIES	KEGG	0.035196688	0.19613795	0.715
KEGG_INOSITOL_PHOSPHATE_METABOLISM	KEGG	0.03586498	0.19137612	0.863
KEGG_BASAL_CELL_CARCINOMA	KEGG	0.047227927	0.194789	0.881
KEGG_GLYCOSPHINGOLIPID_BIOSYNTHESIS_GANGLIO_SERIES	KEGG	0.048117153	0.18487422	0.871

KEGG_CARDIAC_MUSCLE_CONTRACTION	KEGG	0.050607286	0.20072249	0.689
KEGG_CELL_CYCLE	KEGG	0.058091287	0.19673443	0.893
KEGG_GLYCEROLIPID_METABOLISM	KEGG	0.058091287	0.26364276	0.955
KEGG_AMINO_SUGAR_AND_NUCLEOTIDE_SUGAR_METABOLISM	KEGG	0.061728396	0.19481856	0.878
KEGG_LYSOSOME	KEGG	0.070393376	0.18511832	0.831
KEGG_FRUCTOSE_AND_MANNOSE_METABOLISM	KEGG	0.07272727	0.26638505	0.959
KEGG_GLYCOSAMINOGLYCAN_DEGRADATION	KEGG	0.075	0.17296642	0.781
KEGG_PANCREATIC_CANCER	KEGG	0.077083334	0.21625787	0.911
KEGG_VEGF_SIGNALING_PATHWAY	KEGG	0.07789474	0.29774103	0.971
KEGG_BLADDER_CANCER	KEGG	0.079831935	0.30461758	0.975
KEGG_VASCULAR_SMOOTH_MUSCLE_CONTRACTION	KEGG	0.081932776	0.33666486	0.989
KEGG_LONG_TERM_DEPRESSION	KEGG	0.095634095	0.3684003	0.993
KEGG_NEUROTROPHIN_SIGNALING_PATHWAY	KEGG	0.10633947	0.29112107	0.967
KEGG_NOTCH_SIGNALING_PATHWAY	KEGG	0.11087866	0.28159806	0.963
KEGG_GLYCEROPHOSPHOLIPID_METABOLISM	KEGG	0.12916666	0.33866283	0.988
KEGG_LEISHMANIA_INFECTION	KEGG	0.13118279	0.31468186	0.982
KEGG_NATURAL_KILLER_CELL_MEDIATED_CYTOTOXICITY	KEGG	0.1336117	0.33728635	0.986
KEGG_VIRAL_MYOCARDITIS	KEGG	0.14639175	0.3001831	0.975
KEGG_PATHOGENIC_ESCHERICHIA_COLI_INFECTION	KEGG	0.14978904	0.28573647	0.963
KEGG_NOD_LIKE_RECEPTOR_SIGNALING_PATHWAY	KEGG	0.15	0.37239468	0.996
KEGG_ERBB_SIGNALING_PATHWAY	KEGG	0.15351813	0.33045805	0.986
KEGG_FC_EPSILON_RI_SIGNALING_PATHWAY	KEGG	0.17311609	0.36478528	0.993
KEGG_EPITHELIAL_CELL_SIGNALING_IN_HELICOBACTER_PYLORI_INFECTION	KEGG	0.1762295	0.37312937	0.993
KEGG_OTHER_GLYCAN_DEGRADATION	KEGG	0.19456068	0.31330442	0.983
KEGG_DORSO_VENTRAL_AXIS_FORMATION	KEGG	0.1965812	0.37884557	0.997
KEGG_CHRONIC_MYELOID_LEUKEMIA	KEGG	0.19709544	0.2932819	0.971
KEGG_CELL_ADHESION_MOLECULES_CAMS	KEGG	0.20082815	0.33963895	0.989
KEGG_ETHER_LIPID_METABOLISM	KEGG	0.20790021	0.3701103	0.996
KEGG_MTOR_SIGNALING_PATHWAY	KEGG	0.22384937	0.31354818	0.983
KEGG_REGULATION_OF_AUTOPHAGY	KEGG	0.22964509	0.33318263	0.986
KEGG_ENDOMETRIAL_CANCER	KEGG	0.23517382	0.33630246	0.989
KEGG_T_CELL_RECEPTOR_SIGNALING_PATHWAY	KEGG	0.23732251	0.4371119	0.997
KEGG_NON_SMALL_CELL_LUNG_CANCER	KEGG	0.2406639	0.33025697	0.986
KEGG_HUNTINGTONS_DISEASE	KEGG	0.24586777	0.35159418	0.991
KEGG_ACUTE_MYELOID_LEUKEMIA	KEGG	0.24793388	0.3629554	0.993
KEGG_PROSTATE_CANCER	KEGG	0.25155926	0.3374013	0.989
KEGG_RIBOFLAVIN_METABOLISM	KEGG	0.26050422	0.40666646	0.997
KEGG_APOPTOSIS	KEGG	0.2638037	0.3385235	0.989
KEGG_GLYCOSYLPHOSPHATIDYLINOSITOL_GPI_ANCHOR_BIOSYNTHESIS	KEGG	0.26464647	0.30033877	0.977
KEGG_THYROID_CANCER	KEGG	0.27878788	0.41396132	0.997
KEGG_RENAL_CELL_CARCINOMA	KEGG	0.28033474	0.37399065	0.996
KEGG_BIOSYNTHESIS_OF_UNSATURATED_FATTY_ACIDS	KEGG	0.30952382	0.44034547	0.997
KEGG_UBIQUITIN_MEDIATED_PROTEOLYSIS	KEGG	0.31027254	0.36664054	0.993

KEGG_TOLL_LIKE_RECEPTOR_SIGNALING_PATHWAY	KEGG	0.31392932	0.4492608	0.997
KEGG_SPHINGOLIPID_METABOLISM	KEGG	0.32635984	0.43688583	0.997
KEGG_INSULIN_SIGNALING_PATHWAY	KEGG	0.3361169	0.36830994	0.993
KEGG_PURINE_METABOLISM	KEGG	0.35714287	0.43267143	0.997
KEGG_RIBOSOME	KEGG	0.35968378	0.4431438	0.997
KEGG_HOMOLOGOUS_RECOMBINATION	KEGG	0.3884462	0.44224462	0.997
KEGG_ABC_TRANSPORTERS	KEGG	0.4012474	0.51720816	1
KEGG_PENTOSE_PHOSPHATE_PATHWAY	KEGG	0.40319362	0.49504974	0.997
KEGG_N_GLYCAN_BIOSYNTHESIS	KEGG	0.4074074	0.44094044	0.997
KEGG_JAK_STAT_SIGNALING_PATHWAY	KEGG	0.41201717	0.5113484	1
KEGG_ALDOSTERONE_REGULATED_SODIUM_REABSORPTION	KEGG	0.4135021	0.53284806	1
KEGG_NUCLEOTIDE_EXCISION_REPAIR	KEGG	0.41497976	0.4073057	0.997
KEGG_NICOTINATE_AND_NICOTINAMIDE_METABOLISM	KEGG	0.42857143	0.53411853	1
KEGG_AMINOACYL_TRNA_BIOSYNTHESIS	KEGG	0.43927124	0.44516996	0.997
KEGG_CYTOKINE_CYTOKINE_RECEPTOR_INTERACTION	KEGG	0.46088794	0.55773157	1
KEGG_MISMATCH_REPAIR	KEGG	0.50199205	0.4749969	0.997
KEGG_SNARE_INTERACTIONS_IN_VESICULAR_TRANSPORT	KEGG	0.5122449	0.5908051	1
KEGG_DNA_REPLICATION	KEGG	0.51292247	0.50522876	1
KEGG_TYPE_II_DIABETES_MELLITUS	KEGG	0.5157233	0.5533579	1
KEGG_PYRUVATE_METABOLISM	KEGG	0.53578734	0.6179779	1
KEGG_TASTE_TRANSDUCTION	KEGG	0.5536062	0.6410258	1
KEGG_OXIDATIVE_PHOSPHORYLATION	KEGG	0.583501	0.6651935	1
KEGG_BASE_EXCISION_REPAIR	KEGG	0.5883534	0.63621277	1
KEGG_RIG_I_LIKE_RECEPTOR_SIGNALING_PATHWAY	KEGG	0.60692465	0.6725721	1
KEGG_STARCH_AND_SUCROSE_METABOLISM	KEGG	0.6207585	0.6724012	1
KEGG_B_CELL_RECEPTOR_SIGNALING_PATHWAY	KEGG	0.6393443	0.6690297	1
KEGG_PARKINSONS_DISEASE	KEGG	0.6713996	0.7326858	1
KEGG_PRIMARY_IMMUNODEFICIENCY	KEGG	0.6871401	0.66553396	1
KEGG_PYRIMIDINE_METABOLISM	KEGG	0.6895161	0.7514868	1
KEGG_BASAL_TRANSCRIPTION_FACTORS	KEGG	0.700611	0.8069129	1
KEGG_TYPE_I_DIABETES_MELLITUS	KEGG	0.70119524	0.75544345	1
KEGG_RNA_DEGRADATION	KEGG	0.73991936	0.82764167	1
KEGG_CITRATE_CYCLE_TCA_CYCLE	KEGG	0.7464503	0.80769455	1
KEGG_CYTOSOLIC_DNA_SENSING_PATHWAY	KEGG	0.781893	0.7499555	1
KEGG_STEROID_BIOSYNTHESIS	KEGG	0.7949219	0.8252448	1
KEGG_SELENOAMINO_ACID_METABOLISM	KEGG	0.7987805	0.8032862	1
KEGG_NEUROACTIVE_LIGAND_RECEPTOR_INTERACTION	KEGG	0.83914727	0.787934	1
REACTOME_THE_ROLE_OF_NEF_IN_HIV1_REPLICATION_AND_DISEASE_PATHOGENESIS	REACTOME	0	0.48078176	0.151
REACTOME_NCAM_SIGNALING_FOR_NEURITE_OUT_GROWTH	REACTOME	0	0.4148518	0.226
REACTOME_KERATAN_SULFATE_BIOSYNTHESIS	REACTOME	0	0.3341985	0.253
REACTOME_NCAM1_INTERACTIONS	REACTOME	0	0.20037591	0.289
REACTOME_NEF_MEDIATES_DOWN_MODULATION_OF_CELL_SURFACE_RECEPTORS_BY_RECRUITING_THEM_TO_CLATHRIN_ADAPTERS	REACTOME	0	0.17231195	0.289
REACTOME_NEUROTRANSMITTER_RECEPTOR_BINDING_AND_DOWNSTREAM_TRANSMISSION_IN_THE_POSTSYNAPTIC_CELL	REACTOME	0	0.16374151	0.304

REACTOME_AXON_GUIDANCE	REACTOME	0	0.17802835	0.337
REACTOME_TRANSMISSION_ACROSS_CHEMICAL_SYNAPSES	REACTOME	0	0.21958348	0.425
REACTOME_DEVELOPMENTAL_BIOLOGY	REACTOME	0	0.20178899	0.425
REACTOME_O_LINKED_GLYCOSYLATION_OF_MUCINS	REACTOME	0	0.19103965	0.428
REACTOME_ACTIVATION_OF_NMDA_RECEPTOR_UPON_GLUTAMATE_BINDING_AND_POSTSYNAPTIC_EVENTS	REACTOME	0	0.20680486	0.464
REACTOME_GLYCOSAMINOGLYCAN_METABOLISM	REACTOME	0	0.21825135	0.503
REACTOME_INTEGRIN_CELL_SURFACE_INTERACTIONS	REACTOME	0	0.20611614	0.504
REACTOME_SEMAPHORIN_INTERACTIONS	REACTOME	0	0.21163976	0.525
REACTOME_HS_GAG_DEGRADATION	REACTOME	0	0.18634602	0.528
REACTOME_L1CAM_INTERACTIONS	REACTOME	0	0.19282745	0.542
REACTOME_POST_NMDA_RECEPTOR_ACTIVATION_EVENTS	REACTOME	0	0.20142873	0.564
REACTOME_HEPARAN_SULFATE_HEPARIN_HS_GAG_METABOLISM	REACTOME	0	0.19876066	0.574
REACTOME_MUSCLE_CONTRACTION	REACTOME	0	0.21252726	0.606
REACTOME_A_TETRASACCHARIDE_LINKER_SEQUENCE_IS_REQUIRED_FOR_GAG_SYNTHESIS	REACTOME	0	0.22300278	0.63
REACTOME_CHONDROITIN_SULFATE_DERMATAN_SULFATE_METABOLISM	REACTOME	0	0.2411889	0.663
REACTOME_CELL_DEATH_SIGNALLING_VIA_NRAGE_NRIF_AND_NADE	REACTOME	0	0.23381677	0.663
REACTOME_ERK_MAPK_TARGETS	REACTOME	0	0.22738229	0.666
REACTOME_MHC_CLASS_II_ANTIGEN_PRESENTATION	REACTOME	0	0.22801387	0.709
REACTOME_MYOGENESIS	REACTOME	0	0.22809654	0.714
REACTOME_NRAGE_SIGNALS_DEATH_THROUGH_JNK	REACTOME	0	0.24919042	0.741
REACTOME_CREB_PHOSPHORYLATION_THROUGH_THE_ACTIVATION_OF_RAS	REACTOME	0	0.24368389	0.752
REACTOME_CHONDROITIN_SULFATE_BIOSYNTHESIS	REACTOME	0	0.2452073	0.754
REACTOME_NUCLEAR_EVENTS_KINASE_AND_TRANSCRIPTION_FACTOR_ACTIVATION	REACTOME	0	0.24989551	0.767
REACTOME_G_ALPHA_Z_SIGNALLING_EVENTS	REACTOME	0	0.24704373	0.767
REACTOME_G1_PHASE	REACTOME	0	0.24179599	0.767
REACTOME_SIGNALING_BY_RHO_GTPASES	REACTOME	0	0.2371991	0.768
REACTOME_FACTORS_INVOLVED_IN_MEGAKARYOCYTE_DEVELOPMENT_AND_PLATELET_PRODUCTION	REACTOME	0	0.26111913	0.801
REACTOME_LYSOSOME_VESICLE_BIOGENESIS	REACTOME	0	0.27612013	0.834
REACTOME_SIGNALLING_BY_NGF	REACTOME	0	0.28725097	0.852
REACTOME_SIGNAL_TRANSDUCTION_BY_L1	REACTOME	0	0.275578	0.878
REACTOME_SMOOTH_MUSCLE_CONTRACTION	REACTOME	0	0.30001768	0.889
REACTOME_P75_NTR_RECEPTOR_MEDIATED_SIGNALLING	REACTOME	0	0.29895258	0.889
REACTOME_PLC_BETA_MEDIATED_EVENTS	REACTOME	0	0.30219775	0.897
REACTOME_NGF_SIGNALLING_VIA_TRKA_FROM_THE_PLASMA_MEMBRANE	REACTOME	0	0.294335	0.9
REACTOME_KINESINS	REACTOME	0	0.29239932	0.9
REACTOME_REGULATION_OF_INSULIN_SECRETION	REACTOME	0.001915709	0.28572986	0.883
REACTOME_EFFECTS_OF_PIP2_HYDROLYSIS	REACTOME	0.001930502	0.2301776	0.706
REACTOME_POST_CHAPERONIN_TUBULIN_FOLDING_PATHWAY	REACTOME	0.002004008	0.2752618	0.816
REACTOME_OPIOID_SIGNALLING	REACTOME	0.003731343	0.28438777	0.94
REACTOME_SIGNALING_BY_FGFR	REACTOME	0.003809524	0.28697053	0.874
REACTOME_DOWNSTREAM_SIGNALING_OF_ACTIVATED_FGFR	REACTOME	0.003809524	0.28784266	0.936
REACTOME_KERATAN_SULFATE_KERATIN_METABOLISM	REACTOME	0.003875969	0.21886954	0.403
REACTOME_TRAFFICKING_OF_AMPA_RECEPTORS	REACTOME	0.003891051	0.20470771	0.527

REACTOME_GAP_JUNCTION_TRAFFICKING	REACTOME	0.003891051	0.24435814	0.742
REACTOME_NEURONAL_SYSTEM	REACTOME	0.003968254	0.2282235	0.641
REACTOME_CELL_SURFACE_INTERACTIONS_AT_THE_VASCULAR_WALL	REACTOME	0.005576208	0.2837014	0.854
REACTOME_G_ALPHA1213_SIGNALLING_EVENTS	REACTOME	0.005725191	0.28039515	0.878
REACTOME_SIGNALING_BY_PDGF	REACTOME	0.005758158	0.28049356	0.867
REACTOME_COLLAGEN_FORMATION	REACTOME	0.007952286	0.2359617	0.284
REACTOME_TRAFFICKING_OF_GLUR2_CONTAINING_AMPA_RECEPTORS	REACTOME	0.008080808	0.29626918	0.888
REACTOME_CA_DEPENDENT_EVENTS	REACTOME	0.009708738	0.28481632	0.931
REACTOME_SIGNALING_BY_FGFR_IN_DISEASE	REACTOME	0.009784736	0.2846493	0.936
REACTOME_EXTRACELLULAR_MATRIX_ORGANIZATION	REACTOME	0.00984252	0.2632047	0.264
REACTOME_HS_GAG_BIOSYNTHESIS	REACTOME	0.011235955	0.22962146	0.694
REACTOME_INTEGRATION_OF_ENERGY_METABOLISM	REACTOME	0.011472276	0.31968302	0.967
REACTOME_DOWNREGULATION_OF_TGF_BETA_RECEPTOR_SIGNALING	REACTOME	0.011695907	0.29023325	0.94
REACTOME_RAS_ACTIVATION_UOPN_CA2_INFUX_THROUGH_NMDA_RECEPTOR	REACTOME	0.01183432	0.2366375	0.706
REACTOME_REGULATION_OF_KIT_SIGNALING	REACTOME	0.012	0.3381574	0.976
REACTOME_TRANSPORT_OF_INORGANIC_CATIONS_ANIONS_AND_AMINO_ACIDS_OLIGOPEPTIDES	REACTOME	0.012121212	0.3040959	0.917
REACTOME_INTERACTION_BETWEEN_L1_AND_ANKYRINS	REACTOME	0.012145749	0.19521038	0.527
REACTOME_SIGNALLING_TO_RAS	REACTOME	0.013358778	0.29006717	0.935
REACTOME_HEMOSTASIS	REACTOME	0.016917294	0.3003411	0.946
REACTOME_SIGNALING_BY_EGFR_IN_CANCER	REACTOME	0.017142856	0.3014401	0.897
REACTOME_CELL_CELL_COMMUNICATION	REACTOME	0.01734104	0.3019887	0.9
REACTOME_MAPK_TARGETS_NUCLEAR_EVENTS_MEDIATED_BY_MAP_KINASES	REACTOME	0.019157087	0.31617585	0.957
REACTOME_RECYCLING_PATHWAY_OF_L1	REACTOME	0.019493178	0.2894264	0.944
REACTOME_METABOLISM_OF_CARBOHYDRATES	REACTOME	0.019607844	0.29083556	0.94
REACTOME_INSULIN_SYNTHESIS_AND_PROCESSING	REACTOME	0.021153847	0.31331587	0.957
REACTOME_INTEGRIN_ALPHAIIB_BETA3_SIGNALING	REACTOME	0.021696253	0.2955358	0.922
REACTOME_BASIGIN_INTERACTIONS	REACTOME	0.02268431	0.2508921	0.76
REACTOME_DIABETES_PATHWAYS	REACTOME	0.0251938	0.31820694	0.961
REACTOME_DEPOSITION_OF_NEW_CENPA_CONTAINING_NUCLEOSOMES_AT_THE_CENTROMERE	REACTOME	0.025742574	0.30475503	0.897
REACTOME_P130CAS_LINKAGE_TO_MAPK_SIGNALING_FOR_INTEGRINS	REACTOME	0.026052104	0.29431683	0.889
REACTOME_GLUCAGON_SIGNALING_IN_METABOLIC_REGULATION	REACTOME	0.027079303	0.32525852	0.968
REACTOME_PRE_NOTCH_EXPRESSION_AND_PROCESSING	REACTOME	0.02739726	0.30817676	0.948
REACTOME_GRB2_SOS_PROVIDES_LINKAGE_TO_MAPK_SIGNALING_FOR_INTERGRINS_	REACTOME	0.027667984	0.29903898	0.92
REACTOME_ACYL_CHAIN_REMODELLING_OF_PC	REACTOME	0.028680688	0.28872606	0.929
REACTOME_PHOSPHOLIPASE_C_MEDIATED_CASCADE	REACTOME	0.029069768	0.32399777	0.968
REACTOME_CREB_PHOSPHORYLATION_THROUGH_THE_ACTIVATION_OF_CAMKII	REACTOME	0.030710172	0.24728915	0.746
REACTOME_CELL_JUNCTION_ORGANIZATION	REACTOME	0.030828517	0.29578128	0.907
REACTOME_SEMA4D_IN_SEMAPHORIN_SIGNALING	REACTOME	0.032258064	0.2806958	0.856
REACTOME_PLATELET_ACTIVATION_SIGNALING_AND_AGGREGATION	REACTOME	0.0327553	0.3359447	0.979
REACTOME_TGF_BETA_RECEPTOR_SIGNALING_ACTIVATES_SMADS	REACTOME	0.0332681	0.3124869	0.948
REACTOME_PLATELET_AGGREGATION_PLUG_FORMATION	REACTOME	0.03373016	0.32313102	0.965
REACTOME_CYCLIN_A_B1_ASSOCIATED_EVENTS_DURING_G2_M_TRANSITION	REACTOME	0.034749035	0.30294713	0.92
REACTOME_PKA_MEDIATED_PHOSPHORYLATION_OF_CREB	REACTOME	0.034749035	0.32235688	0.965

REACTOME_SIGNALING_BY_ERBB2	REACTOME	0.034816246	0.28717205	0.94
REACTOME_ADHERENS_JUNCTIONS_INTERACTIONS	REACTOME	0.034883723	0.27808312	0.858
REACTOME_OTHER_SEMAPHORIN_INTERACTIONS	REACTOME	0.037401576	0.25583962	0.741
REACTOME_THROMBIN_SIGNALLING_THROUGH_PROTEINASE_ACTIVATED_RECEPTORS_PARS	REACTOME	0.039772727	0.30676264	0.95
REACTOME_CTLA4_INHIBITORY_SIGNALING	REACTOME	0.04054054	0.29363027	0.929
REACTOME_MITOTIC_PROMETAPHASE	REACTOME	0.04474708	0.30941245	0.948
REACTOME_PYRUVATE_METABOLISM	REACTOME	0.051823415	0.29494432	0.926
REACTOME_REGULATION_OF_INSULIN_SECRETION_BY_GLUCAGON_LIKE_PEPTIDE1	REACTOME	0.05212355	0.37154457	0.992
REACTOME_FORMATION_OF_TUBULIN_FOLDING_INTERMEDIATES_BY_CCT_TRIC	REACTOME	0.052734375	0.29753083	0.897
REACTOME_RAP1_SIGNALLING	REACTOME	0.05973025	0.2873766	0.931
REACTOME_UNBLOCKING_OF_NMDA_RECEPTOR_GLUTAMATE_BINDING_AND_ACTIVATION	REACTOME	0.059760958	0.2980257	0.9
REACTOME_SEMA4D_INDUCED_CELL_MIGRATION_AND_GROWTH_CONE_COLLAPSE	REACTOME	0.061657034	0.29340276	0.935
REACTOME_GPVI_MEDIATED_ACTIVATION_CASCADE	REACTOME	0.06403013	0.2903612	0.929
REACTOME_SIGNALING_BY_SCF_KIT	REACTOME	0.06496063	0.3237212	0.968
REACTOME_GABA_B_RECEPTOR_ACTIVATION	REACTOME	0.06563707	0.2849982	0.878
REACTOME_COSTIMULATION_BY_THE_CD28_FAMILY	REACTOME	0.06613226	0.41052425	0.996
REACTOME_PI_3K_CASCADE	REACTOME	0.068	0.41270176	0.997
REACTOME_G_PROTEIN_BETA_GAMMA_SIGNALLING	REACTOME	0.07450981	0.34689555	0.984
REACTOME_GABA_RECEPTOR_ACTIVATION	REACTOME	0.075	0.27882385	0.829
REACTOME_PREFOLDIN_MEDIATED_TRANSFER_OF_SUBSTRATE_TO_CCT_TRIC	REACTOME	0.07569721	0.28868714	0.944
REACTOME_ACTIVATION_OF_CHAPERONE_GENES_BY_XBP1S	REACTOME	0.076171875	0.29346198	0.946
REACTOME_GABA_SYNTHESIS_RELEASE_REUPTAKE_AND_DEGRADATION	REACTOME	0.07630522	0.30005464	0.917
REACTOME_MEIOTIC_RECOMBINATION	REACTOME	0.07858546	0.2917432	0.907
REACTOME_DAG_AND_IP3_SIGNALING	REACTOME	0.080078125	0.3422235	0.979
REACTOME_MITOTIC_G2_G2_M_PHASES	REACTOME	0.08039216	0.3223132	0.964
REACTOME_GRB2_EVENTS_IN_ERBB2_SIGNALING	REACTOME	0.08235294	0.35070333	0.988
REACTOME_PRE_NOTCH_PROCESSING_IN_GOLGI	REACTOME	0.08267716	0.3227793	0.964
REACTOME_SIGNAL_AMPLIFICATION	REACTOME	0.08301158	0.30854735	0.95
REACTOME_EGFR_DOWNREGULATION	REACTOME	0.083984375	0.3507325	0.988
REACTOME_REGULATION_OF_WATER_BALANCE_BY_RENAL_AQUAPORINS	REACTOME	0.08510638	0.3802053	0.994
REACTOME_NUCLEOTIDE_BINDING_DOMAIN_LEUCINE_RICH_REPEAT_CONTAINING_RECEPTOR_NLR_SIGNALING_PATHWAYS	REACTOME	0.0877193	0.41655624	0.997
REACTOME_CELL_CELL_JUNCTION_ORGANIZATION	REACTOME	0.09356725	0.3457019	0.984
REACTOME_INHIBITION_OF_INSULIN_SECRETION_BY_ADRENALINE_NORADRENALINE	REACTOME	0.09375	0.32280883	0.964
REACTOME_MEIOSIS	REACTOME	0.0967118	0.3083016	0.948
REACTOME_PIP3_ACTIVATES_AKT_SIGNALING	REACTOME	0.097222224	0.33911064	0.979
REACTOME_SHC1_EVENTS_IN_ERBB4_SIGNALING	REACTOME	0.1010101	0.39907226	0.996
REACTOME_G1_S_SPECIFIC_TRANSCRIPTION	REACTOME	0.101960786	0.39102685	0.995
REACTOME_POST_TRANSLATIONAL_PROTEIN_MODIFICATION	REACTOME	0.103515625	0.34112415	0.979
REACTOME_LOSS_OF_NLP_FROM_MITOTIC_CENTROSOMES	REACTOME	0.10412574	0.32102895	0.965
REACTOME_SHC_RELATED_EVENTS	REACTOME	0.104961835	0.3235026	0.969
REACTOME_CHROMOSOME_MAINTENANCE	REACTOME	0.107421875	0.34016764	0.975
REACTOME_SIGNALING_BY_ROBO_RECEPTOR	REACTOME	0.10763209	0.33685628	0.976
REACTOME_CELL_CYCLE	REACTOME	0.11045365	0.32630578	0.965

REACTOME_GLUTATHIONE_CONJUGATION	REACTOME	0.11372549	0.33998445	0.979
REACTOME_STRIATED_MUSCLE_CONTRACTION	REACTOME	0.115079366	0.28790358	0.944
REACTOME_NEPHRIN_INTERACTIONS	REACTOME	0.115234375	0.3479337	0.988
REACTOME_YAP1_AND_WWTR1_TAZ_STIMULATED_GENE_EXPRESSION	REACTOME	0.11614173	0.3498673	0.988
REACTOME_ACTIVATION_OF_KAINATE_RECEPTORS_UPON_GLUTAMATE_BINDING	REACTOME	0.11660079	0.3734198	0.993
REACTOME_SIGNALING_BY_BMP	REACTOME	0.11881188	0.3242618	0.965
REACTOME_SIGNALLING_TO_ERKS	REACTOME	0.12151395	0.39729792	0.996
REACTOME_PI3K_EVENTS_IN_ERBB4_SIGNALING	REACTOME	0.12284069	0.40311575	0.996
REACTOME_ADP_SIGNALLING_THROUGH_P2RY1	REACTOME	0.12476008	0.34718356	0.982
REACTOME_SIGNALING_BY_NOTCH	REACTOME	0.1290944	0.3702361	0.993
REACTOME_TRANSMEMBRANE_TRANSPORT_OF_SMALL_MOLECULES	REACTOME	0.12922466	0.41952494	0.997
REACTOME_SYNTHESIS_AND_INTERCONVERSION_OF_NUCLEOTIDE_DI_AND_TRIPHOSPHATES	REACTOME	0.12984496	0.32179585	0.965
REACTOME_INSULIN_RECEPTOR_RECYCLING	REACTOME	0.13257575	0.37271953	0.993
REACTOME_RECRUITMENT_OF_MITOTIC_CENTROSOME_PROTEINS_AND_COMPLEXES	REACTOME	0.13333334	0.31859207	0.965
REACTOME_CGMP_EFFECTS	REACTOME	0.13396226	0.34781662	0.988
REACTOME_MYD88_MAL_CASCADE_INITIATED_ON_PLASMA_MEMBRANE	REACTOME	0.13438736	0.4076223	0.996
REACTOME_SHC_MEDIATED_SIGNALLING	REACTOME	0.13498099	0.32465804	0.965
REACTOME_E2F_MEDIATED_REGULATION_OF_DNA_REPLICATION	REACTOME	0.1374502	0.3713576	0.993
REACTOME_ION_TRANSPORT_BY_P_TYPE_ATPASES	REACTOME	0.1392157	0.41256946	0.996
REACTOME_DOWNSTREAM_SIGNAL_TRANSDUCTION	REACTOME	0.14341846	0.3233648	0.969
REACTOME_AQUAPORIN_MEDIATED_TRANSPORT	REACTOME	0.14424951	0.44950595	1
REACTOME_SIGNALING_BY_ERBB4	REACTOME	0.14486921	0.38610196	0.995
REACTOME_MAP_KINASE_ACTIVATION_IN_TLR_CASCADE	REACTOME	0.14653465	0.3778577	0.994
REACTOME_G_BETA_GAMMA_SIGNALLING_THROUGH_PI3KGAMMA	REACTOME	0.1482966	0.3885977	0.995
REACTOME_CELL_CYCLE_MITOTIC	REACTOME	0.15049505	0.33631337	0.975
REACTOME_PHOSPHORYLATION_OF_THE_APC_C	REACTOME	0.1515748	0.40664765	0.996
REACTOME_PI3K_EVENTS_IN_ERBB2_SIGNALING	REACTOME	0.1521739	0.41088256	0.997
REACTOME_LATENT_INFECTION_OF_HOMO_SAPIENS_WITH_MYCOBACTERIUM_TUBERCULOSIS	REACTOME	0.156	0.36803383	0.99
REACTOME_NETRIN1_SIGNALING	REACTOME	0.15678777	0.40872276	0.997
REACTOME_GAB1_SIGNALOSOME	REACTOME	0.15904573	0.3497291	0.988
REACTOME_MITOTIC_M_M_G1_PHASES	REACTOME	0.16129032	0.34825927	0.988
REACTOME_TELOMERE_MAINTENANCE	REACTOME	0.16247582	0.3893585	0.995
REACTOME_MEMBRANE_TRAFFICKING	REACTOME	0.16370809	0.38127005	0.994
REACTOME_DARPP_32_EVENTS	REACTOME	0.16435644	0.36703435	0.993
REACTOME_GASTRIN_CREB_SIGNALLING_PATHWAY_VIA_PKC_AND_MAPK	REACTOME	0.16538462	0.4187114	0.997
REACTOME_TRAF6_MEDIATED_INDUCTION_OF_NFKB_AND_MAP_KINASES_UPON_TLR7_8_OR_9_ACTIVATION	REACTOME	0.168	0.4516864	1
REACTOME_SRP_DEPENDENT_COTRANSLATIONAL_PROTEIN_TARGETING_TO_MEMBRANE	REACTOME	0.16904277	0.38227147	0.994
REACTOME_ACTIVATED_TLR4_SIGNALLING	REACTOME	0.17025441	0.4334034	0.997
REACTOME_SIGNALING_BY_TGF_BETA_RECEPTOR_COMPLEX	REACTOME	0.17034069	0.38796544	0.995
REACTOME_PYRUVATE_METABOLISM_AND_CITRIC_ACID_TCA_CYCLE	REACTOME	0.17261904	0.3468913	0.988
REACTOME_ASPARAGINE_N_LINKED_GLYCOSYLATION	REACTOME	0.17623763	0.3841761	0.994
REACTOME_APC_CDC20_MEDIATED_DEGRADATION_OF_NEK2A	REACTOME	0.1809145	0.40623954	0.996
REACTOME_PLATELET_HOMEOSTASIS	REACTOME	0.182	0.42106673	0.997

REACTOME_APC_C_CDC20_MEDIATED_DEGRADATION_OF_CYCLIN_B	REACTOME	0.18326694	0.40864065	0.996
REACTOME_NFKB_AND_MAP_KINASES_ACTIVATION_MEDIATED_BY_TLR4_SIGNALING_REPERTOIRE	REACTOME	0.18343195	0.43818533	1
REACTOME_UNFOLDED_PROTEIN_RESPONSE	REACTOME	0.19565217	0.40654758	0.996
REACTOME_TOLL_RECEPTOR_CASCADES	REACTOME	0.19649805	0.43601152	0.997
REACTOME_SHC1_EVENTS_IN_EGFR_SIGNALING	REACTOME	0.19726562	0.36148304	0.988
REACTOME_RNA_POL_I_PROMOTER_OPENING	REACTOME	0.19844358	0.29153597	0.944
REACTOME_IL_2_SIGNALING	REACTOME	0.2	0.41145077	0.997
REACTOME_FRS2_MEDIATED_CASCADE	REACTOME	0.20486815	0.48877507	1
REACTOME_DEGRADATION_OF_THE_EXTRACELLULAR_MATRIX	REACTOME	0.20907298	0.45340747	1
REACTOME_DNA_REPLICATION	REACTOME	0.2112676	0.3684974	0.993
REACTOME_PROTEIN_FOLDING	REACTOME	0.21314742	0.41054735	0.996
REACTOME_INFLAMMASOMES	REACTOME	0.21442126	0.48509818	1
REACTOME_PI3K_AKT_ACTIVATION	REACTOME	0.22134387	0.43072328	0.997
REACTOME_ION_CHANNEL_TRANSPORT	REACTOME	0.22554891	0.4313467	0.997
REACTOME_HOMOLOGOUS_RECOMBINATION_REPAIR_OF_REPLICATION_INDEPENDENT_DOUBLE_STRAND_BREAKS	REACTOME	0.22637795	0.39272046	0.995
REACTOME_NITRIC_OXIDE_STIMULATES_GUANYLATE_CYCLASE	REACTOME	0.22727273	0.42946714	0.997
REACTOME_INHIBITION_OF_THE_PROTEOLYTIC_ACTIVITY_OF_APC_C_REQUIRED_FOR_THE_ONSET_OF_ANAPHASE_BY_MITOTIC_SPINDLE_CHECKPOINT_COMPONENT	REACTOME	0.228	0.4216388	0.997
REACTOME_SYNTHESIS_OF_PIPS_AT_THE_PLASMA_MEMBRANE	REACTOME	0.2310757	0.42788008	0.997
REACTOME_SIGNALING_BY_INSULIN_RECEPTOR	REACTOME	0.23493975	0.4487786	1
REACTOME_RNA_POL_I_TRANSCRIPTION	REACTOME	0.23586744	0.4088002	0.997
REACTOME_G_PROTEIN_ACTIVATION	REACTOME	0.2394636	0.45737216	1
REACTOME_ADP_SIGNALLING_THROUGH_P2RY12	REACTOME	0.23952095	0.44832012	1
REACTOME_DOUBLE_STRAND_BREAK_REPAIR	REACTOME	0.24124514	0.37318012	0.992
REACTOME_ACTIVATED_NOTCH1_TRANSMITS_SIGNAL_TO_THE_NUCLEUS	REACTOME	0.243083	0.43287724	0.997
REACTOME_SLC_MEDIATED_TRANSMEMBRANE_TRANSPORT	REACTOME	0.24649298	0.48561668	1
REACTOME_APOPTOTIC_EXECUTION_PHASE	REACTOME	0.2504817	0.43005306	0.997
REACTOME_TRANSCRIPTIONAL_REGULATION_OF_WHITE_ADIPOCYTE_DIFFERENTIATION	REACTOME	0.25148514	0.45720136	1
REACTOME_CD28_CO_STIMULATION	REACTOME	0.2519685	0.45038685	1
REACTOME_MITOTIC_G1_G1_S_PHASES	REACTOME	0.25201613	0.3874459	0.995
REACTOME_GAP_JUNCTION_ASSEMBLY	REACTOME	0.25244617	0.44849595	1
REACTOME_TERMINATION_OF_O_GLYCAN_BIOSYNTHESIS	REACTOME	0.25390625	0.44991723	1
REACTOME_REGULATION_OF_MITOTIC_CELL_CYCLE	REACTOME	0.2549801	0.4310244	0.997
REACTOME_NEUROTRANSMITTER_RELEASE_CYCLE	REACTOME	0.25656566	0.4470388	1
REACTOME_INHIBITION_OF_VOLTAGE_GATED_CA2_CHANNELS_VIA_GBETA_GAMMA_SUBUNITS	REACTOME	0.25675675	0.4100314	0.997
REACTOME_NEGATIVE_REGULATION_OF_FGFR_SIGNALING	REACTOME	0.25732216	0.48752075	1
REACTOME_PHASE_II_CONJUGATION	REACTOME	0.2620424	0.5321172	1
REACTOME_PRE_NOTCH_TRANSCRIPTION_AND_TRANSLATION	REACTOME	0.26418787	0.4471169	1
REACTOME_G_BETA_GAMMA_SIGNALLING_THROUGH_PLC_BETA	REACTOME	0.27450982	0.46959734	1
REACTOME_TRIF_MEDIATED_TLR3_SIGNALING	REACTOME	0.27667984	0.48728883	1
REACTOME_GLYCEROPHOSPHOLIPID_BIOSYNTHESIS	REACTOME	0.28	0.49940458	1
REACTOME_CONVERSION_FROM_APC_C_CDC20_TO_APC_C_CDH1_IN_LATE_ANAPHASE	REACTOME	0.28031808	0.4500178	1
REACTOME_MEIOTIC_SYNAPSIS	REACTOME	0.28100777	0.4315098	0.997
REACTOME_NUCLEOTIDE_LIKE_PURINERGIC_RECEPTORS	REACTOME	0.28598484	0.4494761	1

REACTOME_TRANSPORT_TO_THE_GOLGI_AND_SUBSEQUENT_MODIFICATION	REACTOME	0.28853756	0.45763624	1
REACTOME_FORMATION_OF_INCISION_COMPLEX_IN_GG_NER	REACTOME	0.28884462	0.42287084	0.997
REACTOME_TRANS_GOLGI_NETWORK_VESICLE_BUDDING	REACTOME	0.2915811	0.4129986	0.997
REACTOME_SIGNALING_BY_FGFR1_MUTANTS	REACTOME	0.29258516	0.47909278	1
REACTOME_PACKAGING_OF_TELOMERE_ENDS	REACTOME	0.2937743	0.40082642	0.996
REACTOME_GLYCOGEN_BREAKDOWN_GLYCOGENOLYSIS	REACTOME	0.29399586	0.44821006	1
REACTOME_G0_AND_EARLY_G1	REACTOME	0.2942346	0.4451967	1
REACTOME_THROMBOXANE_SIGNALLING_THROUGH_TP_RECEPTOR	REACTOME	0.3018868	0.5282362	1
REACTOME_G_ALPHA_Q_SIGNALLING_EVENTS	REACTOME	0.302974	0.5301975	1
REACTOME_IL_RECEPTOR_SHC_SIGNALING	REACTOME	0.30417496	0.48644298	1
REACTOME_AMYLOIDS	REACTOME	0.30604288	0.4174849	0.997
REACTOME_GLUTAMATE_NEUROTRANSMITTER_RELEASE_CYCLE	REACTOME	0.3067961	0.45890266	1
REACTOME_INSULIN_RECEPTOR_SIGNALLING_CASCADE	REACTOME	0.30876493	0.49905595	1
REACTOME_METABOLISM_OF_PROTEINS	REACTOME	0.30923694	0.45905882	1
REACTOME_GOLGI_ASSOCIATED_VESICLE_BIOGENESIS	REACTOME	0.31300813	0.4332224	0.997
REACTOME_POTASSIUM_CHANNELS	REACTOME	0.3151751	0.4866252	1
REACTOME_N_GLYCAN_ANTENNAE_ELONGATION_IN_THE_MEDIAL_TRANS_GOLGI	REACTOME	0.31547618	0.48751122	1
REACTOME_PEPTIDE_CHAIN_ELONGATION	REACTOME	0.31656185	0.528067	1
REACTOME_APOPTOTIC_CLEAVAGE_OF_CELLULAR_PROTEINS	REACTOME	0.31730768	0.46389917	1
REACTOME_G_ALPHA_I_SIGNALLING_EVENTS	REACTOME	0.31800765	0.55852854	1
REACTOME_GLYCOSPHINGOLIPID_METABOLISM	REACTOME	0.31960785	0.46834973	1
REACTOME_G1_S_TRANSITION	REACTOME	0.32931727	0.44339925	1
REACTOME_DOWNREGULATION_OF_SMAD2_3_SMAD4_TRANSCRIPTIONAL_ACTIVITY	REACTOME	0.33066133	0.5335654	1
REACTOME_TCA_CYCLE_AND_RESPIRATORY_ELECTRON_TRANSPORT	REACTOME	0.3313253	0.44752708	1
REACTOME_PROSTACYCLIN_SIGNALLING_THROUGH_PROSTACYCLIN_RECEPTOR	REACTOME	0.33584905	0.54031503	1
REACTOME_SPHINGOLIPID_METABOLISM	REACTOME	0.3365949	0.4986829	1
REACTOME_NOD1_2_SIGNALING_PATHWAY	REACTOME	0.33737373	0.52760565	1
REACTOME_SIGNALLING_TO_P38_VIA_RIT_AND_RIN	REACTOME	0.33797216	0.54919904	1
REACTOME_POST_TRANSLATIONAL_MODIFICATION_SYNTHESIS_OF_GPI_ANCHORED_PROTEINS	REACTOME	0.33858266	0.42857972	0.997
REACTOME_PROTEOLYTIC_CLEAVAGE_OF_SNARE_COMPLEX_PROTEINS	REACTOME	0.3387424	0.52854466	1
REACTOME_APOPTOSIS	REACTOME	0.34169886	0.4490097	1
REACTOME_ACETYLCHOLINE_BINDING_AND_DOWNSTREAM_EVENTS	REACTOME	0.34412956	0.5246868	1
REACTOME_PHOSPHOLIPID_METABOLISM	REACTOME	0.3493014	0.449134	1
REACTOME_AMINO_ACID_TRANSPORT_ACROSS_THE_PLASMA_MEMBRANE	REACTOME	0.3653846	0.53210497	1
REACTOME_RNA_POL_I_RNA_POL_III_AND_MITOCHONDRIAL_TRANSCRIPTION	REACTOME	0.3673077	0.5245159	1
REACTOME_ACTIVATION_OF_BH3_ONLY_PROTEINS	REACTOME	0.36893204	0.52725863	1
REACTOME_ENOS_ACTIVATION_AND_REGULATION	REACTOME	0.37	0.48654595	1
REACTOME_ABC_FAMILY_PROTEINS_MEDIATED_TRANSPORT	REACTOME	0.3721374	0.5546696	1
REACTOME_RESPONSE_TO_ELEVATED_PLATELET_CYTOSOLIC_CA2_	REACTOME	0.3745247	0.53015816	1
REACTOME_ANTIGEN_ACTIVATES_B_CELL_RECEPTOR_LEADING_TO_GENERATION_OF_SECOND_MESSENGERS	REACTOME	0.374761	0.5492197	1
REACTOME_ACTIVATION_OF_THE_PRE_REPLICATIVE_COMPLEX	REACTOME	0.38446215	0.48577118	1
REACTOME_SIGNALING_BY_HIPPO	REACTOME	0.3846154	0.5268564	1
REACTOME_GLOBAL_GENOMIC_NER_GG_NER	REACTOME	0.38508064	0.4584101	1

REACTOME_INTRINSIC_PATHWAY_FOR_APOPTOSIS	REACTOME	0.38966203	0.5309292	1
REACTOME_PLATELET_SENSITIZATION_BY_LDL	REACTOME	0.39029127	0.5462311	1
REACTOME_CITRIC_ACID_CYCLE_TCA_CYCLE	REACTOME	0.4059406	0.5149598	1
REACTOME_SYNTHESIS_OF_GLYCOSYLPHOSPHATIDYLINOSITOL_GPI	REACTOME	0.40688258	0.5313724	1
REACTOME_G2_M_CHECKPOINTS	REACTOME	0.42828685	0.5251618	1
REACTOME_FANCONI_ANEMIA_PATHWAY	REACTOME	0.4302554	0.529813	1
REACTOME_ACYL_CHAIN_REMODELLING_OF_PE	REACTOME	0.43222004	0.6120956	1
REACTOME_SIGNALING_BY_ILS	REACTOME	0.43232325	0.58783746	1
REACTOME_ABCA_TRANSPORTERS_IN_LIPID_HOMEOSTASIS	REACTOME	0.43307087	0.5865741	1
REACTOME_PI_METABOLISM	REACTOME	0.43373495	0.49913457	1
REACTOME_BRANCHED_CHAIN_AMINO_ACID_CATABOLISM	REACTOME	0.43460765	0.5742923	1
REACTOME_INWARDLY_RECTIFYING_K_CHANNELS	REACTOME	0.43469787	0.6086152	1
REACTOME_REGULATION_OF_INSULIN_LIKE_GROWTH_FACTOR_IGF_ACTIVITY_BY_INSULIN_LIKE_GROWTH_FACTOR_BINDING_PROTEINS_IGFBPS	REACTOME	0.4368932	0.59849197	1
REACTOME_DNA_STRAND_ELONGATION	REACTOME	0.43712574	0.5257314	1
REACTOME_CELL_CYCLE_CHECKPOINTS	REACTOME	0.4428858	0.5281712	1
REACTOME_ARMS_MEDIATED_ACTIVATION	REACTOME	0.44354838	0.56559163	1
REACTOME_SIGNALING_BY_NOTCH1	REACTOME	0.44509804	0.56752014	1
REACTOME_BOTULINUM_NEUROTOXICITY	REACTOME	0.4453125	0.60919654	1
REACTOME_CLASS_I_MHC_MEDIATED_ANTIGEN_PROCESSING_PRESENTATION	REACTOME	0.44715446	0.5798507	1
REACTOME_CTNNB1_PHOSPHORYLATION_CASCADE	REACTOME	0.44930416	0.6061521	1
REACTOME_CD28_DEPENDENT_PI3K_AKT_SIGNALING	REACTOME	0.45242718	0.6020288	1
REACTOME_DNA_REPAIR	REACTOME	0.45325205	0.53024083	1
REACTOME_INFLUENZA_VIRAL_RNA_TRANSCRIPTION_AND_REPLICATION	REACTOME	0.45416668	0.5736608	1
REACTOME_ASSOCIATION_OF_TRIC_CCT_WITH_TARGET_PROTEINS_DURING_BIOSYNTHESIS	REACTOME	0.45490196	0.61167264	1
REACTOME_BIOSYNTHESIS_OF_THE_N_GLYCAN_PRECURSOR_DOLICHOL_LIPID_LINKED_OLIGOSACCHARIDE_LLO_AND_TRANSFER_TO_A_NASCENT_PROTEIN	REACTOME	0.45544556	0.58057076	1
REACTOME_TIE2_SIGNALING	REACTOME	0.45783132	0.6195503	1
REACTOME_PI3K_CASCADE	REACTOME	0.47912526	0.6141408	1
REACTOME_TRANSCRIPTIONAL_ACTIVITY_OF_SMAD2_SMAD3_SMAD4_HETEROTRIMER	REACTOME	0.48178136	0.5900052	1
REACTOME_NUCLEOTIDE_EXCISION_REPAIR	REACTOME	0.48303393	0.53104055	1
REACTOME_SIGNALING_BY_FGFR1_FUSION_MUTANTS	REACTOME	0.4852071	0.60593385	1
REACTOME_METABOLISM_OF_LIPIDS_AND_LIPOPROTEINS	REACTOME	0.49101797	0.62966627	1
REACTOME_CYTOSOLIC_TRNA_AMINOACYLATION	REACTOME	0.496994	0.5251059	1
REACTOME_S_PHASE	REACTOME	0.5019841	0.574648	1
REACTOME_PROCESSIVE_SYNTHESIS_ON_THE_LAGGING_STRAND	REACTOME	0.50392157	0.5642427	1
REACTOME_FATTY_ACYL_COA_BIOSYNTHESIS	REACTOME	0.50583655	0.63898367	1
REACTOME_ACTIVATION_OF_ATR_IN_RESPONSE_TO_REPLICATION_STRESS	REACTOME	0.5059761	0.56411296	1
REACTOME_ANTIGEN_PROCESSING_UBIQUITINATION_PROTEASOME_DEGRADATION	REACTOME	0.5060729	0.6488634	1
REACTOME_ANTIVIRAL_MECHANISM_BY_IFN_STIMULATED_GENES	REACTOME	0.50690335	0.5753108	1
REACTOME_HOST_INTERACTIONS_OF_HIV_FACTORS	REACTOME	0.5137795	0.6278368	1
REACTOME_GLUCOSE_METABOLISM	REACTOME	0.516129	0.616868	1
REACTOME_IL_3_5_AND_GM_CSF_SIGNALING	REACTOME	0.527668	0.6596547	1
REACTOME_G_ALPHA_S_SIGNALLING_EVENTS	REACTOME	0.5292969	0.6506361	1
REACTOME_MRNA_CAPPING	REACTOME	0.52953154	0.59987295	1

REACTOME_SIGNALING_BY_CONSTITUTIVELY_ACTIVE_EGFR	REACTOME	0.5310621	0.6279393	1
REACTOME_APC_C_CDC20_MEDIATED_DEGRADATION_OF_MITOTIC_PROTEINS	REACTOME	0.5321285	0.6454813	1
REACTOME_REGULATION_OF_APOPTOSIS	REACTOME	0.5342742	0.6608	1
REACTOME_PROLONGED_ERK_ACTIVATION_EVENTS	REACTOME	0.53438115	0.6122991	1
REACTOME_SYNTHESIS_OF_DNA	REACTOME	0.536	0.60512817	1
REACTOME_TRNA_AMINOACYLATION	REACTOME	0.5403226	0.6013083	1
REACTOME_TRANSFERRIN_ENDOCYTOSIS_AND_RECYCLING	REACTOME	0.54141414	0.6288242	1
REACTOME_CLASS_B_2_SECRETIN_FAMILY_RECEPTORS	REACTOME	0.5424063	0.64030296	1
REACTOME_TRIGLYCERIDE_BIOSYNTHESIS	REACTOME	0.5481928	0.6407359	1
REACTOME_GLUCAGON_TYPE_LIGAND_RECEPTORS	REACTOME	0.5496183	0.6562514	1
REACTOME_RESOLUTION_OF_AP_SITES_VIA_THE_MULTIPLE_NUCLEOTIDE_PATCH_REPLACEMENT_PATHWAY	REACTOME	0.55220884	0.6111032	1
REACTOME_CROSS_PRESENTATION_OF_SOLUBLE_EXOGENOUS_ANTIGENS_ENDOSOMES	REACTOME	0.55263156	0.7164619	1
REACTOME_LAGGING_STRAND_SYNTHESIS	REACTOME	0.55490196	0.5877497	1
REACTOME_FORMATION_OF_THE_HIV1_EARLY_ELONGATION_COMPLEX	REACTOME	0.56	0.6053724	1
REACTOME_TRANSCRIPTION_COUPLED_NER_TC_NER	REACTOME	0.56	0.6110799	1
REACTOME_EXTENSION_OF_TELOMERES	REACTOME	0.5601578	0.6113583	1
REACTOME_CYTOKINE_SIGNALING_IN_IMMUNE_SYSTEM	REACTOME	0.5641026	0.66138947	1
REACTOME_BASE_EXCISION_REPAIR	REACTOME	0.566	0.6122105	1
REACTOME_ANTIGEN_PROCESSING_CROSS_PRESENTATION	REACTOME	0.56626505	0.6616002	1
REACTOME_NUCLEAR_SIGNALING_BY_ERBB4	REACTOME	0.5665962	0.65821195	1
REACTOME_PKB_MEDIATED_EVENTS	REACTOME	0.57	0.6599496	1
REACTOME_SIGNALING_BY_THE_B_CELL_RECEPTOR_BCR	REACTOME	0.5864811	0.6621516	1
REACTOME_PEROXISOMAL_LIPID_METABOLISM	REACTOME	0.5927419	0.69295645	1
REACTOME_GLYCOLYSIS	REACTOME	0.5975855	0.69202584	1
REACTOME_OXYGEN_DEPENDENT_PROLINE_HYDROXYLATION_OF_HYPOXIA_INDUCIBLE_FACTOR_ALPHA	REACTOME	0.5980198	0.6979957	1
REACTOME_M_G1_TRANSITION	REACTOME	0.6	0.68432635	1
REACTOME_RESPIRATORY_ELECTRON_TRANSPORT_ATP_SYNTHESIS_BY_CHEMIOSMOTIC_COUPLING_AND_HEAT_PRODUCTION_BY_UNCOUPLING_PROTEINS_	REACTOME	0.6023857	0.65827185	1
REACTOME_MITOCHONDRIAL_TRNA_AMINOACYLATION	REACTOME	0.60365856	0.71046126	1
REACTOME_APC_C_CDH1_MEDIATED_DEGRADATION_OF_CDC20_AND_OTHER_APC_C_CDH1_TARGETED_PROTEINS_IN_LATE_MITOSIS_EARLY_G1	REACTOME	0.61122245	0.7209448	1
REACTOME_SYNTHESIS_OF_PA	REACTOME	0.61133605	0.6582169	1
REACTOME_PURINE_METABOLISM	REACTOME	0.61491936	0.70608866	1
REACTOME_ENERGY_DEPENDENT_REGULATION_OF_MTOR_BY_LKB1_AMPK	REACTOME	0.61584157	0.71195173	1
REACTOME_REGULATION_OF_IFNA_SIGNALING	REACTOME	0.617357	0.66418004	1
REACTOME_REGULATORY_RNA_PATHWAYS	REACTOME	0.6178862	0.6624037	1
REACTOME_METABOLISM_OF_NUCLEOTIDES	REACTOME	0.6181818	0.7056981	1
REACTOME_INTERFERON_SIGNALING	REACTOME	0.6222664	0.7099393	1
REACTOME_ORC1_REMOVAL_FROM_CHROMATIN	REACTOME	0.62677485	0.7065203	1
REACTOME_ABORTIVE_ELONGATION_OF_HIV1_TRANSCRIPT_IN_THE_ABSENCE_OF_TAT	REACTOME	0.62781185	0.7182027	1
REACTOME_HIV_INFECTION	REACTOME	0.64081633	0.7175351	1
REACTOME_INTERACTIONS_OF_VPR_WITH_HOST_CELLULAR_PROTEINS	REACTOME	0.64257026	0.7183325	1
REACTOME_SYNTHESIS_OF_PIPS_AT_THE_GOLGI_MEMBRANE	REACTOME	0.6502947	0.6628712	1
REACTOME_ACYL_CHAIN_REMODELLING_OF_PI	REACTOME	0.6504065	0.69092846	1
REACTOME_FORMATION_OF_TRANSCRIPTION_COUPLED_NER_TC_NER_REPAIR_COMPLEX	REACTOME	0.66467065	0.7384997	1

REACTOME_FORMATION_OF_ATP_BY_CHEMIOSMOTIC_COUPLING	REACTOME	0.66994107	0.7024975	1
REACTOME_CIRCADIAN_REPRESSION_OF_EXPRESSION_BY_REV_ERBA	REACTOME	0.67820776	0.78063107	1
REACTOME_RESPIRATORY_ELECTRON_TRANSPORT	REACTOME	0.6923077	0.74691916	1
REACTOME_SIGNALING_BY_FGFR_MUTANTS	REACTOME	0.69292927	0.7200638	1
REACTOME_DOWNSTREAM_SIGNALING_EVENTS_OF_B_CELL_RECEPTOR_BCR	REACTOME	0.6955645	0.7947728	1
REACTOME_TRANSPORT_OF_RIBONUCLEOPROTEINS_INTO_THE_HOST_NUCLEUS	REACTOME	0.696	0.78372157	1
REACTOME_SYNTHESIS_OF_PC	REACTOME	0.69959676	0.7839595	1
REACTOME_MICRORNA_MIRNA_BIOGENESIS	REACTOME	0.70408165	0.783652	1
REACTOME_ACTIVATED_TAK1_MEDIATES_P38_MAPK_ACTIVATION	REACTOME	0.7076613	0.7613728	1
REACTOME_INFLUENZA_LIFE_CYCLE	REACTOME	0.716	0.8414284	1
REACTOME_ASSEMBLY_OF_THE_PRE_REPLICATIVE_COMPLEX	REACTOME	0.7172131	0.85179156	1
REACTOME_TRANSCRIPTION	REACTOME	0.7335984	0.79116166	1
REACTOME_TRANSPORT_OF_MATURE_MRNA_DERIVED_FROM_AN_INTRONLESS_TRANSCRIPT	REACTOME	0.73991936	0.8588255	1
REACTOME_CYCLIN_E_ASSOCIATED_EVENTS_DURING_G1_S_TRANSITION_	REACTOME	0.7418033	0.8249075	1
REACTOME_INTERFERON_GAMMA_SIGNALING	REACTOME	0.7465619	0.7584427	1
REACTOME_GLUCOSE_TRANSPORT	REACTOME	0.7525151	0.84672093	1
REACTOME_NOTCH1_INTRACELLULAR_DOMAIN_REGULATES_TRANSCRIPTION	REACTOME	0.7588235	0.7856618	1
REACTOME_DEADENYLATION_OF_MRNA	REACTOME	0.764	0.90708554	1
REACTOME_NEP_NS2_INTERACTS_WITH_THE_CELLULAR_EXPORT_MACHINERY	REACTOME	0.76447105	0.84992707	1
REACTOME_RORA_ACTIVATES_CIRCADIAN_EXPRESSION	REACTOME	0.7712551	0.86210793	1
REACTOME_RNA_POL_II_TRANSCRIPTION_PRE_INITIATION_AND_PROMOTER_OPENING	REACTOME	0.77823406	0.8833742	1
REACTOME_RNA_POL_III_TRANSCRIPTION_TERMINATION	REACTOME	0.78630704	0.8604807	1
REACTOME_ACTIVATED_AMPK_STIMULATES_FATTY_ACID_OXIDATION_IN_MUSCLE	REACTOME	0.790224	0.85941476	1
REACTOME_IMMUNOREGULATORY_INTERACTIONS_BETWEEN_A_LYMPHOID_AND_A_NON_LYMPHOID_CELL	REACTOME	0.7959596	0.8523619	1
REACTOME_SMAD2_SMAD3_SMAD4_HETEROTRIMER_REGULATES_TRANSCRIPTION	REACTOME	0.8	0.84617573	1
REACTOME_GENERIC_TRANSCRIPTION_PATHWAY	REACTOME	0.8019802	0.7905536	1
REACTOME_HIV_LIFE_CYCLE	REACTOME	0.8127572	0.9327706	1
REACTOME_NONSENSE_MEDIATED_DECAY_ENHANCED_BY_THE_EXON_JUNCTION_COMPLEX	REACTOME	0.81390595	0.9031329	1
REACTOME_SHC_MEDIATED_CASCADE	REACTOME	0.820202	0.8516929	1
REACTOME_VOLTAGE_GATED_POTASSIUM_CHANNELS	REACTOME	0.8224852	0.86063164	1
REACTOME_ANTIGEN_PRESENTATION_FOLDING_ASSEMBLY_AND_PEPTIDE_LOADING_OF_CLASS_I_MHC	REACTOME	0.8242424	0.89602566	1
REACTOME_SIGNALING_BY_WNT	REACTOME	0.8320158	0.9746709	1
REACTOME_DESTABILIZATION_OF_MRNA_BY_KSRP	REACTOME	0.83469385	0.8693104	1
REACTOME_TRANSLATION	REACTOME	0.8574423	0.9533876	1
REACTOME_SCFSKP2_MEDIATED_DEGRADATION_OF_P27_P21	REACTOME	0.87096775	0.9612824	1
REACTOME_REGULATION_OF_GLUCOKINASE_BY_GLUCOKINASE_REGULATORY_PROTEIN	REACTOME	0.8717435	0.9544354	1
REACTOME_SCF_BETA_TRCP_MEDIATED_DEGRADATION_OF_EMI1	REACTOME	0.8815261	0.9870531	1
REACTOME_CDT1_ASSOCIATION_WITH_THE_CDC6_ORC_ORIGIN_COMPLEX	REACTOME	0.8946281	0.9928199	1
REACTOME_TRANSPORT_OF_MATURE_TRANSCRIPT_TO_CYTOPLASM	REACTOME	0.8996063	0.9951282	1
REACTOME_LATE_PHASE_OF_HIV_LIFE_CYCLE	REACTOME	0.9018405	0.9926554	1
REACTOME_ACTIVATION_OF_THE_MRNA_UPON_BINDING_OF_THE_CAP_BINDING_COMPLEX_AND_EIFS_AND_SUBSEQUENT_BINDING_TO_43S	REACTOME	0.9131313	0.9591834	1
REACTOME_METABOLISM_OF_NON_CODING_RNA	REACTOME	0.9153226	1	1
REACTOME_DEADENYLATION_DEPENDENT_MRNA_DECAY	REACTOME	0.9215292	0.99485415	1

REACTOME_P53_INDEPENDENT_G1_S_DNA_DAMAGE_CHECKPOINT	REACTOME	0.9224652	1	1
REACTOME_METABOLISM_OF_MRNA	REACTOME	0.9241517	1	1
REACTOME_FGFR_LIGAND_BINDING_AND_ACTIVATION	REACTOME	0.9246436	0.947385	1
REACTOME_REGULATION_OF_MRNA_STABILITY_BY_PROTEINS_THAT_BIND_AU_RICH_ELEMENTS	REACTOME	0.9298597	1	1
REACTOME_FORMATION_OF_THE_TERNARY_COMPLEX_AND_SUBSEQUENTLY_THE_43S_COMPLEX	REACTOME	0.9356137	0.9335302	1
REACTOME_AUTODEGRADATION_OF_CDH1_BY_CDH1_APC_C	REACTOME	0.9386503	0.9989878	1
REACTOME_MRNA_PROCESSING	REACTOME	0.9389764	0.99967253	1
REACTOME_METABOLISM_OF_RNA	REACTOME	0.9472617	1	1
REACTOME_RNA_POL_III_CHAIN_ELONGATION	REACTOME	0.9570552	0.9933826	1
REACTOME_P53_DEPENDENT_G1_DNA_DAMAGE_RESPONSE	REACTOME	0.96311474	1	1
REACTOME_GENERATION_OF_SECOND_MESSENGER_MOLECULES	REACTOME	0.96837944	0.9769819	1
REACTOME_REGULATION_OF_ORNITHINE_DECARBOXYLASE_ODC	REACTOME	0.9773196	0.9965843	1
REACTOME_CDK_MEDIATED_PHOSPHORYLATION_AND_REMOVAL_OF_CDC6	REACTOME	0.9794239	0.999003	1
REACTOME_TCR_SIGNALING	REACTOME	0.98163265	0.89498293	1

Table S5. Significantly enriched gene sets (Nom p < 0.05) in Hep-i(+) cells compared with Hep-i(-) cells (assessed by GSEA)

NAME	Data base	NOM p-val	FDR q-val	FWER p-val
HALLMARK_BILE_ACID_METABOLISM	HALLMARK	0	0	0
HALLMARK_XENOBIOTIC_METABOLISM	HALLMARK	0	0	0
HALLMARK_INTERFERON_ALPHA_RESPONSE	HALLMARK	0	0.00203192	0.009
HALLMARK_INTERFERON_GAMMA_RESPONSE	HALLMARK	0	0.004421538	0.025
HALLMARK_IL6_JAK_STAT3_SIGNALING	HALLMARK	0.001730104	0.004498533	0.032
HALLMARK_FATTY_ACID_METABOLISM	HALLMARK	0.003289474	0.017174626	0.134
HALLMARK_OXIDATIVE_PHOSPHORYLATION	HALLMARK	0.008169935	0.05405483	0.47
HALLMARK_ALLOGRAFT_REJECTION	HALLMARK	0.008250825	0.055827018	0.438
HALLMARK_MTORC1_SIGNALING	HALLMARK	0.019448947	0.09290828	0.688
HALLMARK_INFLAMMATORY_RESPONSE	HALLMARK	0.035256412	0.10364589	0.77
KEGG_ANTIGEN_PROCESSING_AND_PRESENTATION	KEGG	0	0	0
KEGG_INTESTINAL_IMMUNE_NETWORK_FOR_IGA_PRODUCTION	KEGG	0	0.00458059	0.01
KEGG_VIRAL_MYOCARDITIS	KEGG	0	0.007766147	0.024
KEGG_GRAFT_VERSUS_HOST_DISEASE	KEGG	0	0.006760758	0.028
KEGG_ASTHMA	KEGG	0	0.006908039	0.036
KEGG_ALLOGRAFT_REJECTION	KEGG	0	0.00590976	0.037
KEGG_AUTOIMMUNE_THYROID_DISEASE	KEGG	0	0.005643357	0.041
KEGG_TYPE_I_DIABETES_MELLITUS	KEGG	0	0.005461193	0.045
KEGG_HEMATOPOIETIC_CELL_LINEAGE	KEGG	0	0.00900959	0.071
KEGG_HISTIDINE_METABOLISM	KEGG	0	0.009126132	0.075
KEGG_CELL_ADHESION_MOLECULES_CAMS	KEGG	0	0.021682419	0.221
KEGG_GLYCOLYSIS_GLUCONEOGENESIS	KEGG	0	0.027548978	0.29
KEGG_ALANINE_ASPARTATE_AND_GLUTAMATE_METABOLISM	KEGG	0	0.027620552	0.31
KEGG_LEISHMANIA_INFECTION	KEGG	0.001980198	0.024243744	0.242
KEGG_TYROSINE_METABOLISM	KEGG	0.002087683	0.032008834	0.359
KEGG_PEROXISOME	KEGG	0.003875969	0.021683577	0.213
KEGG_NITROGEN_METABOLISM	KEGG	0.003875969	0.066747464	0.598
KEGG_SYSTEMIC_LUPUS_ERYTHEMATOSUS	KEGG	0.004032258	0.02164113	0.193
KEGG_BETA_ALANINE_METABOLISM	KEGG	0.005988024	0.012074138	0.103
KEGG_PRIMARY_IMMUNODEFICIENCY	KEGG	0.008179959	0.059675828	0.562
KEGG_PHENYLALANINE_METABOLISM	KEGG	0.008230452	0.10039674	0.743
KEGG_ARGININE_AND_PROLINE_METABOLISM	KEGG	0.008316008	0.029425777	0.335
KEGG_PRIMARY_BILE_ACID_BIOSYNTHESIS	KEGG	0.010162601	0.077654	0.649
KEGG_GLYCINE_SERINE_AND_THREONINE_METABOLISM	KEGG	0.01443299	0.061130643	0.54
KEGG_NICOTINATE_AND_NICOTINAMIDE_METABOLISM	KEGG	0.014613778	0.06145446	0.556
KEGG_VALINE_LEUCINE_AND_ISOLEUCINE_DEGRADATION	KEGG	0.037698414	0.08356468	0.676
KEGG_OLFACTORY_TRANSDUCTION	KEGG	0.03976143	0.16786934	0.879
REACTOME_DOWNSTREAM_TCR_SIGNALING	REACTOME	0	0.001	0
REACTOME_GENERATION_OF_SECOND_MESSENGER_MOLECULES	REACTOME	0	0.002413546	0.005
REACTOME_TCR_SIGNALING	REACTOME	0	0.005957666	0.019
REACTOME_PD1_SIGNALING	REACTOME	0	0.061128862	0.162

REACTOME_PHOSPHORYLATION_OF_CD3_AND_TCR_ZETA_CHAINS	REACTOME	0	0.08464857	0.232
REACTOME_METABOLISM_OF_AMINO_ACIDS_AND_DERIVATIVES	REACTOME	0	0.10158933	0.289
REACTOME_COSTIMULATION_BY_THE_CD28_FAMILY	REACTOME	0	0.105196856	0.338
REACTOME_INTERFERON_GAMMA_SIGNALING	REACTOME	0	0.09907236	0.371
REACTOME_TRIGLYCERIDE_BIOSYNTHESIS	REACTOME	0	0.107802816	0.423
REACTOME_GLYCEROPHOSPHOLIPID_BIOSYNTHESIS	REACTOME	0.002053388	0.37238064	0.961
REACTOME_TRANSPORT_TO_THE_GOLGI_AND_SUBSEQUENT_MODIFICATION	REACTOME	0.002105263	0.10009334	0.354
REACTOME_NUCLEOTIDE_BINDING_DOMAIN_LEUCINE_RICH_REPEAT_CONTAINING_RECEPTOR_NLR_SIGNALING_PATHWAYS	REACTOME	0.004008016	0.4031425	0.993
REACTOME_CLASS_B_2_SECRETIN_FAMILY_RECEPTORS	REACTOME	0.004115226	0.45542392	1
REACTOME_PLATELET_HOMEOSTASIS	REACTOME	0.004149378	0.41834342	1
REACTOME_METABOLISM_OF_VITAMINS_AND_COFACTORS	REACTOME	0.008213553	0.13511233	0.543
REACTOME_GLUCONEOGENESIS	REACTOME	0.012024048	0.20957358	0.697
REACTOME_ENDOGENOUS_STEROLS	REACTOME	0.012145749	0.27912465	0.869
REACTOME_TRANSPORT_OF_VITAMINS_NUCLEOSIDES_AND_RELATED_MOLECULES	REACTOME	0.012219959	0.25343472	0.825
REACTOME_SYNTHESIS_OF_BILE_ACIDS_AND_BILE_SALTS	REACTOME	0.012371134	0.27232108	0.852
REACTOME_MHC_CLASS_II_ANTIGEN_PRESENTATION	REACTOME	0.013384321	0.38549942	0.972
REACTOME_GLUCOSE_METABOLISM	REACTOME	0.016393442	0.2244454	0.732
REACTOME_SYNTHESIS_SECRETION_AND_INACTIVATION_OF_GLP1	REACTOME	0.018367346	0.23903248	0.769
REACTOME_ACYL_CHAIN_REMODELLING_OF_PI	REACTOME	0.021782178	0.26763445	0.87
REACTOME_ACYL_CHAIN_REMODELLING_OF_PS	REACTOME	0.022403259	0.31277552	0.943
REACTOME_INCRETIN_SYNTHESIS_SECRETION_AND_INACTIVATION	REACTOME	0.02414487	0.27975512	0.907
REACTOME_OLFACTORY_SIGNALING_PATHWAY	REACTOME	0.026748972	0.3648792	0.956
REACTOME_TRANSMEMBRANE_TRANSPORT_OF_SMALL_MOLECULES	REACTOME	0.027079303	0.4785888	1
REACTOME_IRON_UPTAKE_AND_TRANSPORT	REACTOME	0.028169014	0.2610249	0.853
REACTOME_COMPLEMENT_CASCADE	REACTOME	0.031446543	0.30180398	0.931
REACTOME_SLC_MEDIATED_TRANSMEMBRANE_TRANSPORT	REACTOME	0.031936128	0.39421687	0.981
REACTOME_CYTOKINE_SIGNALING_IN_IMMUNE_SYSTEM	REACTOME	0.03646833	0.4711344	1
REACTOME_INNATE_IMMUNE_SYSTEM	REACTOME	0.037113402	0.40370357	0.994
REACTOME_PYRIMIDINE_METABOLISM	REACTOME	0.0375	0.2345572	0.786
REACTOME_SYNTHESIS_OF_BILE_ACIDS_AND_BILE_SALTS_VIA_7ALPHA_HYDROXYCHOLESTEROL	REACTOME	0.0392562	0.36809182	0.973
REACTOME_SYNTHESIS_OF_PA	REACTOME	0.039622642	0.37825236	0.973
REACTOME_REGULATION_OF_GENE_EXPRESSION_IN_BETA_CELLS	REACTOME	0.041152265	0.40426937	0.994
REACTOME_SULFUR_AMINO_ACID_METABOLISM	REACTOME	0.04225352	0.42253336	0.981
REACTOME_BILE_ACID_AND_BILE_SALT_METABOLISM	REACTOME	0.046938777	0.26946566	0.883
REACTOME_INTERFERON_SIGNALING	REACTOME	0.04863813	0.38702476	0.984
REACTOME_TRANSPORT_OF_GLUCOSE_AND_OTHER_SUGARS_BILE_SALTS_AND_ORGANIC_ACIDS_METAL_IONS_AND_AMINE_COMPOUNDS	REACTOME	0.04897959	0.39470455	0.987

Table S6. Significantly enriched (NOM p < 0.05) gene sets in hCLiP-chimera-derived hepatocytes in comparison with PHHs

NAME	Data base	NOM p-val	FDR q-val	FWER p-val
HALLMARK_NOTCH_SIGNALING	HALLMARK	0	0.14523014	0.114
HALLMARK_APICAL_SURFACE	HALLMARK	0	0.15693645	0.214
HALLMARK_HYPOXIA	HALLMARK	0	0.23320402	0.308
HALLMARK_KRAS_SIGNALING_DN	HALLMARK	0	0.21433364	0.308
HALLMARK_COAGULATION	HALLMARK	0	0.18801166	0.308
HALLMARK_HEDGEHOG_SIGNALING	HALLMARK	0	0.20412263	0.402
HALLMARK_MYOGENESIS	HALLMARK	0	0.2369269	0.519
KEGG_NITROGEN_METABOLISM	KEGG	0	1	0.431
KEGG_DORSO_VENTRAL_AXIS_FORMATION	KEGG	0	0.8070004	0.532
KEGG_RENIN_ANGIOTENSIN_SYSTEM	KEGG	0	0.67188025	0.737
KEGG_GLYCOLYSIS_GLUCONEOGENESIS	KEGG	0	0.5798928	0.737
KEGG_STEROID_HORMONE_BIOSYNTHESIS	KEGG	0	0.4406415	0.737
KEGG_BUTANOATE_METABOLISM	KEGG	0	0.42509153	0.737
KEGG_METABOLISM_OF_XENOBIOTICS_BY_CYTOCHROME_P450	KEGG	0	0.38385913	0.737
KEGG_BASAL_CELL_CARCINOMA	KEGG	0	0.35087314	0.737
KEGG_PROPANOATE_METABOLISM	KEGG	0	0.2907683	0.737
KEGG_DRUG_METABOLISM_CYTOCHROME_P450	KEGG	0	0.31267843	0.737
KEGG_GRAFT_VERSUS_HOST_DISEASE	KEGG	0	0.3060045	0.737
KEGG_RETINOL_METABOLISM	KEGG	0	0.2978703	0.737
KEGG_ARRHYTHMOGENIC_RIGHT_VENTRICULAR_CARDIOMYOPATHY_ARVC	KEGG	0	0.30322078	0.737
KEGG_COMPLEMENT_AND_COAGULATION_CASCADES	KEGG	0	0.29349664	0.737
KEGG_AUTOIMMUNE_THYROID_DISEASE	KEGG	0	0.31930727	0.779
KEGG_ALPHA_LINOLENIC_ACID_METABOLISM	KEGG	0	0.34937185	0.894
KEGG_MATURITY_ONSET_DIABETES_OF_THE_YOUNG	KEGG	0	0.35212293	0.894
KEGG_GALACTOSE_METABOLISM	KEGG	0	0.34549597	0.894

KEGG_STARCH_AND_SUCROSE_METABOLISM	KEGG	0	0.32447046	0.894
KEGG_ASCORBATE_AND_ALDARATE_METABOLISM	KEGG	0	0.33308324	0.894
KEGG_CELL_ADHESION_MOLECULES_CAMS	KEGG	0	0.32254976	0.942
KEGG_ARACHIDONIC_ACID_METABOLISM	KEGG	0	0.316469	0.942
KEGG_TERPENOID_BACKBONE_BIOSYNTHESIS	KEGG	0	0.31435984	0.942
KEGG_HEDGEHOG_SIGNALING_PATHWAY	KEGG	0	0.31573096	0.942
KEGG_GLYCOSPHINGOLIPID_BIOSYNTHESIS_LACTO_AND_NEOLACTO_SERIES	KEGG	0	0.36563307	0.942
KEGG_STEROID_BIOSYNTHESIS	KEGG	0	0.40754798	0.942
REACTOME_PRE_NOTCH_PROCESSING_IN_GOLGI	REACTOME	0	0.45624468	0.258
REACTOME_SYNTHESIS_OF_PA	REACTOME	0	0.49582168	0.551
REACTOME_ACYL_CHAIN_REMODELLING_OF_PG	REACTOME	0	0.35054788	0.551
REACTOME_AMINE_COMPOUND_SLC_TRANSPORTERS	REACTOME	0	0.5495397	0.819
REACTOME_NA_CL_DEPENDENT_NEUROTRANSMITTER_TRANSPORTERS	REACTOME	0	1	0.913
REACTOME_GLYCOLYSIS	REACTOME	0	1	0.913
REACTOME_TRANSPORT_OF_VITAMINS_NUCLEOSIDES_AND_RELATED_MOLECULES	REACTOME	0	0.9796463	0.913
REACTOME_ACYL_CHAIN_REMODELLING_OF_PS	REACTOME	0	0.8588539	0.913
REACTOME_FORMATION_OF_FIBRIN_CLOT_CLOTTING_CASCADE	REACTOME	0	0.85995644	0.913
REACTOME_BIOLOGICAL_OXIDATIONS	REACTOME	0	0.80131924	0.913
REACTOME_CYTOCHROME_P450_ARRANGED_BY_SUBSTRATE_TYPE	REACTOME	0	0.8075716	0.913
REACTOME_INTRINSIC_PATHWAY	REACTOME	0	0.760971	0.913
REACTOME_PHASE1_FUNCTIONALIZATION_OF_COMPOUNDS	REACTOME	0	0.7406763	0.946
REACTOME_INTERACTION_BETWEEN_L1_AND_ANKYRINS	REACTOME	0	0.6859455	0.946
REACTOME_ACYL_CHAIN_REMODELLING_OF_PC	REACTOME	0	0.69108987	1
REACTOME_HS_GAG_BIOSYNTHESIS	REACTOME	0	0.69282025	1
REACTOME_EFFECTS_OF_PIP2_HYDROLYSIS	REACTOME	0	0.7313041	1
REACTOME_A_TETRASACCHARIDE_LINKER_SEQUENCE_IS_REQUIRED_FOR_GAG_SYNTHES	REACTOME	0	0.70685107	1
REACTOME_ACYL_CHAIN_REMODELLING_OF_PE	REACTOME	0	0.6834588	1

REACTOME_HEPARAN_SULFATE_HEPARIN_HS_GAG_METABOLISM	REACTOME	0	0.68222684	1
REACTOME_HS_GAG_DEGRADATION	REACTOME	0	0.664482	1
REACTOME_PRE_NOTCH_EXPRESSION_AND_PROCESSING	REACTOME	0	0.6609847	1
REACTOME_GRB2_SOS_PROVIDES_LINKAGE_TO_MAPK_SIGNALING_FOR_INTERGRINS_	REACTOME	0	0.66925216	1
REACTOME_AMINE_DERIVED_HORMONES	REACTOME	0	0.6552516	1
REACTOME_METABOLISM_OF_STEROID_HORMONES_AND_VITAMINS_A_AND_D	REACTOME	0	0.6392642	1
REACTOME_ACYL_CHAIN_REMODELLING_OF_PI	REACTOME	0	0.6242897	1
REACTOME_TRANSPORT_OF_GLUCOSE_AND_OTHER_SUGARS_BILE_SALTS_AND_ORGANI	REACTOME	0	0.6194206	1
REACTOME_METABOLISM_OF_LIPIDS_AND_LIPOPROTEINS	REACTOME	0	0.6084904	1
REACTOME_ANTIGEN_ACTIVATES_B_CELL_RECEPTOR_LEADING_TO_GENERATION_OF_SE	REACTOME	0	0.68690026	1
REACTOME_STEROID_HORMONES	REACTOME	0	0.6336788	1
REACTOME_RESPONSE_TO_ELEVATED_PLATELET_CYTOSOLIC_CA2_	REACTOME	0	0.6231095	1
REACTOME_CLASS_B_2_SECRETIN_FAMILY_RECEPTORS	REACTOME	0	0.63061726	1
REACTOME_GLUCAGON_TYPE_LIGAND_RECEPTORS	REACTOME	0	0.6273213	1
REACTOME_CHOLESTEROL_BIOSYNTHESIS	REACTOME	0	0.6142165	1
REACTOME_G_ALPHA_S_SIGNALLING_EVENTS	REACTOME	0	0.63354135	1
REACTOME_PHOSPHOLIPID_METABOLISM	REACTOME	0	0.64769787	1